Studies on Utilisation of Agro-Waste for Fabrication of Sustainable Bio-composites

Thesis submitted in partial fulfilment of the requirements for the degree of

DOCTOR OF PHILOSOPHY

by

Sayan Kumar Bhattacharjee

Roll No. 156107013

DEPARTMENT OF CHEMICAL ENGINEERING

INDIAN INSTITUTE OF TECHNOLOGY GUWAHATI

Assam, Guwahati - 781039

(April 2023)

This thesis is dedicated to my Grandparents, my beloved

Parents, my beautiful Wife and my In Laws

For their Endless Love, Support and Encouragement

Department of Chemical Engineering

Indian Institute of Technology Guwahati

CERTIFICATE

This is to certify that the research work in the thesis entitled "**Studies on Utilisation of Agro-Waste for Fabrication of Sustainable Bio-Composites**" is carried out by me at the Chemical Engineering Department, Indian Institute of Technology Guwahati, under the supervision of Prof. Vimal Katiyar and Dr. Raghvendra Gupta. The results documented in this thesis are achieved my me and has not been submitted to any other University or Institute for the award of any degree or diploma.

(**Sayan Kumar Bhattacharjee)**
Roll No.: 156107013

Department of Chemical Engineering

Indian Institute of Technology Guwahati

Guwahati – 781039, India

Department of Chemical Engineering

Indian Institute of Technology Guwahati

CERTIFICATE

This is to certify that the research work in the thesis entitled "**Studies on Utilisation of Agro-Waste for Fabrication of Sustainable Bio-Composites**", being submitted by **Sayan Kumar Bhattacharjee** for the award of Ph.D. degree has been carried out by him at the Chemical Engineering Department, Indian Institute of Technology Guwahati, under our guidance and supervision. The work documented in this thesis has not been submitted to any other University or Institute for the award of any degree or diploma.

(Prof. Vimal Katiyar)
Professor

Department of Chemical Engineering

Indian Institute of Technology Guwahati

Guwahati – 781039, India

(Dr. Raghvendra Gupta)
Associate Professor

Department of Chemical Engineering

Indian Institute of Technology Guwahati

Guwahati – 781039, India

Acknowledgement

The journey of completing the thesis is a potpourri of countless incidents and experiences, which have sculpted the path of intellectual exploration and self-awareness. I acknowledge this period of student-hood as the most enriching stage of my personal growth.

It is my utmost privilege to be a student on the campus of the Indian Institute of Technology, Guwahati, where life thrives with vibrance, exuberance and strive for excellence. I express my deep sense of gratitude to the Department of Chemical Engineering, where my foundation of understanding the fundamentals of complex natural phenomenon from an engineering perspective have been built.

I express my deep sense of gratitude to my supervisors Prof. Vimal Katiyar and Dr. Raghvendra Gupta, whose perseverance, encouragement and valuable input played a pivotal part in shaping this thesis. Their critical thinking, depth of knowledge and teaching skills are nothing short of exemplary. I am grateful to my doctoral committee members Dr. Amit Kumar, Prof. Anugrah Singh (Department of Chemical Engineering), and Dr. Poonam Kumari (Department of Mechanical Engineering), for their valuable suggestions, constructive criticisms and encouragement. I would like to thank to the Central Instruments Facility (CIF) and the Centre for Sustainable Polymers (CSP) formerly known Coe-SusPol for carrying out instrumental analysis part of my research work. I would also like to thank to the Head of the Department of Chemical Engineering, Prof. Kaustubha Mohanty and all authorities of the department of chemical engineering for providing me all research and analytical facilities required for my work. I am extremely thankful to the technical staff of the chemical engineering department, particularly Mr. Debajit Borah, Mr. Dipak Kumar Barman, Mr. Harsaraj Biswanath and non-technical staffs Mr. Bhagya Boro, Mr. Deepjyoti Sinha for their kind co-operation during the entire doctoral work.

I am indebted to my lab seniors specially to Dr. Gourhari Chakraborty, Dr. Akhilesh Kumar Pal. Dr. Surendra Singh Gaur, Dr. Narendren Soundararajan, Dr. Prodyut Dhar, Dr. Riddhi Mahansaria for their valuable suggestions, advice and encouragement. I sincerely thank to my lab mates Kona, Abhishek, Munmi, Chethana, Srijeeb, Pankaj, Bhanupriya, Arnab, Manoj, Khisitij, Amrit, Parul, Kuhelika, Mandavi for their sincere help and for making the workplace so joyful and homely. I acknowledge the support and help I received form my contemporaries Dr. Bikash, Dr. Rupam, Dr. Rupam, Dr. Barnali, Dr. Kuldeep, Saptarshi and seniors Dr. Pradip, Dr. Atanu, Dr. Shounak, Dr. Suman. The start of my academic journey at IIT Guwahati would not have been possible without the warmth and friendship of my batchmates Dr. Sounak, Dr. Aparajita, Dr. Subhojit, Dr. Debojit, Dr. Siddhant. I would extremely cherish the fun-filled years in hostels I had spent with my friends Dr. palash, Dr. Kundan, Rahul, Anindya, Anjishnu, Parvej, Riddhiman, Sayan, Milan, Priyam, Adhiraj, Oishik, Victor, Amit, Pritam.

Most importantly, I am eternally indebted to my parents for their continuous support, sacrifice, and encouragement throughout my doctoral journey. I would treasure their integrity, values, ethics, perseverance, and optimism for the rest of my research life. I am blessed to have a beautiful wife, Dr. Debarati, in my life. How could I forget her immense support and encouragement during my doctoral life? Lastly, I thank my in-laws for their motivation and encouragement.

Sayan Kumar Bhattacharjee

IIT Guwahati

Abstract

The present scenario encompasses the increased environmental concerns about reducing carbon footprint and rising prices of petrochemicals have attracted much attention towards developing green and sustainable biodegradable polymers and nanomaterials, which will help secure the planet's ecological balance. As a result, lignocellulosic biomass has become an alternative route of fossil resources to compensate for the increasing trend of the world's demand for petroleum usage. The lignocellulosic resources include:

1. Agricultural wastes (rice straw, sugarcane bagasse, coconut husks, wheat rice).
2. Industrial and municipal wastes (waste paper).
3. Food wastes (Plate waste, by-products from food and beverage processing).
4. Forest residues (hardwood and softwood).

With growing environmental awareness, researchers are focusing on eco-friendly materials, with terms such as "renewable," "recyclable," "sustainable," and "triggered biodegradable" becoming buzzwords. The development of such materials has been a great motivating factor for materials scientists and an essential provider of opportunities to improve the standard of living of people worldwide. Natural fibers from agricultural waste are gaining importance in the polymer industry because they are lightweight, low-cost, and environmentally friendly. Rice straw (RS), a type of natural fiber obtained from agro-industrial waste, can be used as a filler in the various polymer matrixes to develop polymer composites.

Therefore, this doctoral thesis focuses on the valorisation of agricultural waste in the form of rice straw and the fabrication of different polymeric bio-composites and nanocomposites. Other value-added products in the nanometres range were chemically synthesized from RS, i.e., nano-silica (NS), cellulose nanocrystal where these nanofillers are incorporated in various thermoplastic biopolymer matrix, i.e., Poly (lactic acid), Poly (butylene succinate). However, in the melt extrusion process at higher temperatures, miscibility and the phase separation

between the polymer matrix and these nanofillers is still challenging for the scientific community as these tend to aggregate due to small size effects, high surface energy, and relatively poor interaction between the filler and the polymer matrix which in turn decreases the mechanical property of the composites. Various compatibilisers and cross-linking agents were incorporated into the systems to improve the miscibility during melt processing. This thesis also investigates the influence of different nanofiller content on the thermal, mechanical, and rheological properties of the bio-composites and nanocomposites. The structure-properties relationship of the composites was explored in terms of the mechanical properties, thermal properties, crystallisation behaviour, and rheological properties, which have been summarized in six different chapters and explained in detail in subsequent sections.

Table of Contents

CHAPTER 5

EXTRACTION OF CELLULOSE NANOCRYSTALS (CNC) FROM RICE STRAW (RS) AND FABRICATION AND CHARACTERISATION OF POLY (LACTIC ACID) (PLA) – CNC BASED BIO-NANOCOMPOSITES BY MELT EXTRUSION PROCESS

List of Figures

List of Tables

Nomenclature

Abbreviations

CNC	Cellulose nanocrystals
DTG	Derivative thermogram
DCP	Di cumyl peroxide
DSC	Differential Scanning Calorimetry
FESEM	Field Emission Scanning Electron Microscope
FTIR	Fourier Transform Infrared Spectroscopy
HDT	Heat Distortion Temperature
LVE	Linear Viscoelastic Region
MA	Maleic Anhydride
NS	Nano Silica
PBS	Poly (butylene succinate)
PCL	Poly (caprolactone)
PE	Polyethylene
PHB	Poly (hydroxybutyrate)
PLA	Poly (lactic acid)

PP	Polypropylene
RS	Rice Straw
RSF	Rice Straw Flour
TGA	Thermogravimetric Analysis
UTM	Universal Testing Machine
UTS	Ultimate Tensile Strength
XRD	X-ray Diffraction
Y	Young's Modulus

Notations

%E	Elongation at break
T_{10}	Temperature at which 10% weight loss occurs
T_{max}	Maximum decomposition temperature
T_g	Glass Transition temperature
T_{cc}	Cold crystallisation temperature
T_m	Melting temperature
X_c *(%)*	Percentage crystallinity
G'	Storage Modulus (Pa)
G''	Loss Modulus (Pa)

ω	Angular frequency (rad/s)
η^*	Complex Viscosity (Pa.s)
$\tan\delta$	Loss factor
m	Fluid consistency co-efficient
n	Flow behaviour index
η'	Real part of the Complex Viscosity (Pa. s)
η''	Imaginary part of the Complex Viscosity (Pa. s)

Chapter 1

Introduction & Literature Review

1.1 Introduction

The increasing demand for eco-friendly materials, increasing depletion rate, and soaring prices of petroleum-based plastics and pressing environmental regulations have all triggered a growing interest towards the field of composites [1,2]. Composites materials are formed by combining two or more materials to improve properties of their original components. When one or more of the materials used are derived from biological origins, they are then defined as bio-composites [3]. In general, polymer composites consist of a polymer resin as the matrix and one or more fillers are added to serve specific objectives or requirements. For example, composites for aerospace and sports applications require high mechanical and thermal properties. Traditionally synthetic fibers such as carbon or glass fibers have been used to reinforce composites and are able to produce such properties. However, with the growing global environmental concerns, their slow biodegradability is a disadvantage. Therefore, researchers are finding other viable approaches to enhance or accelerate the biodegradability of polymeric composites. For this reason, natural fibers provide good prospective as reinforcements fillers in thermosets, thermoplastics, and elastomers. Some main advantages of using natural fibers in composites are low cost, sustainability, light weight, and being nonabrasive and non-hazardous and more importantly they can accelerate biodegradability of the polymeric composites [4,5]

Rice (Oryza sativa L.) is a primary source of food for billions of people and one of the major crops in the world. It covers around 1% of the earth's surface [1]. Statistics show that, during

the period of 2010–2013, the average annual global production of rice was 725 million metric tons with Asia region alone producing over 90% of the total global rice production [6]. Rice straw (RS) is an inexpensive byproduct of rice processing and is separated from rice grain during the rice milling process. It is reported that, for every ton of rice produced, about 0.23 tons of RS is formed [7]. Rice milling is one of the most important industries in countries such as China, India, Indonesia, Malaysia, and Bangladesh [8]. RS is a cellulose-based fibrous material with a wide range of aspect ratios [8]. Due to its high availability, low bulk density (90–150 $kg\,m^{-3}$), toughness, abrasiveness in nature, resistance to weathering, and unique composition, a variety of applications have been proposed in the literature. RS has the potential to be utilized as an insulating material, in the production of organic chemicals [9], panel boards and activated carbon [10], and supplementary cementing material [4]. Potential of RS as source of power generation and its financial viabilities have also been studied and have produced encouraging results [11, 12]. Even though it is converted into the above-mentioned end products, however, like many other agricultural by products, the industrial applications of this biomass are still limited with little economic value. Therefore, it is very important to find pathways to fully utilize the RS and an intense research scrutiny is currently undertaken worldwide to identify potential applications and to develop economically feasible processes for these applications on a commercial scale.

Societies, especially among the rice millers, often dispose of the RS waste using open burning. This situation directly leads to environmental concerns and becomes a great environmental threat causing damage to the land and the surrounding area in which it was dumped. Different methods for straw disposal, including finding a commercial use for the waste have been suggested; however, it has proven to be a difficult fuel for gasification and fluidized bed combustion. This is a result of the high ash content resulting in carbon conversion inefficiency. Previous reports on the commercial use of RS have focused more on surface modification to

improve filler–matrix interaction in composite applications. Another way to use RS involves the exploitation of its cellulose content. RS consists of 30-45% cellulose, 20-25% hemicellulose, 15-20% lignin and minor organic compounds [13]. Therefore, this thesis highlights that using RS as the primary source for producing nanocrystals is promising. In addition, the extraction of nano-silica (NS), a common inorganic filler from RS, has yet to be widely researched but could be considered of interest to researchers for the fabrication of different thermoplastic polymer-based bio-composites which primarily applied in the packaging industry.

1.2 Bioplastics/Bio based biodegradable plastics

Currently, the total production of plastics in the world has been significantly marked up by the use of bioplastics. The major disposing problem owing to the use of petroleum-based plastics is that they are not biodegradable as they are produced by chemical extraction.

The bio-based plastics are differentiated accordingly:

- Biopolymers are kinds of polymers that are occurred in nature using biological actions like starch, cellulose, natural rubbers, proteins and poly (hydroxyalkanoates).
- Bio-based polymers are polymers that are based on the polymerization of monomers that are biomass derived like Poly (lactic acid).

Thereby plastics can be termed as bioplastics if they are either biobased, biodegradable, or consist of bot properties having a biological source whether completely or significantly. They can be biodegradable or non-biodegradable depending on different standards where biodegradability, disintegrate and compostability conditions need to be followed. Consequently, bioplastics can also be recycled or reutilised to avoid plastic pollution [14]. Bio compostable plastics/ polymers are degraded by biological means during composting conditions to yield CO_2, H_2O, inorganic compounds, and biomass at a consistent rate without

leaving distinguishable or hazardous residues [15, 16]. The classification of bioplastics is shown in **Figure 1.1.**

(a)

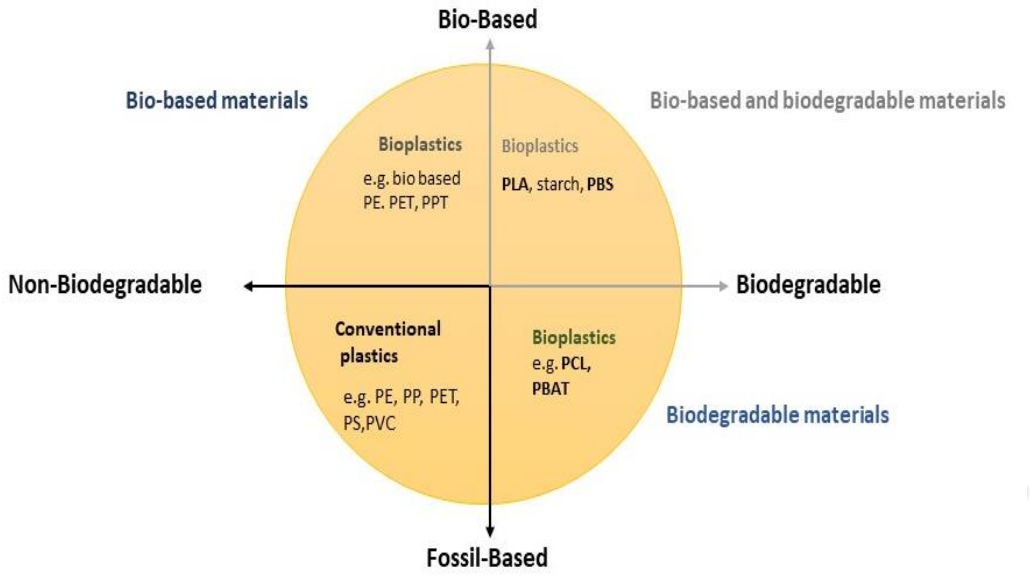

(b)

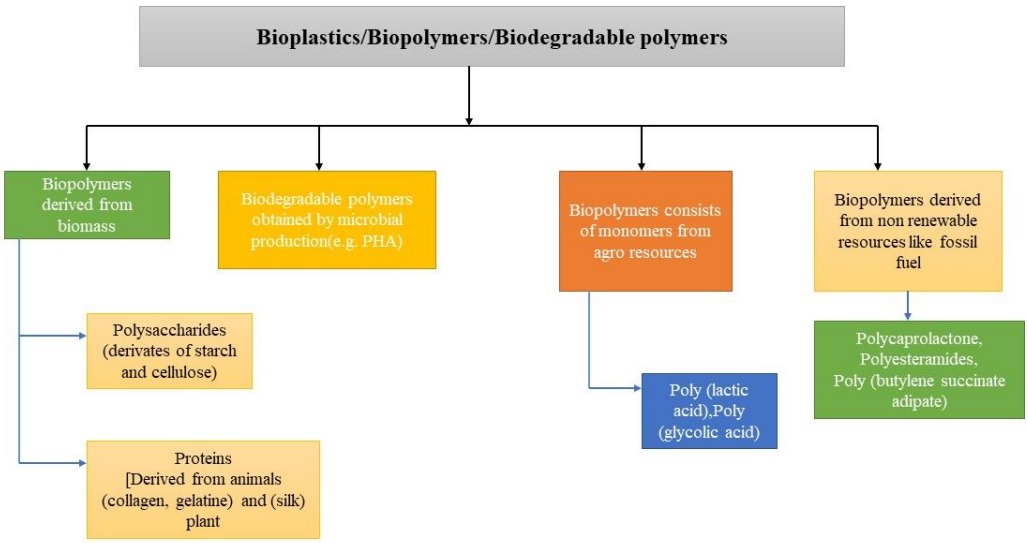

Fig 1.1: (a) differentiation between bioplastics and petroleum-based bio-plastics. **(b)** Flowchart of different kinds of bioplastics.

1.2.1 *Global production of Bioplastics*

Environment-friendly products demand is increasing in the market as shown in Figure 1.2. The global bioplastics market was estimated as 3,123.24 kilo tons by 2021 and expected to grow to a CAGR of 26.03%, during the period (2021-2023). The presence of a large amount of feedstock causes the highest production of bioplastics in Asia-Pacific. The global production capacity of bioplastics recorded by the European Bioplastics Association is 2.11 million tons in 2020, due to the growing demands from countries, like China, India, South Korea, and Japan. Concerning the pros and cons that though bioplastics are the remedies for solving global problems but biodegradability is also an important agenda that is to be followed. Out of the various bioplastics Poly (lactic acid) is more advantageous because of its natural feedstock and biodegradable and compostable nature. The global market value of poly (lactic acid) (PLA) was USD 698.27 million, by revenue, in 2021, and estimated to reach USD, 2,091.29 million by 2023, at an estimated CAGR of 20.06% [17, 18].

(a)

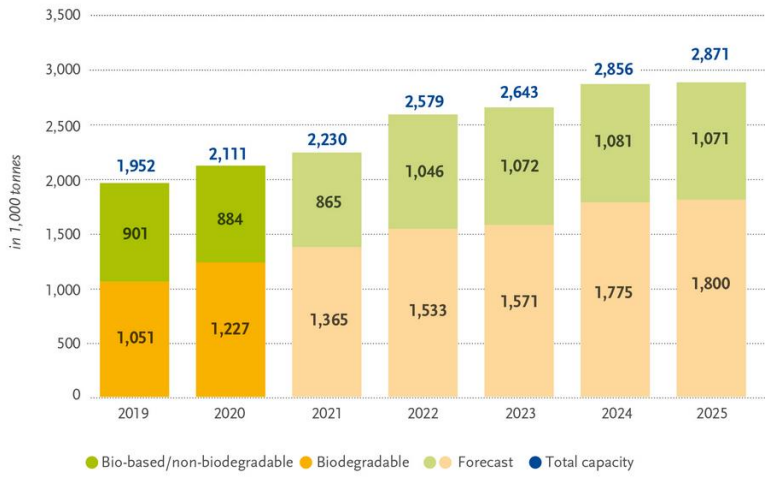

Fig 1.2 (a) Global production capacities of bioplastic

Source: *European bioplastics, nova institute (2020)*

(b)

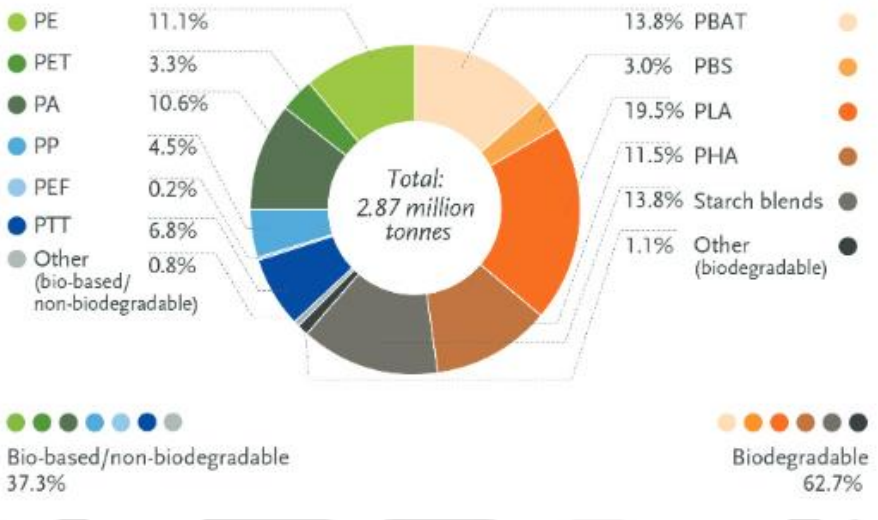

Fig 1.2 (b) Global production capacities of bioplastic 2025 (material type)

Source*: European bioplastics, nova institute (2020)*

1.2.2 Applications of Bioplastics

Bioplastics are found to have enormous potential in various applications.

- Present end use of bioplastics: Bioplastic have been utilised to make biodegradable and short-lived products such as extensive packaging (shopping bags, tray and films for food items and compostable bag for waste material collection), disposable catering products [19], mulch films [20], textile [21], medical sectors including bone fixation, sutures [22], drug delivery and tissue engineering [23]. Also, these are potentially used in pharmaceutical sectors to make pills and capsules along with durable products such as automotive interiors and mobile cases.

- Possible emerging end use of bioplastics: The major emerging applications of bioplastic include 3D printing, metalized biaxially oriented PLA based food packaging films [21, 24] and modified durable automotive products.

1.3 Biodegradable Polymers

Biodegradable polymers are a specific type of polymer that breaks down after its intended purpose to result in natural by products such as gases (CO_2, N_2), water, biomass and inorganic salts. These polymers are found both naturally and synthetically made, and largely consist of ether, ester and amide functional groups.

1.3.1 Properties of Biodegradable Polymers

Biodegradable polymers have strong carbon backbones that are difficult to break, such that degradation often starts from the end groups. Some important properties of biodegradable polymers are:

- Thermoplasticity
- Hydrophobicity
- Microbial resistivity
- Mechanical stability
- Biocompatibility
- Non-toxic

1.3.2 Applications

Biodegradable polymers can be applied in these following fields-

- Food packaging

- Tissue engineering
- Bio-medical applications
- Drug-delivery
- Material for sensor and conducting substances

1.3.3 Examples of Bio-degradable polymers

Some commercially available biodegradable polymers are given in the following section.

Poly lactic acid (PLA):

PLA is highly versatile, thermoplastic aliphatic polyester derived from renewable resources [6] such as corn, potato, sugarcane and beet roots. PLA can be synthesized from lactic acid by two methods: a) Direct polycondensation, b) Ring opening polymerization. PLA has a glass transition temperature 60-65 ºC, melting temperature 173-178 ºC. PLA can withstand temperatures of 110 ºC. PLA has similar mechanical properties to PET polymer. PLA is relatively easy to breakdown, easy to hydrolyse. It is brittle at room temperature. It has poor gas barrier properties, melt viscosity for further processing and high production cost limit the application of this polymer. It is used for decomposable packaging material, much film, in food packaging and disposable tableware.

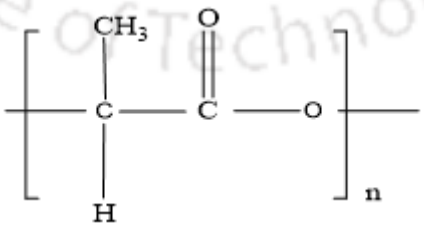

Fig. 1.3 Chemical Structure of PLA

Poly Butylene Succinate (PBS):

PBS is thermoplastic aliphatic biodegradable polyester with properties that are comparable to polypropylene. PBS has a glass transition temperature of -40^{0}C and melting point of 115^{0}C. The direct esterification of succinic acid with 1,4-butanediol is the most common way to produce PBS. The scope of PBS application fields is still growing and several areas can be identified but it remains difficult to know precisely in which specific object PBS is actually used. PBS could be processed into films, bags or boxes for both food and cosmetic packaging. Other application of PBS could be found as disposable products such as tableware or medical articles.

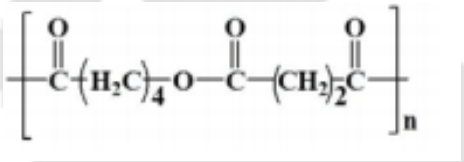

Fig. 1.4. Chemical Structure of PBS [25]

Poly (hydroxybutyrate) (PHB)

PHB is aliphatic polyester produced from the microbial fermentation. The wide range applicability of PHB is due to its complete biodegradability, biocompatibility and renewability[11]. PHB is insoluble in water and relatively resistant to hydrolytic degradation. It has good oxygen permeability and ultra-violet resistance but poor resistance to acids and bases. PHB has melting point 173-180°C and glass transition temperature of approximately 1-5^{0}C. Major drawback of PHB is its brittleness, high crystallinity, narrow processing window, higher production cost, and brittle characteristics. To overcome these problems, PHB has been subjected to polymer-polymer blending, bio-filler and nano-filler loading.

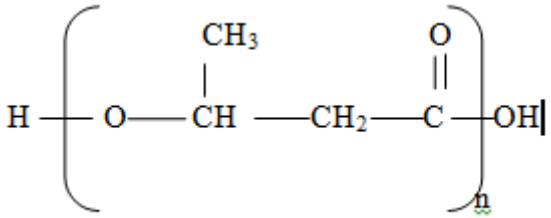

Fig. 1.5 Chemical structure of PHB

1.4 Value added products from Agro-Waste

Rice straw (RS), lignocellulosic biomass, is a very common agro-waste generated in the agriculture system after the post-harvesting of rice. Incorporating the crop and harvesting method, approximately 40–60% of residual biomass comprises RS. The complex structure limits the usability of RS. Being a quick, easy, and cheap process, most farmers opt for open field burning as the most preferred approach to dispose of RS in agricultural fields. This practice also adversely reduces the nutrient composition in the soil. The elemental carbon, nitrogen, and sulphur become completely burnt and emit hazardous gases such as methane, nitrogen oxide, and ammonia, causing austere atmospheric pollution. These gases also contribute and add up to the existing ozone pollution. Burning releases fine particles known to aggravate chronic heart and lung diseases. The scientific fraternity has recently been fascinated to produce some value-added industrially essential products from the RS described in the following section. These important materials could be an effective bio-filler for fabricating bio-composites, which can be applied in the packaging field.

1.4.1 Nano Silica (NS)

The scientific community has successfully utilized the potential of nanotechnology to develop different products and materials at the nanoscale for societal welfare. Silica is an important inorganic material with a panoramic range of applications in the textile industry, automobile

industry, biology, medicine, adsorbents, drug delivery system, etc. NS has received considerable attraction in the past few years. Many kinds of research proved that NS reinforced polymer composites have enhanced properties because of their size and high surface energy.

1.4.2 Nanocellulose

Nanocellulose, are an important class of emerging bio-nanoparticles of 21st century, because of their numerous unique properties which makes them potentially applicable in diverse fields of scientific and technological advancements. Due to their interesting structural and physicochemical properties, they have attracted researchers to develop nanocellulose-based technologies and led to an increase in demand among industries for the successful commercialization of the developed technologies. Some of the noteworthy exceptional properties of nanocellulose include tunable aspect ratio, controlled morphology, excellent structural (mechanical) properties, high specific surface area and hydroxyl functionality that can be chemically modified depending on targeted applications. In addition to, the abovementioned characteristics, these bio-nano particles possess several attractive properties such as improved biocompatibility, biodegradability, non-toxicity and bio-based origin which further enhance the research interest and widen their range of applications [26]. The abundant availability of initial cellulosic precursors in the form of renewable biomass resources makes the manufacture of nano cellulosic products particularly attractive and environment-friendly, in comparison to petroleum-based polymers which are derived from the depleting fossil-fuel reserves. To meet the increasing demand worldwide, scalable technologies for production of CNCs have been developed and its commercialization through industrial processes are actively carried out by companies in parts of Canada, USA and Finland [27]. Nanocellulose, can be tailored and functionalized into different types of materials and structures such as films, nanofibers, nanofluids, foams, hydrogels, xerogels, aerogels, emulsions or as pastes which

opens up a plethora of technological innovations and commercial opportunities [28]. Till date nanocellulose have been extensively used in high performance applications for the development of wide range of value-added products, and finds potential applications in daily life such as: (i) in the development of polymeric nanocomposites as reinforcing agents for fabrication of high strength fibers, textiles or 'smart' packaging [29] , (ii) as drug delivery vehicles[30], (iii) scaffolds for bone replacement/ tissue engineering [31], (iv) as rheological modifiers for paints, coatings, adhesives or inks [32], (v) as building blocks to strengthen the concrete used in construction [32], or in the manufacturing of paper and related products [33], (vi) in optically tunable liquid crystalline materials [34] and (vii) as paper based flexible electronics [35] forming portable batteries [36] substrate to solar cells [37] or fuel cell membranes [38]. The utilization of sustainable and renewable nanomaterials in the designing and manufacturing of myriad newer products with exciting applications will help address some of the issues and global challenges related to environmental pollution and shortage of petroleum resources. Nanocellulose consists of primarily crystalline domains of cellulose which are of three different types depending on the degree of crystallinity and morphology of such crystalline segments: (i) cellulose nanocrystals (CNCs) or cellulose nano-whiskers (CNWs) with high crystallinity generally have small crystalline fragments, are of low aspect ratio and are usually fabricated through controlled acid hydrolysis, (ii) cellulose nanofibrils (CNF) are of comparatively lower crystallinity with high aspect ratio and are generally fabricated through mechanical disintegration process using intense homogenization or ultra-sonication, and (iii) bacterial cellulose (BC) composed of thin bundles of randomly assembled microfibrils which are microbially produced through the fermentation process [39].

1.4.2.1 Cellulose nanocrystal (CNC)

CNCs usually consist of parallelly stacked crystalline segments of short cellulosic chains which induce anisotropic mechanical behaviour with the elastic modulus E‖~110–220 GPa along axial direction and E⊥~2–50 GPa along transverse directions [40]. The elastic modulus is comparable to most of the strongest materials such as carbon-nanofiber (~125- 181 GPa) and Kevlar (70-122 GPa). Moreover, the inexhaustible availability of precursor materials and easy processing methodologies makes CNCs comparatively cost- effective than other known nanomaterials. The aforementioned mechanical properties of the CNCs are known to be significantly depend on the source of biomass origin, pre-treatment method followed for the extraction of cellulose, type of acid hydrolysis methodology selected, cellulose polymorphism and functionality [29]. Due to its distinct rod-like morphology, CNCs have the capability to act as strong reinforcing agents, the degree of which depends on its aspect ratio and inter/intra-molecular hydrogen bonding. Different applications of CNC are depicted in **Figure 1.6.**

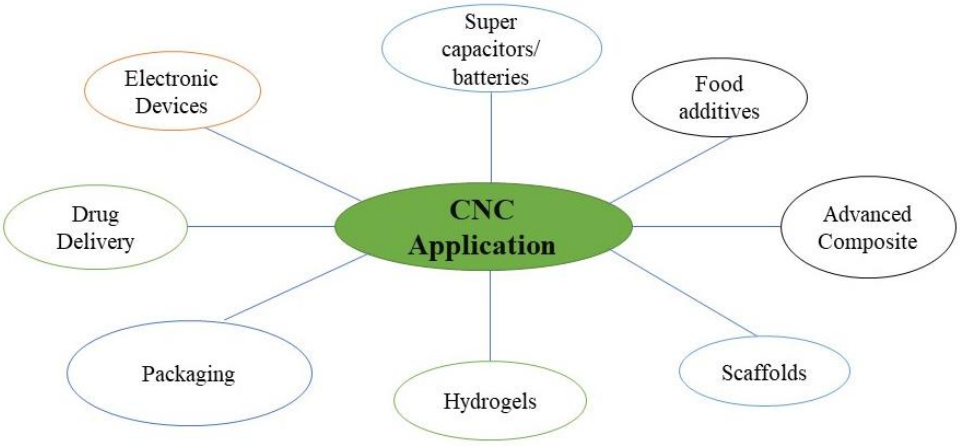

Fig 1.6 Applications of CNC

1.4.2.2 Cellulose Nanofiber (CNF)

Cellulose nanofibers (CNFs) are typically as long as several micrometers and 5 to 20 nm wide. They are not soluble in aqueous solutions but are highly dispersed to make a suspension with a given viscosity. They possess anisotropic physical characteristics. The highly crystalline cellulose nanofibers elastic modulus, which is known as the ratio of their stress to the corresponding strain, is 150 GPa and 50 GPa for longitudinal and transverse directions, respectively. Cellulose nanofibers (CNF) have been considered as potential matrix for various applications like optoelectronic conversion, energy storage, packaging, drug delivery, bioimaging and biomedical materials, nanofillers, protective coatings, barrier membranes and filtration media, transparent films, antimicrobial activity, pharmaceuticals etc [41]. CNFs are renewable, low cost and low-density material with less abrasive property [42]. The properties of CNF such as purity, biocompatibility, crystallinity, wettability and surface tuneable structure have intense effect on various environmental applications. Biocompatibility of CNF is an important property that makes them highly suitable for various biomedical applications especially in scaffold development for tissue engineering. This is also an important property for its environmental applications [43].

1.5 Nanocomposites

Nanocomposites are engineered materials, in which biodegradable polymers are used as Matrix and different reinforcing agents are added to enhance the applicability. The fillers may be 100% biodegradable or inorganic substances depending on the polymer and the application. In nanocomposites one of the components should have one dimension in the range of nanometre. Reinforcing substance may be fiber or particulate matter.

1.5.1 Need of fabrication of nanocomposites

i) Replacement of conventional commodities with cost-effective better quality light weight easy to handle composite materials.

ii) In nanocomposites, filler has high aspect ratios. It improves the interaction between matrix and reinforcing substances, thus enhances strength, modulus.

iii) Nanocomposites serves dual purposes as it possesses both the properties of matrix and filler, thus range of application enhances.

iv) In case of polymer nanocomposites, filler enhances thermal stability, conductivity, barrier property and controls degradation of biopolymers hence generates improved versatile product.

v) In case of membranes, catalysts, adsorbents, antimicrobial agent nanocomposites are highly effective.

1.5.2 Applications

Some of the important applications of the nanocomposites are given in the following section.

- **Packaging-** Permeability properties are considered as most important parameters than other properties in case of packaging applications. Nano clays incorporation enhances the barrier property most. PLA, PHB, Starch based nanocomposites are attractive packaging materials. Oxygen, water vapour barrier properties improved by 15-48% and 40-50% for PLA-clay nanocomposites compared to PLA.
- **Electronics, Sensors and Energy Application-** Flexible, degradable electronics materials are more desirable for using, so nanocomposites get extensive attention. From

Cellulose nanofibers transparent, flexible compounds which are capable to produce displays, solar cells, organic light emitting diode. PLA-Cellulose whiskers materials also highly applicable. PLA/MWCNT, PLA/Graphene composites can be used in detection of solvents, vapours, Glucose etc. Electromagnetic shielding devices, Thermo-electronic systems, photovoltaic cells can also be produced by bio-nanocomposites.

- **Medical applications-** Essential features of biomaterials is biocompatibility in case of medical application, the ability of proper functionality in the human body to come up with desired clinical outcome, without causing negative/side effects. Recognition of bio-based polymers are increasing as biocompatible materials for clinical use. For example, plastics and films made from corn proved to be non-cytotoxic and non-inflammatory to clinical use. Soy-derived polymers are useful as bone filling material. It is reported that in tissue engineering PLLA, Chitosan based Nanocomposites can be used. LDH based Nanocomposites can be used as materials for drug delivery. Nucleic acid bio polymer reinforced with LDH can be utilised for gene therapy.

1.5.3 Comparative Studies of Fabrication Techniques of Bio-nanocomposites

Bio-nanocomposites are usually prepared using three main techniques: (i) In-situ Polymerization, (ii) Solution Casting, and (iii) Melt Processing. Recently other preparation techniques such as electro spinning and processing under supercritical conditions (e.g., supercritical carbon dioxide) has gained interest.

- **i)** In situ Polymerization: During in situ polymerization, the nanoparticles are premixed with the liquid monomer or monomer solution. Then polymerization is initiated by heat, radiation or suitable initiators. In this process no solvent is required; Separation process also can be done easily. But not applicable for large scale production.

- **ii)** Solution Casting: In the solution casting process, one solvent is used to dissolve the polymer and separate the suspension/solution of filler with the same solvent prepared. Then the solution is mixed well, and the films are fabricated by solvent evaporation. Organic solvents like chloroform, DCM, THF, etc. are used as solvents depending upon solubility parameters, boiling point, and type of polymer and filler. This technique is advantageous for the lab scale investigation without much processing complexity. Good dispersion also can be achievable. But not applicable in large-scale production.
- **iii)** Melt Processing: In the melt processing technique, the nanoparticles are mixed with the polymer in the molten state. The formation of bio-nanocomposites via polymer melt intercalation depends upon the thermodynamic interaction between the polymer and the nanoparticle. For clays, this interaction will also depend upon the transport/diffusion of polymer chains from the bulk melt into the silicate interlayers. The polymer needs to be sufficiently compatible with nanoparticle surface to ensure proper dispersion. This technique is applicable for large scale production. Dispersion of filler and chance of degradation of biopolymer are the major problem in this case. Different types of Melt Processing units are- Micro compounder, Extruder, Injection moulding, blown moulding, Thermoforming etc.

1.5.4 *Problems of Fabrications of Bio-nanocomposites*

Uniform/desired dispersion of the nano fillers within the polymer matrix are the biggest problem. As most of the bio fillers are hydrophilic and polymers like PLA, PBS are hydrophobic so interaction between filler and matrix are not good. Particles also have high Van der walls force to the trends to agglomerate as a result Phase separation takes place and various defects within the polymer occurs. It reduces the activity of the polymer.

1.6 Reactive Compatibilization

Reactive compatibilization in the presence of chain extenders, compatibilizers have been postulated as one of the possible solutions to improve the limitation of bio-composites [44, 45]. Chain extender often contains various types of functionalities and reactive species offering radicals for the generation of free radical on the backbone of the main chain allowing modification either compatibilization [46] or developing more cross-linked/branched sites [44]. The active sites of chain extenders like peroxide can react with hydroxyl and carboxyl group and easily abstract the H atom from the main chain for radical formation at the back bond [47]. However, if modification involves the free radical sites generation on one component can further react to the second component during melt mixing, the phases can be linked chemically to modify the structure and tailored the properties [48]. Properties of bio-nanocomposite have controlled by nature of the chain extender, other polymer or filler composition in the polymeric matrix and processing parameters. Dicumyl peroxide (DCP) has been selected as a free radical initiator at high temperature and possess structural modification to improve compatibility or melt strength. Whereas, the use of compatibilizers is one method in which the compatibility between the matrix and the filler is improved during melt processing. A compatibilizer could enhance interfacial adhesion by reducing the interfacial tension between the two immiscible phases, improving the mechanical properties of the composites. Maleic anhydride (MA) and Luban gum have been selected as a compatibilizer in this present study.

1.7 Rheological Analysis

Rheology is a powerful tool which attaining much attention because of analysing ability of various properties related to filler-matrix interaction and it may provide information on deformation of polymer due to impact of fillers, impact of filler orientation, nature of dispersion of nanomaterial within polymer matrix and structure-property correspondence in

biodegradable composites [49]. In addition to this rheology investigation also provides information related to processability of any polymer matrix and filler combination. Different processing characteristics through rheological investigation of these composites can lead to information about fillers loading, temperature, screw speed for fabrication of final composite materials [50].

Different aspects of the matrix-reinforcement interactions of composites can be understand using rheological data. Oscillatory mode experiments including frequency sweep and strain sweep using fix plate geometry provides information on the complex viscosity, storage and loss modulus, phase angle and polymer chain relaxation. Nature of complex viscosity in varying frequency plots indicates shear thinning behaviour of the bio-composites along with the extent of adherence to power law. Nature of interaction of polymer filler i.e., miscibility and dispersion can be visualized from the Cole–Cole plots (a plot between imaginary and the real viscosity) and the Han plot (a plot between storage to the loss moduli). In addition to this, molecular weight and impact of processing on distribution can be known from the data of the cross-over point which is value the frequency where loss modulus (G″) is same as storage modulus (G′). Non-linear flow behaviour of storage modulus in low frequency domain indicates towards possible network formation within the composite in the melt state. Impact of temperature on the flow behaviour i.e., on G′, G″ and η can be determined and flow activation energy of polymer matrix and nanocomposites can be investigated. Through melt rheology investigation and analysing rheological data processability and operation condition optimization of different melt processes can be done for a particular biodegradable polymer matrix and filler [51].

Along with normal homo-polymeric composite system processing different composite system with chain modifiers like cross-linker, plasticizer and compatibilizer can be studied using rheology tool. In case of composite containing polymer blend as matrix rheological behaviour

gives variation in characteristic parameters which are proportional to the nature of the blend as well as filler-polymer interaction. Extent of crosslinking and change in chain relaxation behaviour can be examined from rheology data for different crosslinking systems (peroxide linker for reactive extrusion, chemical linker for gel) [52].

Rheology investigation for polymeric solution using rotational field gives information about nature of flow of polymeric solution i.e., shear stress (τ) with respect to shear rate (γ^o) and viscosity (η) with shear rate. These investigations are significant for cellulose, chitosan, protein and other hydrophilic polymers which are capable of gel formation. Rheology investigation generates information about flowability and gel point of this polymers which helps in optimization of polymer loading and gel preparation parameters optimization [53]. Rheological investigation of magnetorheological polymeric solutions gives indication of applicability of this polymer in the arena of ferrofluid [54].

Rheology investigation also provides information about molecular weight alteration of matrix due to incorporation of different nanofillers, chain modifiers and processing condition. Different deferent rheology parameter gives information about deformability, melt strength, nature of flow under shear, yield stress, percolation point of a composite system. Rheology information's in together reveals the effectivity of a composite and suitability of the processing path.

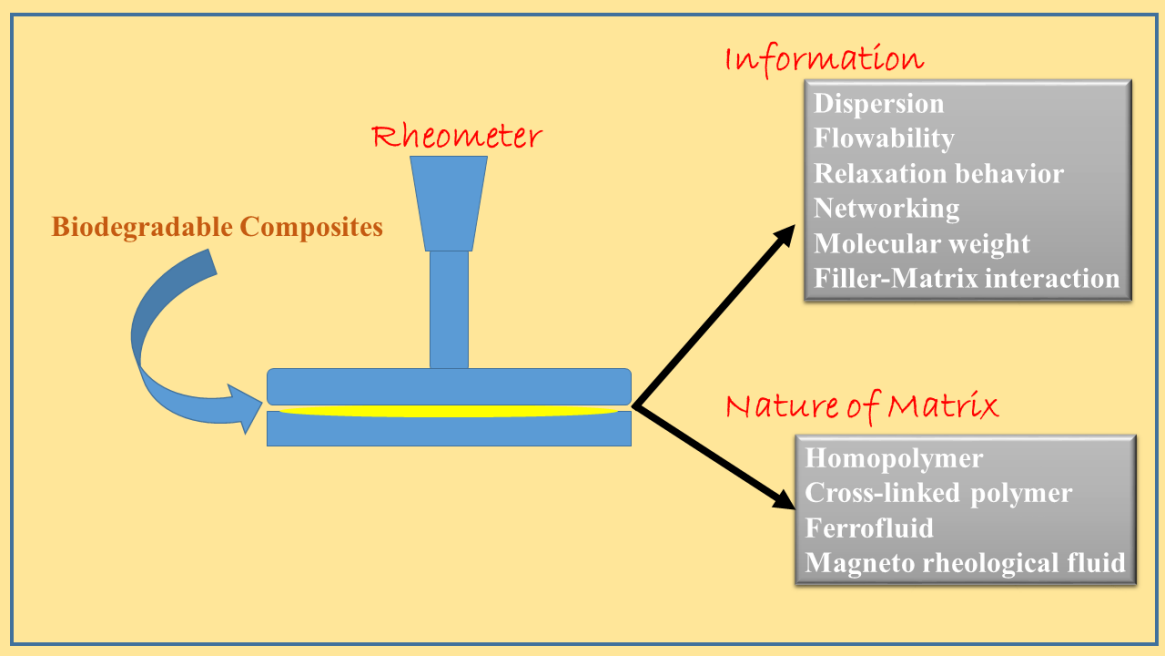

Fig. 1.7 Impact of rheology study on Biodegradable composites

1.7.1 Rheological studies of biodegradable composites

Melt rheology: Industrial applications of polymers need different melt processing operations during synthesis of composite as well as during application-oriented object casting. Biodegradable polymeric composite production efficiency also depends on proper selection of processing condition. As melt strength, dispersion of filler and deteriorations of molecular weight are the prime factors which determines process cost efficiency and composite quality.

(a)Melt flow properties of composite

Rheological properties of polymeric melts such as storage modulus (G'), loss modulus (G'') and complex viscosity (η) gives information of the flowability and flow nature of the composites. Composite loading also determined from the optimum values of the rheology parameters. Shojaeiarani et al., 2019 investigated different flow properties of melt PLA/CNC nanocomposites with different loadings of CNC. Rheology study was conducted in oscillatory mode using parallel plate geometry at 170 °C. Incorporation of CNC has increased the viscosity

of the nanocomposite for both the fabrication pathways (film casting and spin coating). G′ and G″ found to be increasing with respect to the CNC loading it indicates possible increase of melt strength and chain entanglements due to addition of CNC within PLA matrix [56]. Recycling of polymer is a major domain which can reduce the cost of production as well as will reduce the disposal problem. It is a challenge to intact the original properties of polymer even after reprocessing. Recycling ability of bio degradable polymer also can be examined by measuring rheological parameters of different recycle products. In case of silk incorporated PLA nanocomposites melt extrusion at 200 °C was carried out and recycled for 4 times. The effectivity of recycling was investigated using different characterization techniques and change in rheology properties of the composites were also inspected. Lowering of cross-over was noticed for NPLA and SNC/NPLA composites with increase of recycle number possibly due to degradation of molecular weight and variation in polydispersity. Storage modulus found to be decreased due to recycling for NPLA (710 kPa) to 3 times recycled NPLA (670 kPa). However, in case of SNC reinforced storage modulus almost similar for all the recycled composites. Thus, in this study rheology investigation implies suitability of SNC as filler for PLA products where product can be recycled [52]. Thus, for recasting of polymer composites adequate melt strength is required for maintenance of actual shape for respective application. High melt strength is also increasing the cost of operation. So, in case of melt casting proper information of rheology parameters are needed for synthesis of cost-effective composite. Similar investigation was conducted by Lee et al.,2019 for clay reinforced composites of PLA based biodegradable polymeric systems. In this study PLA based blends were used as matrix with 20% incorporation of poly(ε-caprolactone) (PCL), poly (butylene adipate-co-terephthalate) (PBAT) and poly (butylene succinate-co-adipate) (PBSA) into 80% PLA separately. Different closite clays (Closite 30B, Cloisite 20A) were used as reinforcement for melt mixing with PLA and PLA based blends. Rheology study was conducted in oscillatory

mode at the processing condition 190 °C. It was observed that in incorporation of the modified clays inside the blend systems G′ and G″ has increased. It also recorded that for 7 wt.% loading of closite 30B clay the increase is maximum from the others. Increasing trend was also noticed for complex viscosity with loading of clay [57]. Similarly, rheology investigation of PLA/PBAT blend was studied and effect of multiwall carbon nanotube (MWNT) on the structure of blend system also investigated for composites. G′ and G″ has increased with increase of MWNT loading. Complex viscosity observed to be dependent on the loading as well as nature of polymer matrix [58]. In some of the investigations of solution processed polymeric film melt rheology was investigated in order to check impact of filler towards melt strength and flowability of bio-nanocomposites [59].

(b)Dispersion of reinforcement

Impact of reinforcement of filler sometimes alters the homo-polymeric nature of matrix prepared through melt processing route. Through rheology investigation it is possible to understand the nature of dispersion of filler within polymer matrix. In some cases, where different modified techniques are utilized prior to master batch dilution technique through melt processing effectivity of the process on the dispersion and flowability of matrix polymer chain can be studied. Dispersion of graphene in PLA matrix was studied using melt processing and in this study master batch of graphene was coated over the PLA pellets prior to extrusion [51]. Miscibility and dispersion were observed to be improved in case of masterbatch coated nanocomposites from Han plot and Cole-Cole plot. Incorporation of master batch coated graphene into PLA matrix found to improve the flowability of the composites. Homo-polymeric nature was not altered due to the nanocomposite fabrication. These effects are important issues during large-scale PLA film production. Rheology properties o PLA/chitosan-graft-lactic acid oligomer (CH-g-OLLA) bio-nanocomposite films were studied in order to check the flow properties as well as nature of dispersion of chitosan in the PLA matrix [60]. It

was observed that G' and G" increased with ω when oscillatory rheology investigations were carried out for the composite melts at 180 °C. However, viscous nature of the composite melt was noticed from the higher value of G" with respect to G' possibly due to inclusion of short chain oligomers along with chitosan. Newtonian flow characteristics for PLA and PLA–CH-g-OLLA (1%) films were noticed up to angular frequency 0.3 rad/s. Shear-thinning flow behaviour was detected in the film samples.

1.8 Literature Review

A detailed literature reviews are recorded in this following section. This entire section consists of the preparation of bio-composites using different fillers, different biodegradable polymers. Different processing techniques, applications and improvements in the property of the prepared bio-composites are also summarised in the following section.

1.8.1 Biodegradable polymer/natural fibers-based bio-composites

Joseph K et al. (2000) investigated the hybridization effect on the tensile properties of jute-cotton woven fabric reinforced polyester composites as functions of the fiber content, orientation and roving texture. It was observed that the tensile properties of the bio-composites increased steadily with the fiber content (up to 50%) and the tensile strength of the jute reinforced composites is about 220% higher than pure polyester resin [61].

David Plackett et al. (2003) prepared biodegradable composites using jute fibre and L-polylactide. They have reported the tensile properties of the composites were 40% higher than those of polylactide alone which were produced at temperature in the range of 180-200^{0}C. So, in this case jute fibre acts as a reinforcing agent. However, impact resistance is decreased [62].

Mangal R et al. (2003) prepared bio-composites consisting of phenol formaldehyde reinforced with pineapple leaf fiber using the transient plane source (TPS) technique. The effective thermal conductivity and the effective thermal diffusivity of the composites decreased as compared with pure phenol formaldehyde as the fraction of fiber loading increases [63].

Wong S et al. (2004) mentioned about the improvement of the interfacial adhesion of the PHB/flax composites with the addition of TDP at various concentrations (up to 10% v/v). The thermal stability, flexural properties were also improved after the incorporation of TDP. With the increase of TDP content, improvements were observed in the fibre-matrix bonding and a change in the matrix from brittle to ductile [64].

Alvarez et al. (2004) prepared a biodegradable starch-based bio-composites using sisal fibres. The interaction effectiveness of the matrix in the fibers is directly linked to the rheological behaviour. A significant improvement of the thermal properties and the composite creep resistance were observed with the addition of sisal fibres to the polymeric matrix [65].

Pothan LA et al. (2006) prepared a banana reinforced polyester composites with special reference to the effects of fiber loading, frequency and temperature. The value of the storage modulus of the composites with the 40% fiber loading was found to be highest. The incorporation of abaca fiber in the polyester matrix induces reinforcing effects. Increased dynamic modulus value and low damping value proves that the interactions between the fiber and matrix improved [66].

Zini et al. (2007) reported that the composites of PHB and long fiber mats by compression moulding showed better mechanical properties as compare to the composites obtained by batch mixing fibres with molten polymer and the adhesion property was also improved by acetylation method [67].

Huda et al. (2007) fabricated a bio-composites of PLA/recycled newspaper fiber with the addition of silane and talc. The thermal stability of the prepared composites increased with the addition of fibers as compare to the neat PLA and the heat deflection temperature of the composites was found to be comparable to that of the glass fiber-reinforced PLA composites. The flexural and impact strength was found to be significantly higher of the silane treated talc reinforced PLA/ recycled newspaper fiber compared to the without silane treated composites. The flexural strength and flexural modulus of the silane treated composites were 132MPa and 15.3GPa respectively while the flexural strength and flexural modulus of the untreated composites were 77MPa and 6.7GPa respectively [68].

Xu H et al. (2008) manufactured thermoplastic biodegradable composites of PLA/PCL matrix reinforced with ramie fiber by the in-situ polymerization method. In this work they employed a silane coupling agent for the improvement of the interfacial adhesion of the bio-composites. The tensile strength and impact strength were highest when a silane coupling agent was employed; the ramie fiber length was 5-6mm and when the fiber content was 45% [69].

Bledzki et al. (2009) prepared a bio-composites of PLA using abaca and man-made cellulose fibre and compared with the polypropylene (PP) composites. The composites were prepared by the combined moulding technology: two step extrusion coating process followed by an injection moulding. The tensile strength and modulus were increased significantly by the factors of 1.45 and 1.75 respectively with the 30wt% of cellulose and with 30wt% of abaca fibres the elastic modulus and tensile strength were increased by the factors of 2.40 and 1.20 respectively [70].

Marsyahyo E et al. (2009) developed bulletproof panels by hand lay-up process using ramie fiber as a reinforcing agent and epoxy as a matrix. These prototype bulletproof panels were much lighter and economically cost effective than the conventional bulletproof panels [71].

J.D.D. Melo et al. (2012) fabricated a biodegradable composite using carnauba fibres and poly (hydroxybutyrate) (PHB) as a matrix. In this study, carnauba fibres were modified by alkali, peroxide, potassium permanganate and acetylation treatment and used for the development of a biodegradable composite. They have reported that the hydrogen peroxide treatment has given the better mechanical properties of the PHB based composite than any other treatment considered and also improved the wettability. Strength and elastic modulus of composites made from peroxide treated carnauba fibers randomly dispersed was superior to those using untreated fibers or any other fiber treatment and similar to neat PHB. Storage modulus measured by dynamic mechanical analysis was lower than that of the neat PHB at temperatures below the glass transition, but higher above the T_g. Carnauba fiber reinforced PHB biodegradable composite may prove as an alternative to plain PHB with cost reduction and similar mechanical properties. The addition of these fibers to PHB may provide a smaller reduction in modulus at higher temperatures, where the matrix modulus is lower. However, the lower strength of the composites when compared to the plain PHB indicates that fiber–matrix interface adhesion still needs improvement, which should be the subject of future work [72].

Mechanical properties of jute fibre reinforced thermoplastic and biodegradable polymer composites are given in **Table 1.1**.

Table 1.1 Mechanical properties of jute fibre reinforced thermoplastic composites

Reinforcement	Matrix	Tensile Strength (MPa)	Tensile Modulus (GPa)	Flexural Strength (MPa)	Flexural Modulus (GPa)	Impact Strength	Ref.
Non-woven jute fabric	Poly (L-lactic acid) (PLLA)	55	0.867	67	2.83	12.98kJ /m^2	**Khan et al. (2013)**
Jute strand	Starch	22.2	2.47	36.4	-	10.5kJ/ m^2	**Vilaseca et al. (2007)**
Non-woven jute	Soy	37.1	1.040	38.4	1.120	-	**Behera et al. (2012)**
Jute	Biopol	81.42	1.92	-	-	-	**Hossain et al. (2011)**
Jute	Unsaturated polyester resin	-	-	34	1.8	-	**Mistri et al. (2001)**
Jute	Soy protein	64	6.1	24.1	4.074	-	**Reddy et al. (2001)**

1.8.2 Biodegradable Polymer/ CNC based Nanocomposites

Hao-Yang Mi et al. (2014) developed Poly **(**ε-caprolactone) (PCL)/CNC based foamed nanocomposites by twin screw extrusion. Both solid and foamed samples with higher levels of CNC content showed higher tensile moduli, complex viscosities, and storage moduli due to the reinforcement effects of CNCs. The addition of CNCs caused a reduction of the decomposition temperature and an increase in the glass transition temperature, crystallization temperature, and crystallinity of PCL. Moreover, the biocompatibility of the foamed nanocomposites with low CNC content was verified by 3T3 fibroblast cell culture [73].

Andrea Arias et al. (2014) prepared PLA-based CNC nanocomposites via a novel two-step process for improving the nano-level dispersion of CNC. The first step consisted in the encapsulation of the nanocrystals using polyethylene oxide (PEO) as a polymer carrier via a solution-mixed procedure, followed by freeze-drying. In a second step, the binary blend formed by PEO and CNC was melt- mixed in the PLA matrix. High and low molecular weights (MW) PEO were chosen and four PEO/CNC ratios were evaluated (two for each MW). Morphology of nanocomposite microtome surfaces showed that the number of agglomerates was reduced as the H-PEO/CNC ratio raised from 0.25 to 1.0, suggesting that part of the CNC had been dispersed as primary particles difficult to observe in SEM, due to the presence of PEO. When using the L-PEO and higher ratios (i.e., 1.25 and 12.5) the agglomerates completely disappeared, indicating a much finer dispersion of CNC. Mechanical properties under uniaxial tension showed that the brittle behaviour of PLA could be transformed to ductile as the L-PEO content increased. L-PEO exhibited very good performance as a carrier and dispersing agent for CNC, leading to the formation of well-dispersed PLA/PEO/CNC nanocomposites. Synergistic effects between plasticization and reinforcement at higher contents of CNC might

represent an interesting way to improve further the properties of these largely bio-based materials [74].

Prodyut et al. (2016) fabricated a thermally stable polylactic acid (PLA) grafted cellulose nanocrystal (PLA-g-CNC) nanocomposite films by reactive extrusion process using dicumyl peroxide as a cross networking agent. They had also recycled the PLA-g-CNC nanocomposites without breaking the molecular structure of PLA significantly. After the incorporation of CNC into the PLA matrix, the thermal stability and the mechanical properties were improved significantly due to the formation of C-C bonds with the CNCs. The Tensile strength and young's modulus were improved by 41% and 490% respectively whereas the value of filler effectiveness coefficient (C_{FE}) has decreased. It suggests that the grafted CNC acts as an efficient reinforcing agent [75].

Nooshin Noshirvani et al. (2017) prepared biodegradable nanocomposites from plasticized starch-polyvinyl alcohol (PS-PVA) composite using CNC by solution casting method. It is observed that after incorporation of CNC into the PS-PVA matrix, the ultimate tensile strength (UTS), glass transition temperature (T_g), melting point (T_m) are increased. However, the solubility, water absorption, water vapour permeability (WVP) and strain at break (SB) decreased. The results suggest that as a green reinforcement for elaboration of biodegradable packaging, CNC is a good replacement for mineral reinforcement such as silicates [76].

Shasanka Sekhar Borkotoky et al. (2017) fabricated bio-nanocomposite foam consisting of bio-based PLA and CNC. The porosity of the bio-nanocomposite foam is found to be 80%. The storage modulus of the foam for the compressive and tensile mode increased to 1.7 and 2.2 respectively. Almost 13% increment is observed in crystallinity at the highest loading of CNCs as compared to neat PLA. Detailed decomposition behaviour is studied by using hyphenated thermogravimetric analysis – Fourier transform infrared spectroscopy (TGA-FTIR) system.

Approximately ~10 folds reduction in the density of PLA and the nanocomposite foams compared to PLA carries much significance in specialized application areas where weight is an important concern [77].

Prodyut et al. (2017) fabricated PLA/CNC based nanocomposite films by reactive extrusion for food packaging applications which improved processability, melt strength and rheological behaviour and reduced the necking property. The molecular architecture, such as gel fraction yields, grafting efficiencies, and Mw characteristics, are significantly altered from ~16%−68%, 14%−67%, and ~158−207 KDa, respectively, with varying compatibilizers used during reactive extrusion. Oxygen properties and water vapour properties are reduced significantly from (20%-65%) and (27%-50%) respectively. Improved thermomechanical properties are observed of the reactively processed films. This film is potentially applicable for the storage of oil and dairy based products, which show shelf lives of ~5 months and ~2 weeks, respectively, and are within the standard migration limits, as per the set legislations. Hence, this work provides a novel, easily processable extrusion-based approach for manufacturing sustainable PLA/ CNC-based green and eco-friendly films with improved recyclability, biodegradability, and nontoxicity for potential applications as food packages on a commercial scale [78].

Kaili Song et al. (2017) developed a keratin-based biopolymer film reinforced by surface modified CNCs which is naturally derived and environmentally friendly. Surface functionalization of CNCs resulted in the introduction of aldehyde groups on its backbone which endowed it with dual-functional effects as both reinforcing and cross-linking agents. The bio-composites exhibited significantly improved mechanical properties and excellent water stability. It was found that the formation of percolating nanofiller network in keratin matrix and improved interfacial adhesions were responsible for the imperative reinforcing effect of the bio-composites. This reinforcing as well as cross-linking strategy by functionalized CNC could

enrich the exploration of high-performance composites and extend exploration of the applications of keratin materials in the fields of tissue engineering or drug delivery [79].

Shaoying Cui et al. (2018) prepared poly (propylene carbonate) based biodegradable composite using graphite nanoplates-spherical nanocrystalline cellulose (GNP-SNCC). In this work, cellulose and graphite were co-milled by ball milling and spherical nanocrystalline cellulose (SNCC) was expected to be in-situ prepared and partially adhere to the surface of graphene layers by physical and chemical bonds to obtain the graphite nano- plates-spherical nanocrystalline cellulose (GNP-SNCC) nanohybrids. The mechanical properties, electrical conductivity is improved significantly. The value of the yield strength increased to 52.8MPa. Glass transition temperature (T_g) increased drastically to 51.3^{0}C which is quite higher as compare to the neat PPC of 34.0^{0}C. The percolation threshold decreased drastically from 15 to 5wt% [80].

Shasanka Sekhar Borkotoky et al. (2018) investigated the thermal degradation and non-isothermal crystallization behaviour of PLA foam and PLA/CNC based foams at three different loadings of CNC (i.e., 1%, 2%, 3%) and named as PLA/CNC1, PLA/CNC2, PLA/CNC3. Effect of porosity and CNC reinforcement towards thermal degradation and crystallization of the PLA is thoroughly investigated by using mercury intrusion porosimetry (MIP). "Model-free" and "modelistic" approaches like Friedman, Flynn-Wall-Ozawa (FWO), Kissinger-Akahira-Sinouse (KAS), Kissinger and Augis & Bennet have been utilized for non-isothermal degradation kinetics of the fabricated foams. The apparent activation energy calculated from FWO is ~175.8 kJ/mol, ~198.6 kJ/mol, ~175.5 kJ/mol and ~174.7 kJ/mol for nPLA, PLA/CNC 1, PLA/CNC 2 and PLA/CNC 3 respectively. It is also observed that at higher conversions, complex three-dimensional diffusion mechanism of degradation might be taking place in accordance with Criado plots [77].

1.9 Objectives

In the above context, the present thesis explores the valorisation of agricultural waste in the form of RS and to produce different value-added products and their different application in different fields. The objectives of the present work are as follows,

- Utilisation of Agro-waste (Rice Straw) for the fabrication of PBS based bio-composites by melt compounding method.
- Synthesis of nano silica from waste RS and fabrication of PLA-nano-silica based bio nanocomposites and evaluation of their properties.
- Extraction of the CNC from RS and fabrication and characterisation of PLA-CNC based bio nanocomposites by melt extrusion process.

1.10 Proposed thesis orientation

The content of the thesis has been divided into six different chapters

Chapter I: Introduction and literature review

Chapter II: Materials and methods

Chapter III: Utilisation of agro waste (Rice Straw (RS)) for the fabrication of PBS based bio-composites by melt compounding method.

Chapter IV: Extraction of nano silica from waste RS and fabrication of PLA-nano silica based bio nanocomposites and evaluation of their properties.

Chapter V: Synthesis of the CNC from RS and fabrication and characterisation of PLA-CNC based bio nanocomposites by melt extrusion process.

Chapter VI: Overall conclusions and future scope.

Chapter 2

Materials & Methods

This chapter discusses the details of materials, chemical reagents and experimental procedures for undergoing the current thesis work.

2.1 Materials

PBS (Grade 1001MD) having M_n (number average molecular weight) ~ 88,000 Daand PDI (polydispersity index) ~2.2 was supplied by Showa High Polymer Singapore Pte. Ltd. (Japan). PLA granules of grade 4032 D (Mn~150,000 Da; PDI~1.3) were supplied from Nature works (USA). Rice straw (RS) was collected from the local paddy fields (Amingaon, North Guwahati, India). Maleic anhydride (MA) and dicumyl peroxide (DCP, purity >99.5%) was purchased from Sigma Aldrich (India). Sodium hydroxide (NaOH), sodium hypochlorite (NaOCl), hydrogen peroxide (H_2O_2), and sulphuric acid (H_2SO_4) are used for the pre-treatment and extraction of CNCs. For the fabrication magnetic CNCs, chemical required such as ammonium hydroxide (NH_4OH) (>99% purity), ferric (III) chloride ($FeCl_3$) (96%), ferrous (II) chloride ($FeCl_2$) (98%) were purchased from SISCO research laboratories (SRL chemicals, India). Ultrapure water synthesized from Milli- Q synthesis unit, Millipore® (TOC<10ppb; particles<0.22µ/ml; resistivity: ~18.2MΩ.cm at 25°C) was used as solvent for all the experiments reported in the thesis. All the chemicals are utilised for the required analyses the way it is received without any additional refinement.

2.2 Methods

2.2.1 Extraction of silica nano particles from waste rice straw

Nano silica (NSs) were synthesized by the following way:

A 10-gm sample of SRL, SOL, and OSL was heated at 700 ◦C for 3 h in a muffle furnace. The resulting grey powdered ash (~1 gm) was treated with 6.0 N HCl at 70°C for 12 h with continuous stirring to dealuminate the ash and remove iron in the ash. The resulting suspension was filtered, and the solid residue was washed with distilled water five to six times to remove acid and metal ions present in the mixture. The resulting solid was then treated with 2.5 N NaOH to remove metal impurities in silica suspension and stirred at 70 ◦C for 12 h to produce sodium silicate.

Further, the mixture was acidified to pH 2.5 by dropwise addition of concentrated H_2SO_4. The resulting white slurry was filtered, and the solid residue containing silica precursor was again repeatedly washed with distilled water and dried at 60 ºC for 6 h. The dried mass (~500 mg) was subjected to pyrolysis in a muffle furnace for 2 h at 450 ◦C. The principal chemical reaction can be represented as follows:

Rice straw ash + HCl → Leached ash (SiO_2)

$2NaOH + SiO_2 \rightarrow Na_2SiO_3 + H_2O$

$Na_2SiO_3 + H_2SO_4 \rightarrow SiO_2 + Na_2SO_4 + H_2O$

The synthesized SNPs, which appeared as a fine white powder (~200 mg, Yield: 64 % based on silicic acid precursor), were stored in an airtight glass vial for further characterization.

2.2.2 Extraction of cellulose nanocrystals (CNCs) from rice straw (RS)

2.2.2.1 Pre-treatment

The pre-treatment method, which consists of the alkali and bleaching process, was performed to remove the hemicellulose and lignin content from rice straw (RS).

i) Alkali treatment

After washing several times with distilled water to remove the dirt particles and drying in a vacuum oven at 60°C for 24h, RS was ground with a high-speed universal disintegrator (FW100) to produce rice straw flour (RSF) and stored at room temperature. The dried RSF was treated with 6 wt.% NaOH solution at 80°C for 2 h under reflux conditions. The solid pulp was filtered with excess distilled water several times. The alkali treatment was repeated thrice.

ii) Bleaching process

After the alkali treatment, the bleaching process was carried out using 2wt.% NaOCl and 2wt.% H_2O_2 at 90°C for 2h under reflux condition. The reaction mixture was again filtered several times using excess distilled water, and this process was also repeated three times. Finally, the pulp was kept in a hot air oven at 60°C to obtain the dried cellulose.

2.2.2.2. Acid hydrolysis

After the alkali and bleaching process, the acid hydrolysis treatment of the cellulose pulp (2.0 g) was conducted with sulphuric (H_2SO_4) acid (64wt.%, 100ml) under vigorous magnetic stirring (~700 rpm) at 100°C for 4 h. Chilled deionized water was added to the reaction mixture to stop the hydrolysis reaction, followed by centrifugation (~10,000 rpm, 15 min) to remove the excess acid. The CNC suspension was transferred to the cellulose acetate dialysis membrane (molecular weight cut off =~14KDa, Sigma Aldrich) against filtered water for several days until a neutral pH of~ 7 was reached. Subsequently, the final neutral suspension of CNC was centrifuged to separate the substantial parts, followed by lyophilization of the precipitated mass to obtain the freeze-dried CNC powder.

2.2.3 Melt extrusion of PBS-RSF bio-composites

Both PBS granules and RSF was vacuum dried overnight at 80℃ to remove any adsorbed moisture. DCP (2 wt.%) was dissolved in acetone and mixed with the PBS granules and different weight percentages of RSF, particularly towards the higher loading (5, 10 wt.%). Beyond that ($> 10\ wt\%$) , some serious operational problems were found because of the agglomeration or clogging of RSF. For the proper dispersion of DCP on the surface of PBS and RSF, excess acetone was removed by vacuum drying. Melt extrusion was done using a HAAKE Minilab co-rotating twin screw extruder. The process parameters were as follows:

i. Processing temperature- 140℃

ii. Screw speed- 100 rpm

iii. Residence time- 2min

The different PBS-RSF bio-composites were designated as NPBS (Neat PBS), PBS-RS1(PBS + 5wt% RSF), PBS-RS2(PBS + 10wt% RSF), PBS-RS1-DCP (PBS + 5wt% RSF+ 2wt% DCP), PBS-RS2-DCP (PBS + 10wt% RSF+ 2wt% DCP).

2.2.4 Fabrication of PLA/CNC based bio-nanocomposites via melt extrusion

Both PLA granules and freeze-dried CNC powder was vacuum dried at 40°C overnight before melt compounding. MA(3wt.%), used in this study as a compatibilizer was dissolved in acetone (10ml) and sprayed on the PLA. Excess acetone was removed by the vacuum drying of PLA before processing. The MA coated PLA was mixed manually in a beaker with the different weight percentages of CNC (1→3 wt.%). PLA-CNC based bio-composites with or without MA were melt mixed using a HAAKE Minilab (Thermofisher Scientific) co-rotating twin-screw extruder where the process parameters are given below:

i) Processing Temperature- 180°C

ii) Screw Speed- 50 rpm

iii) Residence time- 300s

Hereafter, the detailed composition of PLA-CNC based bio-composites in the presence of MA with different loadings of CNC are summarised in Table 2.1.

Table 2.1 Composition of the bio-composites

Sample designation	PLA (wt.%)	CNC (wt.%)	MA (wt.%)
Neat PLA (NPLA)	100	-	-
PLA-CNC1(PC1)	99	1	-
PLA-CNC2(PC2)	98	2	-
PLA-CNC3(PC3)	97	3	-
PLAgMA(PM)	96.7	-	3
PLAgMACNC1(PCM1)	95.7	1	3
PLAgMACNC2(PCM2)	94.7	2	3
PLAgMACNC3(PCM3)	93.7	3	3

2.2.5 Fabrication of PLA/NS based nanocomposites via melt extrusion

Both PLA granules and freeze-dried NS powder was vacuum dried at 40°C overnight before melt compounding. Luban gum (G)(1wt.%), used in this study as a compatibilizer. The PLA, NS, and G was mixed manually in a beaker with the different weight percentages of NS (2→6wt.%). PLA-NS based bio-composites with or without G were melt mixed using a HAAKE Minilab (Thermofisher Scientific) co-rotating twin-screw extruder where the process parameters are given below:

i) Processing Temperature- 170°C

ii) Screw Speed- 50 rpm

iii) Residence time- 300s

Hereafter, the detailed composition of PLA-NS based bio-composites in the presence of G with different loadings of NS are summarised in Table 2.2.

Table 2.2 Composition of the bio-composites

Sample designation	**PLA (wt.%)**	**NS (wt.%)**	**G (wt.%)**
Neat PLA (NPLA) (B1)	100	-	-
PLA-NS (2%) (B2)	98	2	-
PLA-NS (4%) (B3)	96	4	-
PLA-NS (6%) (B4)	94	6	-
PLA-NS (2%)- G (1%) (B5)	97	2	1
PLA-NS (4%)- G (1%) (B6)	95	4	1
PLA-NS (6%)- G (1%) (B6)	93	6	1

2.3 Analytical Instrumentation and Characterisation

2.3.1 Gel Content (%)

The extruded strips of PBS-RSF bio-composites in presence of DCP were washed using HPLC grade chloroform for ~24 h to remove the unreacted DCP. Subsequently, the suspension was vacuum filtered and the gel was washed with excess chloroform for several times. Finally, the gel was vacuum dried at ~50℃ to remove the trapped chloroform. The gel fraction was calculated using the following equation (1).

$$\text{Gel content (\%)} = \frac{W_{gel}}{W_i} \times 100$$

Where W_i is the initial weight of the extruded strips and W_{gel} final weight of the dried gel after vacuum drying.

2.3.2 X-ray diffraction

XRD studies were carried out using D8 Advance diffractometer (Bruker, Germany) equipped with Cu-Kα radiation (λ= 0.1541 nm) as X-ray source operating (40 kV, 40 mA) at a scan rate of 0.05° per 0.5 s in the 2θ range 10–80°. The crystallinity index (C.I.) and degree of crystallinity were determined using the Reflex module in the Materials Studio software. The program deconvoluted the XRD data to remove the background noise and calculated the degree of crystallinity from the difference in area of crystalline peak to amorphous fractions.

2.3.3 Fourier Transform Infrared Spectroscopy (FTIR)

FTIR spectroscopic studies for powdered samples, FTIR spectra were recorded using diffuse reflection spectroscopy (DRS) mode using dried KBr pellets as the background. It was carried out using PerkinElmer spectrometer scanned in the range of 4000-500 cm^{-1} with a resolution of 4 cm^{-1} for 128 scans.

2.3.4 Morphological Property Analysis

The surface morphological properties of the bio-composites were determined using field emission scanning electron microscopy (FESEM) (ZEISS, USA). The samples were gold sputtered for 180s before being subjected to FESEM analysis at an accelerated voltage of 2-3 kV.

2.3.5 Thermogravimetric Analysis (TGA)

The thermal degradation behaviour of the bio-composites was studied by thermo-gravimetric analysis (TGA) using a PerkinElmer TGA 4000 instrument (USA). The samples (7-8mg) were heated at the rate of 10°C/min from 30 to 600°C in an inert nitrogen gas atmosphere.

2.3.6 Differential Scanning Calorimetry (DSC)

The thermal properties of the bio-composites were analysed using a differential scanning calorimeter (DSC) (Netzsch, Germany). All the samples of weight 5-6 mg were heated from 30°C to 150°C at a heating rate of 10°C/min. An isothermal condition was maintained at 150°C for 3min in order to remove the thermal history after the first heating cycle. The samples were cooled down to -60°C with the same scan rate, followed by a second heating cycle to 150°C with the same scan rate as that in the first heating cycle. The glass transition temperature (T_g), melting temperature (T_m), crystallization temperature (T_c), degree crystallinity (% X_c) were estimated from the thermal profile of the second heating cycle. The degree of crystallinity was calculated using the following equation

$$X_c = \frac{\Delta H_m^a}{\Delta H_m^o}$$

Where ΔH_m^o is the melting enthalpy of pure PBS which was taken as 110 J/g and ΔH_m^a is the melting enthalpy corresponding to the second heating cycle.

2.3.7 Mechanical Property Analysis

The mechanical properties of the extruded strips of the bio-composites were determined using the universal testing machine (UTM) (Kalpak Instruments), equipped with a load cell of 500 N at a constant speed of 10 mm/min, following the ASTMD 882 standard protocol.

2.3.8 Rheological Property Analysis

The rheological measurements of the bio-composites were carried out using a controlled stress rheometer (Anton Parr) having parallel plate arrangements (25 mm in diameter) in the melt state. The temperature range was chosen as such so that the operation could be done above the melting temperature of the bio-polymer. Residual thermal histories of the test samples were eliminated by heating for 5 min. The dynamic frequency sweep test was performed with a strain level in the linear viscoelastic region (LVE), was determined experimentally by the amplitude sweep test.

Chapter 3

Utilisation of Agro-waste (Rice Straw (RS)) for the fabrication of Poly (butylene succinate) (PBS) based bio-composites by melt compounding method

Abstract

The present study involves valorisation of rice straw (RS) in the form of flour (RSF) for the fabrication of poly (butylene succinate) (PBS) based bio-composites through a melt extrusion method, using dicumyl peroxide (DCP) as the cross-networking agent, and study of the morphological, thermal, mechanical and rheological behaviours of the bio-composites. A layered like morphology with homogeneous dispersion of RSF in the PBS matrix was observed from X-ray diffraction and field emission scanning electron microscopic analysis. Thermo gravimetric analysis showed that the incorporation of RSF improved the thermal stability of PBS whereas, the value of the different thermal properties i.e., glass transition temperature (T_g), melting temperature (T_m) are almost identical. Addition of DCP (2 wt.%) into the PBS-RSF systems increased both the value of tensile strength and elongation at break (EB) (%) specifically for the 5 wt.% loading of RSF. Rheological investigation of the bio-composites showed storage modulus (G') <loss modulus (G") over the angular frequency (ω) range until crossover, corroborating the viscous behaviour of the samples. The complex viscosity, η' was constant when ω<1 rad/s for all the samples, showing Newtonian characteristics. Shear thinning behaviour was observed when ω>1 rad/s. Furthermore, no phase separation was observed from the Han plot and good compatibility was noticed from the Cole-Cole plot which signified good rheological properties of the bio-composites.

GRAPHICAL ABSTRACT:

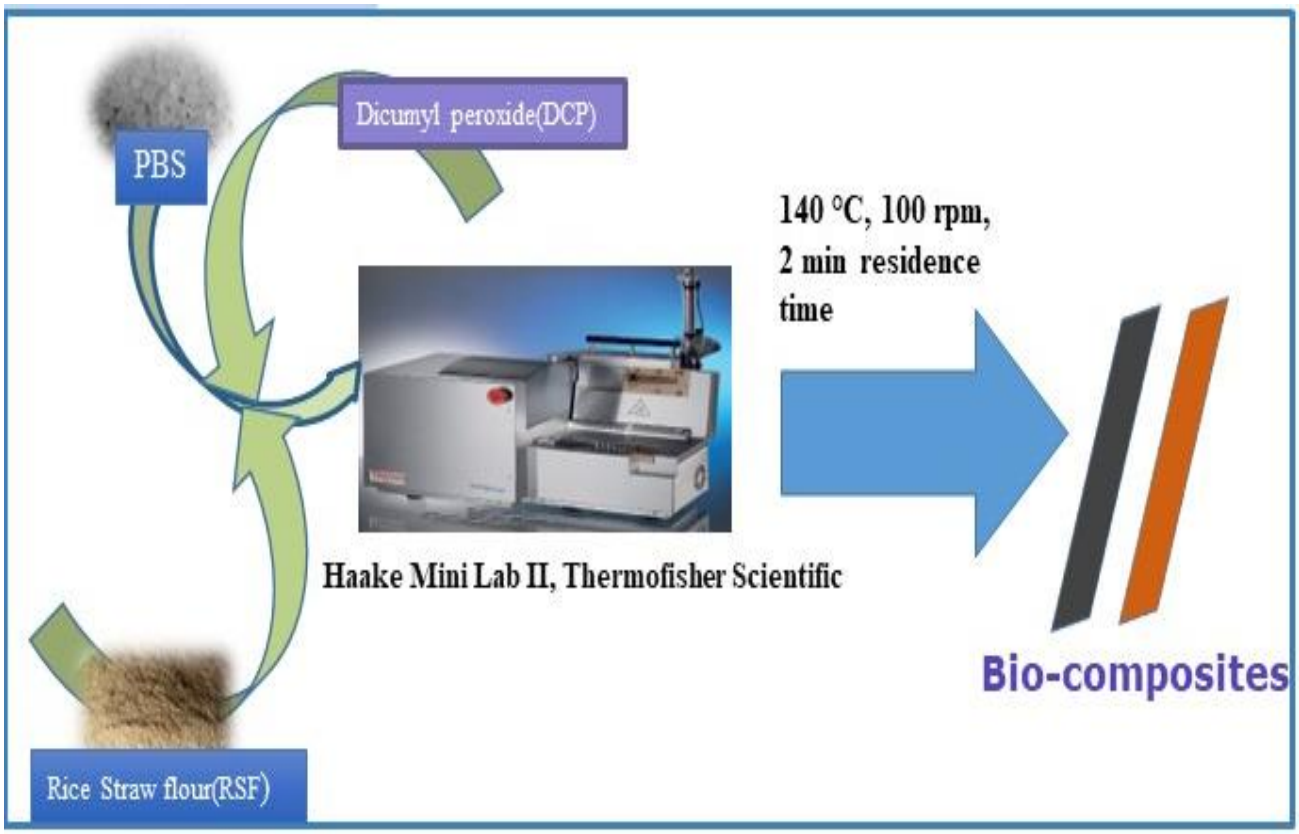

3.1 INTRODUCTION

Production of sustainable and renewable biodegradable polymers have generated enormous interest in the recent times as the conventional petroleum-derived synthetic polymers are the major source of environmental pollution and lead to massive waste management problems [81-83]. Biodegradable polymers made from renewable resources have several applications in packaging and biomedical industries [84]. Poly (butylene succinate) (PBS) is one of the most promising bio-degradable aliphatic thermoplastic polyester which is chemically synthesized from two bio-based renewable monomers, 1,4-butanediol and succinic acid, through poly-condensation reaction [85]. PBS possesses some excellent properties like melt processability, thermal and chemical resistance in comparison to other biodegradable polymers [86-87]. It has a melting point and glass transition temperature in the range of 90-120℃ and -45 to -10℃, respectively, which are between the temperatures reported for polyethylene (PE) and polypropylene (PP) [88]. Furthermore, PBS undergoes biodegradation during disposal in moist soil, compost and seawater [89]. However, some properties of PBS such as tensile strength, elastic modulus, gas barrier properties, softness, melt viscosity and high production cost hinder its extensive applications and further market development [90]. The most effective approach to overcome these shortcomings is to blend PBS with other biodegradable polymers or natural fibers [91].

Natural fibers derived from agricultural wastes are gaining steady importance in the polymer industry due to their light weight and low cost. Rice straw (RS) is an important agricultural waste found mostly in the Asian, Pacific and North American regions and has generally been used as a bedding material for animals. RS has several good properties like low bulk density, toughness, abrasiveness, resistance to weathering and it also has a unique composition. However, industrial applications of RS have been very limited. So, RS-based biodegradable polymer bio-composites are attracting much attention due to their potential biomass energy

[92]. There have been many reports where some natural fibers like starch, cellulose, wood flour and lignin had been reinforced with PBS to create bio-composites having favourable characteristics [93-104]. However, no such literature is available describing the utilities and properties of PBS-RS based biodegradable polymer composites.

In the present work, a PBS-RSF bio-composite was prepared by the melt extrusion process in the presence of dicumyl peroxide (DCP), wherein RSF and DCP were used as the bio-filler and the cross-linking agent, respectively. The impact of different loadings of RSF on the melt extruded PBS based bio-composites, with or without DCP content, was studied extensively, including the influence of different RSF concentrations on the morphological, thermal and mechanical properties of the bio-composites. As per our knowledge, a detailed rheological study of the PBS-RSF based bio-composites is being reported for the very first time, and the effect of RSF on the flow properties of PBS chains, both with or without DCP content, is also being reported.

3.2 RESULTS AND DISCUSSIONS

3.2.1 Gel Content

$$\text{Gel content (\%)} = \frac{W_{gel}}{W_i} \times 100 \ldots (1)$$

It was observed that the PBS-RSF based composites (both for PBS-RS1-DCP and PBS-RS2-DCP) in presence of DCP (2 wt.%) formed a micro gel like structure because of the cross-linking. The Gel content (%) of NPBS and PBS-RSF based composites at different loadings of RSF (5, 10 wt.%) in presence of fixed amount of DCP (2 wt.%) are determined by the extraction process. The gel (%) value of NPBS is (5±0.3), calculated from the equation (1). The gel fraction value of the PBS-RS1-DCP (13±2) of 5 wt.% RSF and at 2 wt.% DCP is much higher than that of NPBS because of the formation of the cross-linking sites. But at the higher loading of RSF (10 wt.%) the gel fraction value of PBS-RS2-DCP (8±0.6) is decreased, possibly due to the reduction in cross-linking efficiency [105].

3.2.2 FTIR Analysis

FTIR analysis is used to investigate the structural modification of NPBS and PBS-RSF based bio-composites with or with without DCP. Fig. 3.1. shows the FTIR spectra of NPBS and its bio-composites. Characteristic FTIR peaks at 1144-1264, 1710-1713 cm^{-1} corresponds to the stretching of -C-O-C- group and the C=O stretching vibrations of the ester groups in PBS chains. The peak around 2920 cm^{-1} represents the asymmetric deformational vibrations of $-CH_2$ group in the main chains of PBS [106]. The absorption band at 3450 cm^{-1} and 2920 cm^{-1} corresponds to the C-H, O-H functional groups which confirms the presence of RSF in the PBS-RSF based bio-composites for all the samples [107]. Addition of DCP into the PBS-RSF systems (for both PBS-RS1-DCP, PBS-RS2-DCP) doesn't alter or shift the position of peak. It can be concluded that the interaction of PBS and RSF in the presence of DCP exist.

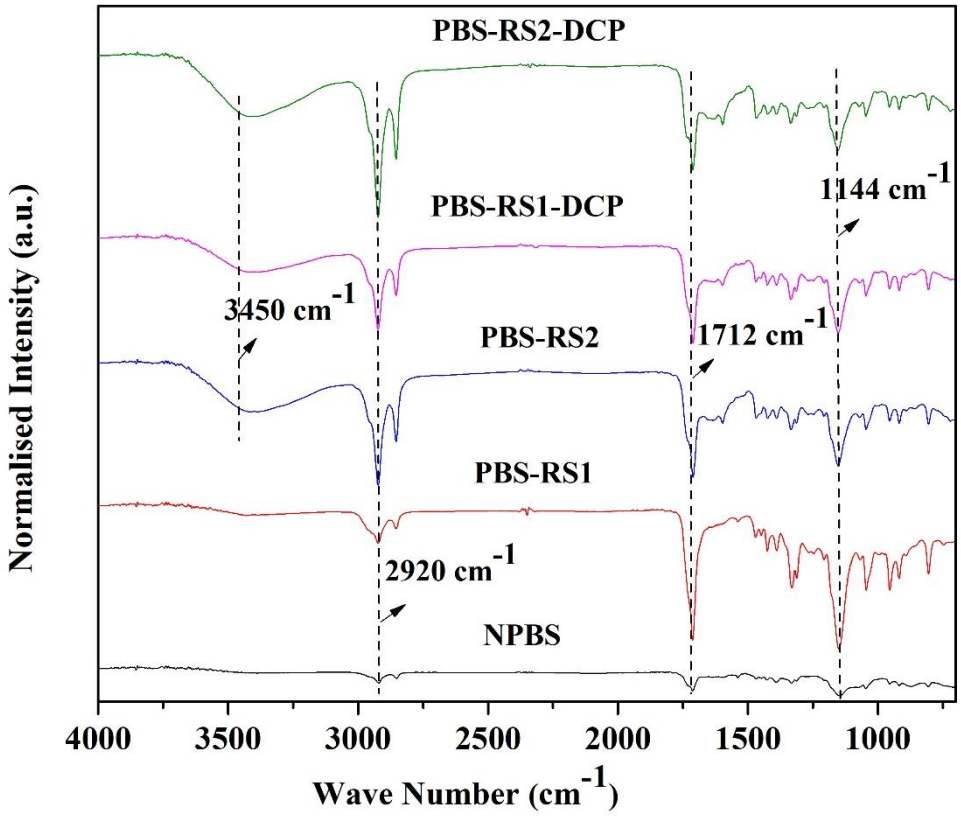

Fig 3.1. FTIR spectra of NPBS and its bio-composites

3.2.3 XRD Analysis

The crystalline structure of NPBS and its composites is studied with XRD as shown in Fig. 3.2. The XRD pattern shows two broad and intense peaks for NPBS at 19.6^{o} and 22.6^{o}, which corresponds to the (020) and (110) planes, respectively. It indicated that PBS was a semi crystalline polymer [108]. It is noteworthy to mention that the addition of RSF (5 and 10 wt.%) and DCP (2wt%) into NPBS did not alter the crystallographic structure of the PBS-RS bio-composites, indicating similar crystal structure. It happened due to the homogeneous dispersion of RSF in the PBS matrix.

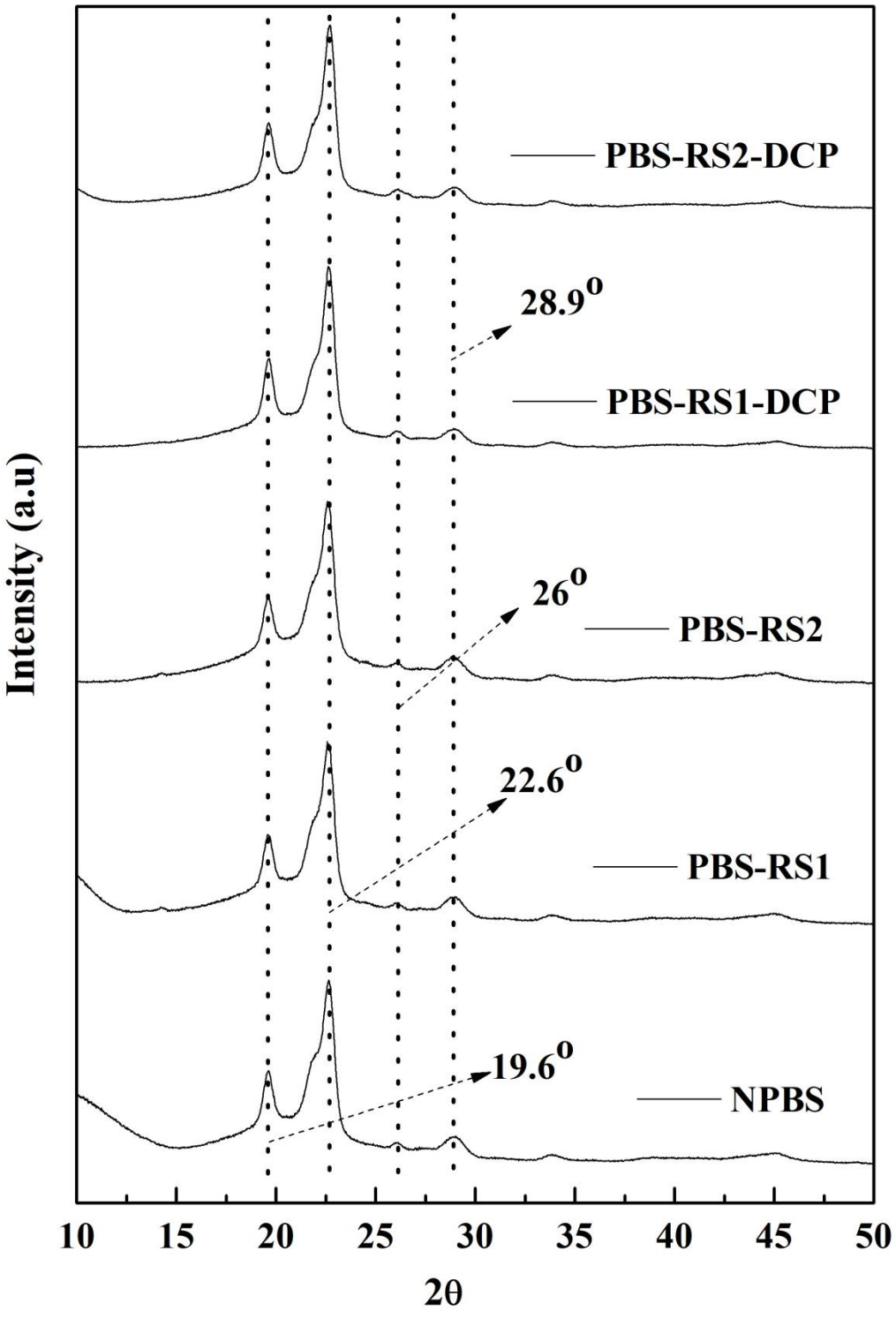

Fig. 3.2. XRD patterns of NPBS and its bio-composites.

3.2.4 Morphological Studies

The morphological structures of the NPBS and PBS-RSF based bio-composites with or without DCP observed by FESEM analysis. Fig. 3.3. (a) represents the topographical image of NPBS. Addition of RSF into the PBS matrix with and without DCP is displayed in Figs. 3.3.(b) and 3.3. (c), respectively and their higher magnification micrographs are represented by Figs. 3.3. (b') and 3.3. (c'), respectively. It can be seen both from the Fig. 3.3. (b, c) that, RSF (5 wt.%) is well dispersed into the PBS matrix which indicates the good miscibility between RSF and PBS matrix with or without DCP respectively. It is also found from the Fig. 3.3. (b, c) that RSF is agglomerated into the PBS matrix. A layered like morphology of RSF was observed showing a good adhesion between RSF and PBS matrix. The dimensions of the RSF were: length: - 10.749± 3.05µm; width: - 2.539± 0.95µm; thickness: - 0.41± 0.11µm.

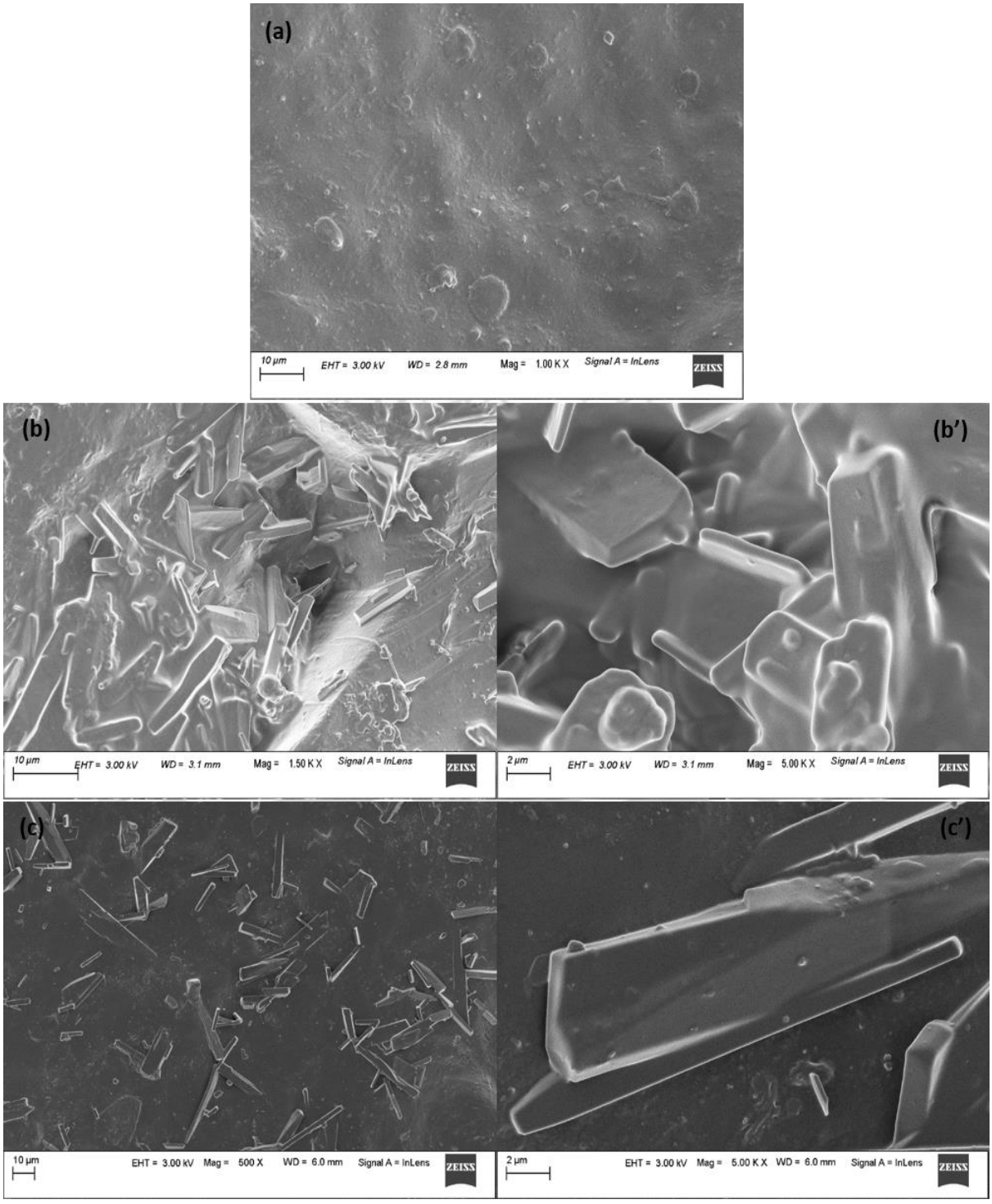

Fig. 3.3. FESEM images of PBS based bio-composites: **(a)** NPBS, **(b, b')** PBS-RS1, **(c, c')** PBS-RS1-DCP.

3.2.5 Analysis of Mechanical Properties of the Bio-composites

The three different mechanical properties i.e., ultimate tensile strength (UTS), elongation at break (EB) (%) and young's modulus (Y) give an idea of plasticity, brittleness, toughness characteristics of NPBS and its composites. Fig. 3.4. displays the mechanical properties of pristine PBS and its bio-composites and the values of the different mechanical properties are listed in Table 3.1. It was seen from the Table. 3.1 that the ultimate tensile strength (UTS) of NPBS was 19.4 MPa. The value of UTS deteriorated progressively upon the addition of 5 wt.% RSF (PBS-RS1) and 10 wt.% RSF (PBS-RS2) to the PBS matrix, in the absence of DCP. As compared to NPBS, the UTS of PBS-RS1 and PBS-RS2 decreased to 15.2 MPa (21.6%) and 10.36 MPa (46.5%) respectively. This significant reduction in UTS could be ascribed to the weak interfacial adhesion between the RSF and PBS matrix, which indicated the generation of micro-cracks at the interfacial area [29]. A similar kind of behaviour had been observed previously for PBS/ polyamide and poly (lactic acid)/ rice hull-based composites [109, 110]. But, addition of DCP (2 wt.%) to the PBS-RS1 and PBS-RS2 composites raised the values of UTS to 18.86 MPa (PBS-RS1-DCP) and 19.56 MPa (PBS-RS2-DCP) which was an increment of ~19.4% and ~47% from the UTS value of PBS-RS1 and PBS-RS2 composites without DCP, respectively. The formation of entanglement and cross-linked structures of the blends were found to be responsible for the increment of UTS, which in turn improved the miscibility of RSF into the PBS matrix and enhanced the toughening property of PBS.

On the contrary, it was observed from the Fig. 3.4. that the addition of different loadings (5, 10 wt.%) of RSF without DCP doesn't change the value of elongation at break (EB) (%) much, as compared to the value of NPBS (18.96 MPa). Whereas, incorporation of DCP into the PBS-RSF systems leads to the significant improvement of the value of elongation at break (%), (96.48%) specifically for the case of 5 wt.% loading of RSF (PBS-RS1-DCP). This is possibly due to the presence of more active free radical sites of peroxide at 2 wt.% loading of DCP

which acts as a depolymerizing catalyst and leads to the fragmentation of some of PBS chains So, both crosslinking as well as chain breaking effect was noticed for the PBS-RS1-DCP. However, this value is drastically decreased for the higher loading of RSF (10 wt.%) of PBS-RS2-DCP composite (30.68%). Hence, the decrement of chain breaking effect and the increment of cross-linking effect was observed for PBS-RS2-DCP.

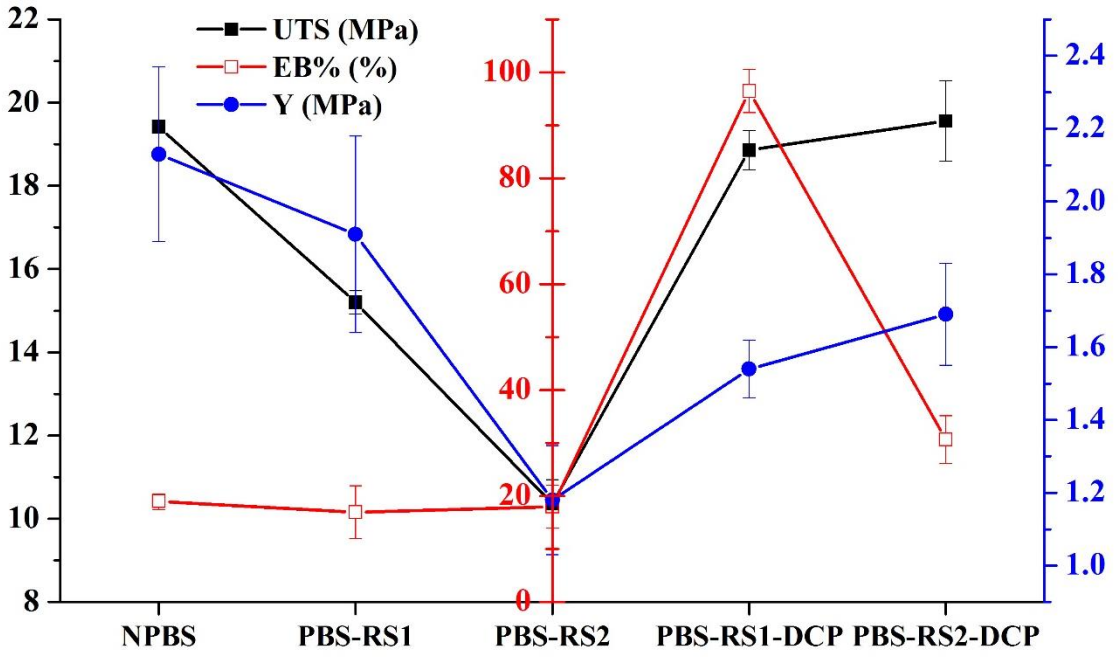

Fig. 3.4. Mechanical properties i.e., **UTS (MPa), EB (%), Y (MPa)** of NPBS and its bio-composites.

Table 3.1 Mechanical properties of NPBS and its bio-composites

Formulation	UTS (N/mm^2)	Young's Modulus (N/mm^2)	Elongation at break (%)
NPBS	19.4±0.1	2.1±0.2	18.9±1.4
PBS-RS1	15.2±0.2	1.9±0.2	16.9±4.9
PBS-RS2	10.3±0.5	1.1±0.1	17.9±4.0
PBS-RS1-DCP	18.5±0.4	1.5±0.0	96.4±4.0
PBS-RS2-DCP	19.5±0.9	1.6±0.1	30.6±4.5

3.2.6 Analysis of Thermal Properties of the Bio-composites

Thermogravimetric Analysis (TGA) is used to determine the thermal stability of a polymer and its composites. Fig. 3.5. (a), (b) shows the thermal degradation behaviour of NPBS and its bio-composites, both with and without DCP and the neat bio-filler, RSF respectively. TGA analysis was done to investigate the different thermal stability parameters such as T_{10}(temperature at which 10% weight loss occurs), T_{max} (maximum decomposition temperature) of the extruded samples. The values of these parameters have been given in Table 3.2. All the samples follow a two-stage degradation process, revealed by the first derivative thermograms as depicted in Fig. 3.5. (c). It was observed that the thermal stability of NPBS, both with and without DCP, improved on the addition of RSF (5 and 10wt %) and all the thermal stability parameters shifted to a higher temperature.

With an increase in the weight percentage of RSF (without DCP), all the thermal stability parameters increased progressively as compared to NPBS. The value of $T_{10\%}$ of the PBS-RS1 and PBS-RS2 systems (chosen as the initial decomposition temperature) was raised by ~2 °C and ~6 °C than that of NPBS. It implied that the enhancement in thermal stability was due to the incorporation of RSF in the PBS matrix. This is possibly due to the good interfacial adhesion between the matrix and the filler and also because of the layered like morphology of RSF which actually retards the emission of the degraded gas. On the contrary, incorporation of DCP into the PBS-RSF system (PBS-RS1-DCP and PBS-RS2-DCP) resulted in a slight reduction of all the thermal stability parameters.

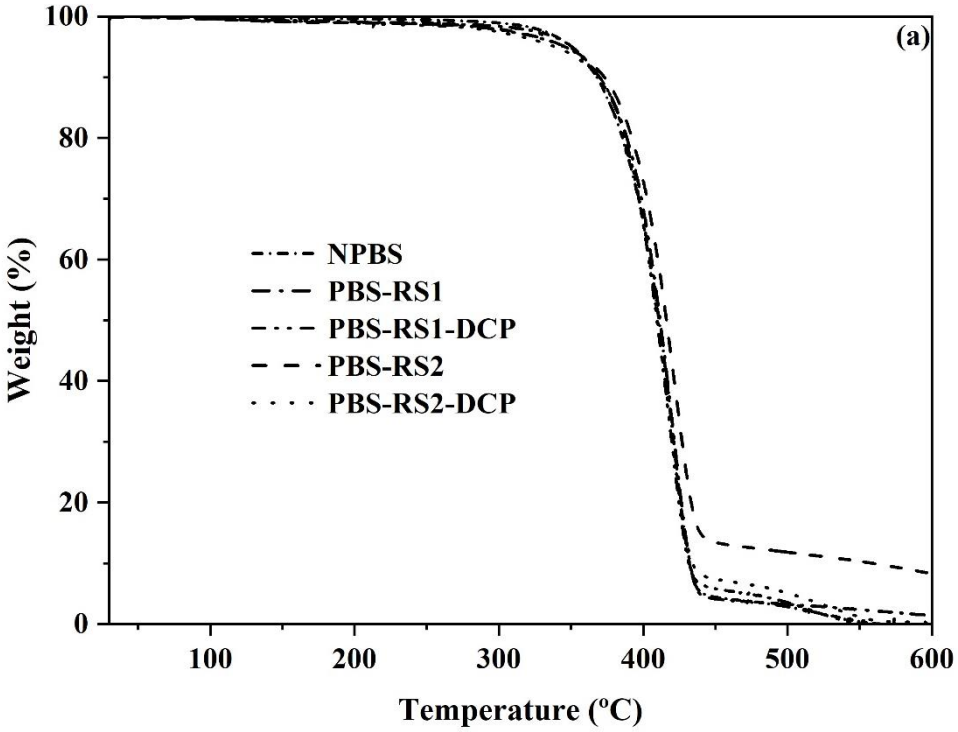

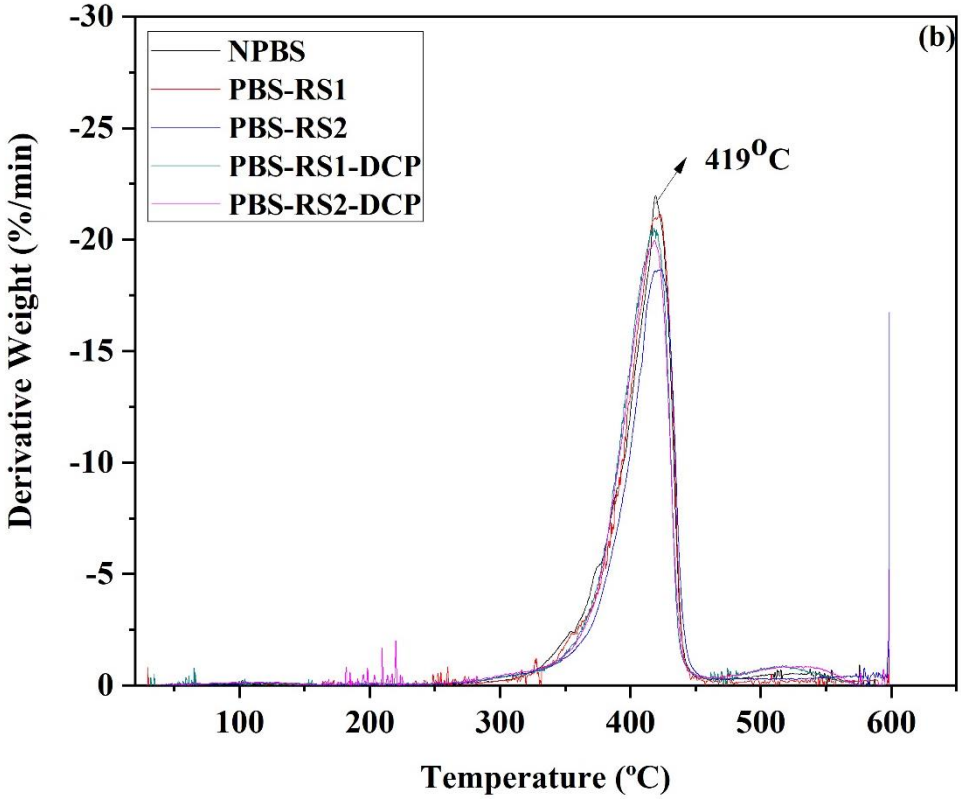

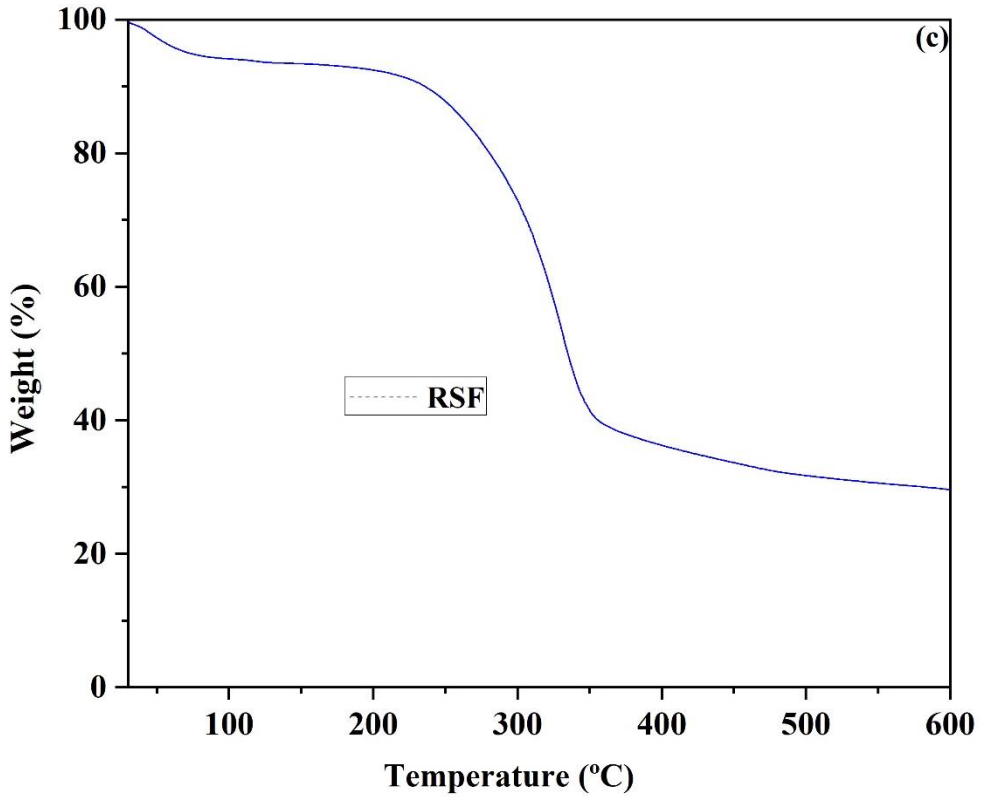

Fig. 3.5. Comparison of **(a)**TGA and **(b)** DTG curves of NPBS and its bio-composites and **(c)** TGA profile of neat bio-filler, RSF.

DSC measurements were carried out to investigate the chain folding behaviour of NPBS and its bio-composites in presence of RSF and DCP. The obtained second heating curves are depicted in Fig. 3.6. and the different thermal properties parameters are listed in Table 3.2. The glass transition temperature (T_g) values of NPBS (-44 °C) and its composites are found to be similar which signifies the similar secondary chain relaxation behaviour. Crystallisation temperature (T_c) values are also quite similar of PBS-RS1 and PBS-RS2 as compare to NPBS (80 °C) whereas, after the addition of DCP into the PBS-RSF systems a slight improvement has noticed of the PBS-RS1-DCP (91.4 °C) and the PBS-RS2-DCP (91.8 °C) composites possibly due to the nucleation effect. The melting temperature (T_m) of NPBS (113.9 °C) and its composites are identical which signifies the similar melting nature of the crystallographic plane. Because of the large crystallisation domain, the values of the percentage crystallinity

were decreased progressively after the addition of different loadings of RSF (5,10 wt.%) as compared to NPBS, possibly due to the restriction of higher crystal domain formation [111] and incorporation of DCP into the PBS-RSF systems resulted in further decrement of the value of the percentage crystallinity, compared to PBS-RSF based systems. For PBS-RS1-DCP and PBS-RS2-DCP, the value of the percentage crystallinity is 61.9 and 34.4, which is decreased from the value of 67.3 and 59.5, compared to PBS-RS1 and PBS-RS2, respectively. The possible reason behind this is the enhanced chain stability or the heterogeneous nucleation effect.

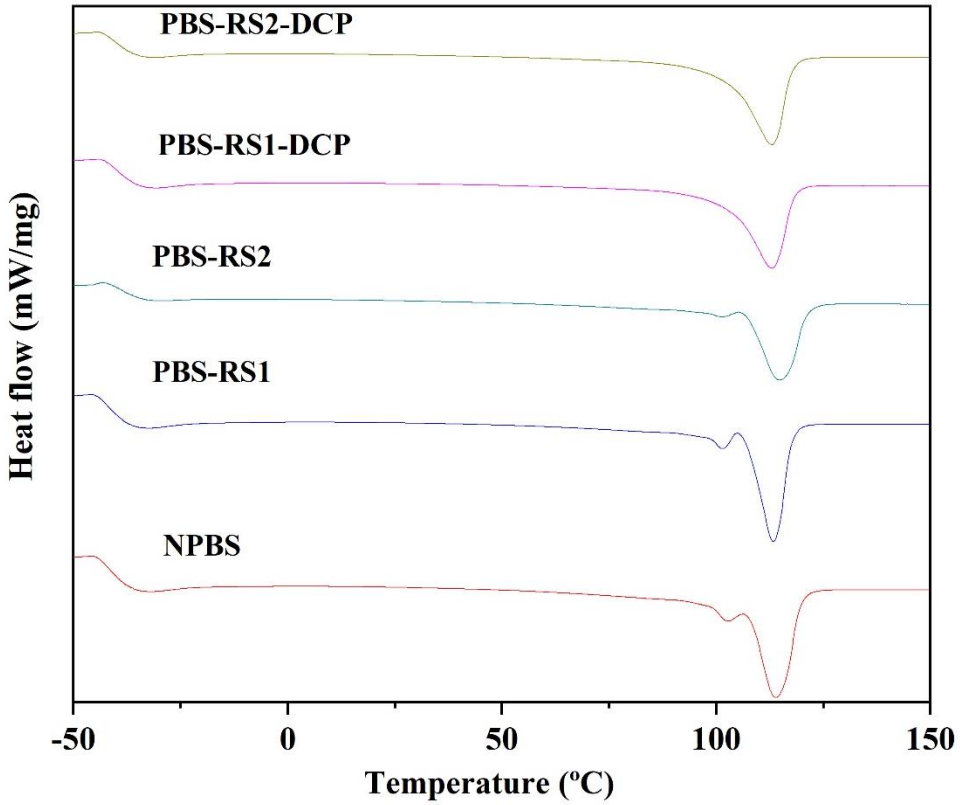

Fig. 3.6. DSC thermograms for NPBS and its bio-composites

Table 3.2 Thermal properties of NPBS and its bio-composites.

Samples	T_{10} (°C)	T_{max}(°C)	Weight loss (%) at 500°C	T_g (°C)	T_c (°C)	T_m (°C)	X_c (%)
NRSF	206	362	31.9	-	-	-	-
NPBS	367.6	419.39	2.8	-44	80	113.9	79.1
PBS-RS1	369.6	422.31	3.2	-43.9	79.7	113.3	67.3
PBS-RS2	373	423.6	11.8	-42.4	77.1	114.8	59.5
PBS-RS1-DCP	369.4	417.9	3.5	-42.4	91.4	112.9	61.9
PBS-RS2-DCP	368	418.5	5.1	-43.5	91.8	113	34.4

3.2.7 Analysis of Rheological Properties of the Bio-composites

Parallel disc oscillatory shear test was performed to find the relationship between the melt rheological properties of the materials and their frequency at a specific temperature without affecting the internal structure of the materials. The storage modulus (G') and loss modulus (G") of NPBS, PBS-RSF and PBS-RSF-DCP composite samples are shown in Figs. 3.7 (a) & 3.7 (b). According to the linear viscoelastic theory, G' and G" increase monotonically with an increase in angular frequency, ω, in the polymer composites. It could be clearly observed from Fig.3.7 that the PBS based bio-composites obey the linear viscoelastic theory showing an

increase in both G' and G" with increasing ω. As the experiment was conducted at 140 °C, all the samples were in the molten state. It implied that viscous nature was dominant in NPBS and its composites when G' was less than G" for the samples over the frequency range until the crossover point. On increasing the content of RSF from 5wt.% to 10 wt.%, G' and G" increased slightly due to better dispersion of RSF on the PBS matrix. It was also observed that the incorporation of DCP (2 wt.%) into the PBS-RSF system (for both 5 and 10 wt.% of RS) resulted in a rapid increase in G' and G". In the terminal flow region, $G' \propto \omega^2$ and $G'' \propto \omega$ are the common characteristics of a homopolymer. The values of the slope of ln G" vs ln ω in the low-frequency region ($0.1 \leq \omega \leq 10$) was near to 1 for all the samples and for the slope of ln G' vs ln ω, the value was near 2; except for the PBS-RSF (5%)-DCP (2%) and PBS-RSF (10%)-DCP (2%) composites, which deviated from the power law relationship. It suggested the characteristics of intense grafting. The values of the slopes for all the samples are given in Table 3.3.

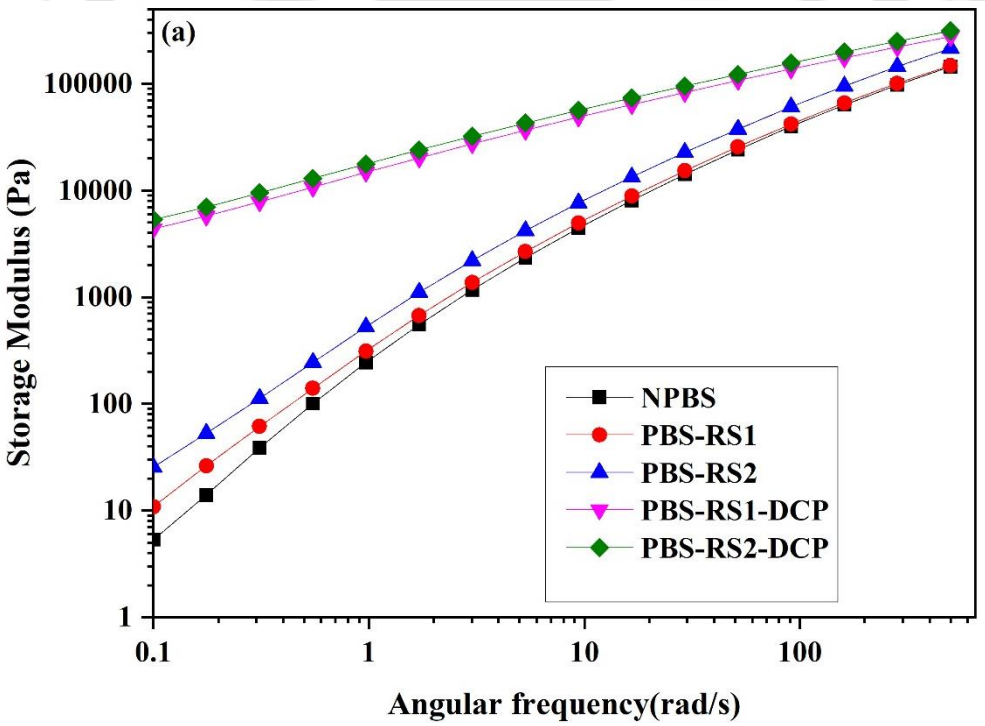

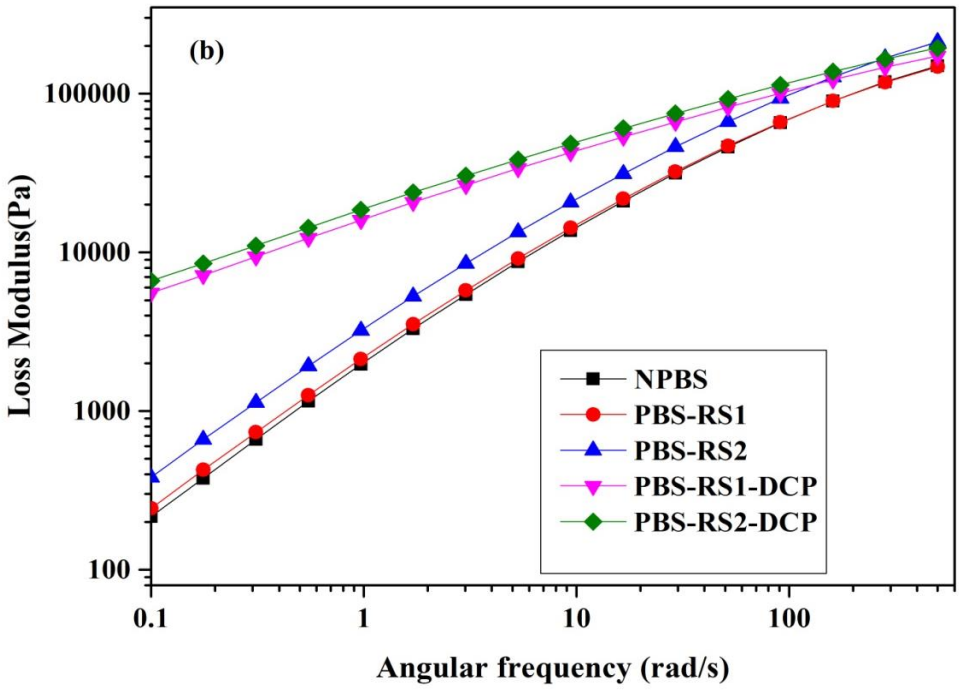

Fig. 3.7. (a) Storage modulus and **(b)** Loss modulus of NPBS and its bio-composites.

The data of complex viscosity (η^*)as a function of angular frequency is displayed in Fig.3.8. It was found that η^* decreased with an increase in ω for all the samples and a similar trend was observed for NPBS and PBS-RSF systems without DCP. The samples showed Newtonian fluid-like behaviour when η^* was nearly independent of ω (ω $\leq$1 rad/s), and followed non-Newtonian fluid-like behaviour when η^* was dependent on ω (ω>1rad/s), which is termed as the Power-law region. In comparison to NPBS, the complex viscosity of the composites increased with an increase in the content of RSF (5-10 wt.%), as addition of fillers hindered the movement of PBS chains.

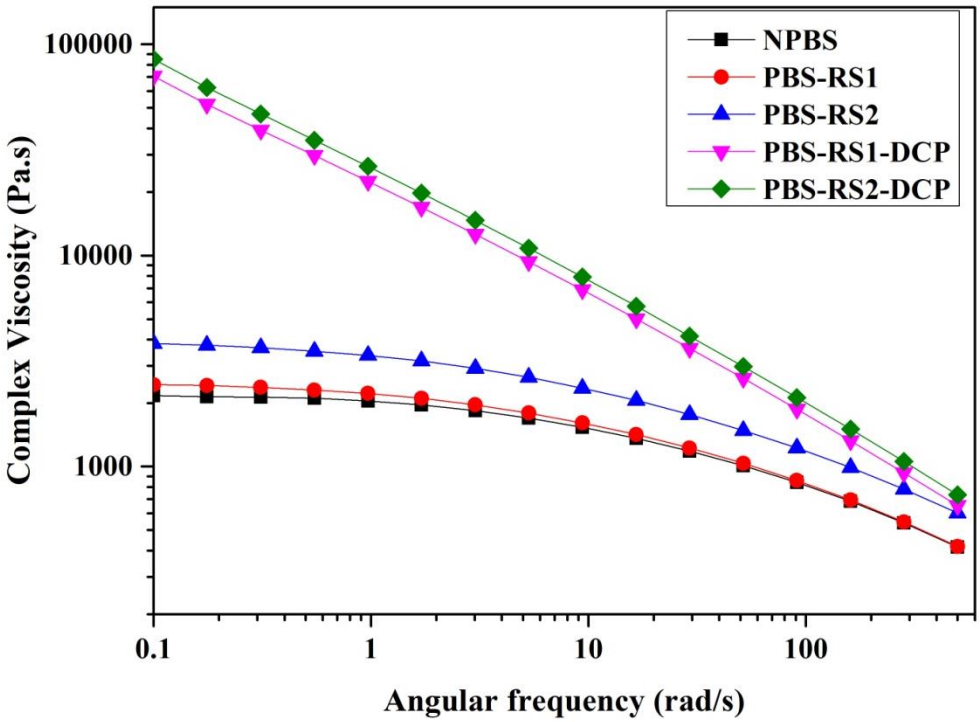

Fig. 3.8. Complex viscosity of NPBS and its bio-composites.

In this study, RSF acted as a reinforcing agent due to which the complex viscosity was increased by 12.7% and 77.1% on the addition of 5 wt.% and 10 wt.% RSF, respectively, at a frequency of 0.1 rad/sec compared to NPBS. Furthermore, when DCP (2 wt.%) was added to the PBS-RSF system, the complex viscosity enhanced even more. The reason for this pronounced improvement in complex viscosity of the bio-composites was the effect of cross-linking and long chain branching due to the formation of entangled networks by the restriction of mobility of the macromolecules. Shear thinning behaviour was observed in all the samples of NPBS and its composites due to the effect of shear on the entanglements.

The loss factor ($\tan\delta$) data, defined by the ratio of G" to G', plotted against angular frequency is shown in Fig. 3.9. Crossover points for all the samples were obtained by drawing a horizontal line that passed through $\tan\delta$ equal to unity. For the PBS-RSF system (for both, 5 wt.% and 10wt% RSF), crossover points occurred at higher frequency values and after the inclusion of DCP into the PBS-RSF system, it shifted to lower frequency values, whereas no crossover point was found for NPBS.

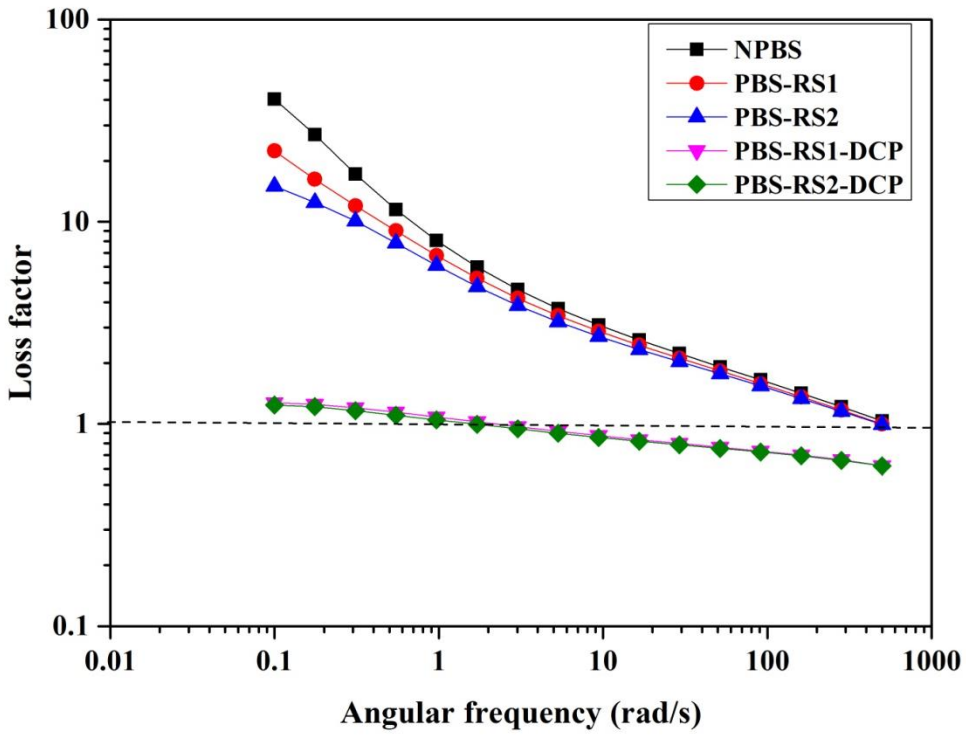

Fig. 3.9. Variation in loss factor of NPBS and its bio-composites with 'ω'.

The crossover frequency data of all the samples are listed in Table 3.3. The value of $\tan\delta$ was lower than unity beyond the crossover point for PBS-RSF (5 wt.%)-DCP (2wt.%) and PBS-RSF (10wt%)-DCP (2wt%) systems. This implied that G' was greater than G". There is a direct correspondence between the crossover frequency and the molar mass of a polymer. If the crossover point occurs at a lower frequency, then the molar mass of a polymer is relatively higher. In this investigation, the molar masses of the PBS-RSF (5wt%)-DCP (2wt%) and PBS-RSF (10wt%)-DCP(2wt%) composites were relatively higher as compared to NPBS and PBS-RSF composites without DCP. The complex viscosity increased only slightly at the crossover point when RSF was incorporated into the PBS matrix, but addition of DCP into the PBS-RSF system led to a significant increase in the complex viscosity values (Table 3.3).

The dependence of angular frequency on the torque in NPBS and its composites has been displayed in Fig. 3.10. With an increase in ω, the values of the torque increased significantly

for all the samples which happened due to the change in viscosity with respect to the angular frequency.

The torque of PBS-RS2 was higher as compared to NPBS and this effect magnified even more when DCP was added to the PBS-RSF systems (for both 5wt.% and 10wt.% RSF). The increase in complex viscosity on the addition of fillers and further incorporation of DCP into the polymer matrix were responsible for the above phenomenon.

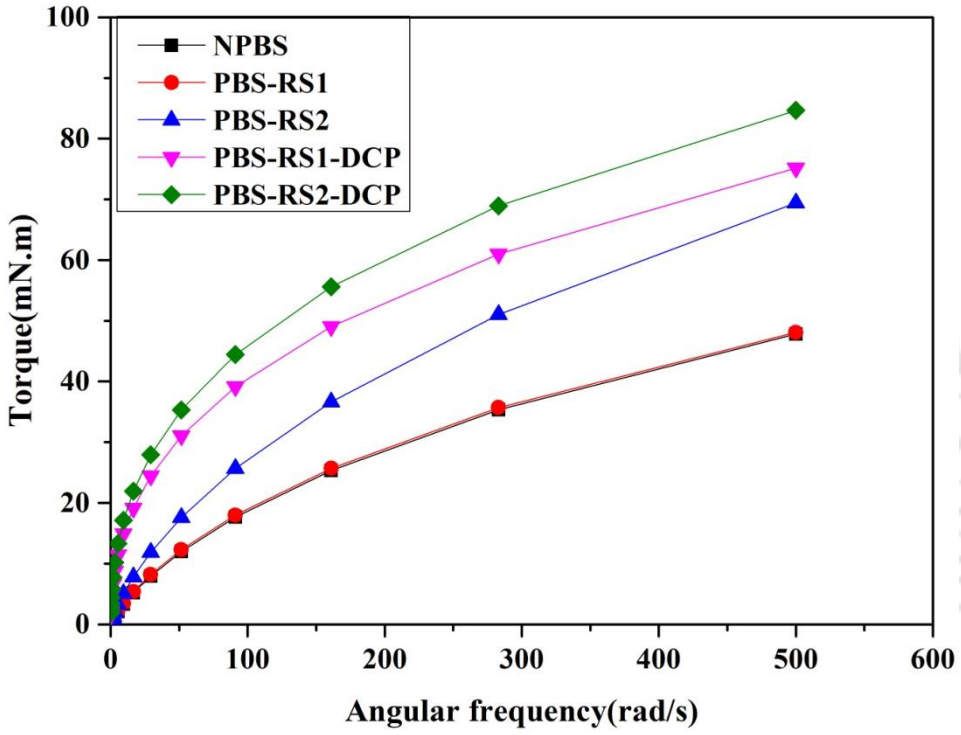

Fig. 3.10 Variation in torque of NPBS and its bio-composites with 'ω'.

Power law model

It was clearly observed that all the samples of NPBS and its composites followed the phenomenon of shear thinning behaviour. The power law model explains the shear thinning behaviour of a sample through the following equation (2) [112].

$$\eta = m(\dot{\gamma})^{n-1} \qquad (2)$$

Where ‘m’ and ‘n’ were the fluid consistency coefficient and the flow behaviour index, respectively.

This model fits in the transition region between the Newtonian and the non-Newtonian range. Cox and Merz [113] proposed that there is a correspondence between the steady state shear viscosity, η, which is plotted against the shear rate, γ, and the magnitude of complex viscosity, $|\eta^*|$, which is plotted against the angular frequency, ω. The value of the fluid behaviour index, n, designates the deviation from the Newtonian behaviour, and the non-Newtonian behaviour is determined from the slope of (n-1) of the plot between η^* against ω considering the Cox-Merz rule: $(\eta^*(\omega)|_{\omega\to 0} = \eta(\gamma^{\cdot})|_{\gamma\to 0})$.

It was seen that the value of ‘n’ was less than ‘1’ for all the samples justifying the shear thinning behaviour of NPBS and its composites (Table 3.3).

Table 3.3 Rheological properties of NPBS and its bio-composites.

Sample	Crossover properties			Power law model	Terminal region		Han plot	
	ω_c (rad/s)	G'= G" (kPa)	η^* (Pa.s)	n	ln G'-lnω	ln G"-lnω	Slope	R^2
NPBS	-	-	-	0.82	1.49	0.91	1.5	0.998
PBS-RS1	496.33	147.24	419.56	0.80	1.35	0.89	1.46	0.999
PBS-RS2	489.69	210.44	608.48	0.71	1.27	0.88	1.42	0.999
PBS-RS1-DCP	2.19	22.88	14848	0.46	0.53	0.45	1.20	0.999
PBS-RS2-DCP	1.39	21.64	21962.91	0.45	0.52	0.44	1.19	0.999

Han plot

The logarithmic plot between G' and G" termed as Han plot, is used to investigate the micro structural changes in the polymer composites. In this investigation, Han plot (log G' vs log G") [114, 115] was employed to study the changes in the microstructure of NPBS and its composites at a fixed temperature of 140 °C, as shown in Fig. 3.11. It was observed that the Han plot of NPBS and its composites of PBS with 5 wt.% and 10 wt.% loading of RSF (without DCP) did not coincide with each other up to 239 Pa of G'. This clearly suggested the structural

changes between NPBS and PBS-RSF (for both 5 wt.% and 10 wt.% RS) composites, and although at higher values of G", the composites of PBS-RSF (for both 5wt% and 10 wt.% RSF) coincided with NPBS. The values of the slope of NPBS and PBS-RSF composites with 5 wt.% and 10 wt.% loading of RSF were 1.5, 1.46 and 1.42 respectively, which were almost comparable to each other. Thus, it could be concluded that the reinforcement of RSF was not creating any phase separation in the composites. However, it was found from Table 3.3 that the slopes decreased to 1.20 and 1.19 when DCP (2 wt.%) was added into the PBS-RSF composites with 5 wt.% and 10 wt.% loading of RSF, respectively. The possible reason behind is the formation of branched and crosslinked structure.

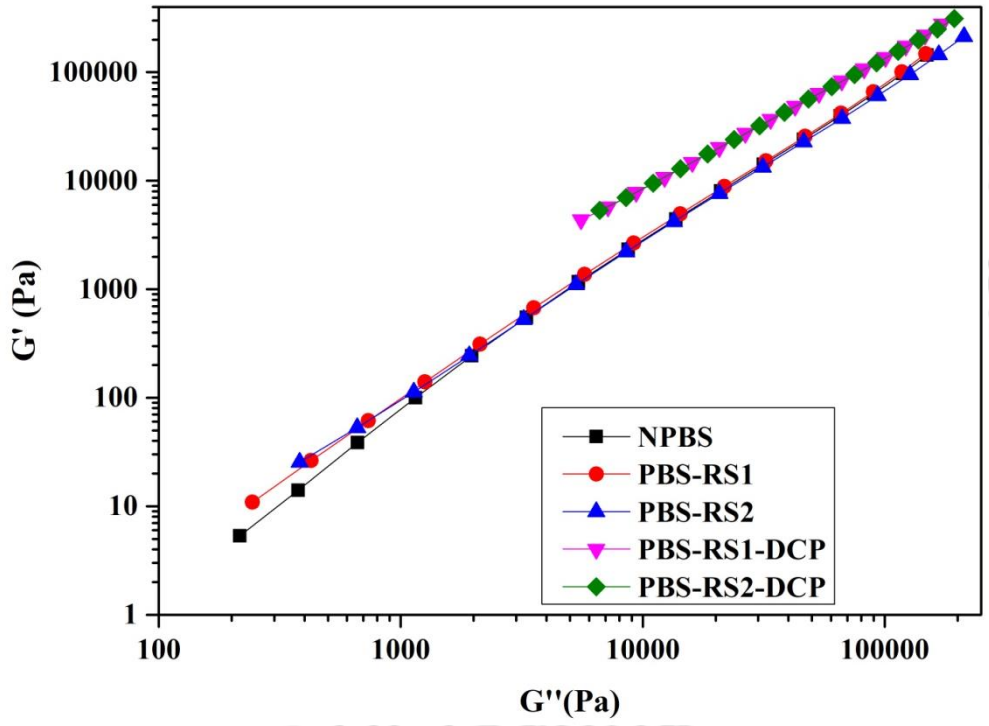

Fig. 3.11 Han plot of NPBS and its bio-composites.

Cole-Cole plot

Cole-Cole plots [116] are used to describe the viscoelastic properties of a composite with a relaxation time distribution consisting of a real and an imaginary part of the complex viscosity. The real, η' and imaginary, η" parts are obtained by the following equations (3) and (4).

$$\eta' = G''/\omega \quad (3)$$

$$\eta'' = G'/\omega \quad (4)$$

It was observed that NPBS and PBS-RSF (for both 5 wt.% and 10 wt.% RSF) systems without DCP content showed a semicircle curve with similar characteristic shapes (Fig. 3.12), which suggested similar relaxation mechanisms of the composites. The arc of the semicircle curve become larger and wider with the addition of RSF (from 5wt.% to 10wt.%), which indicated good compatibility and dispersion of RSF on the PBS matrix, and which in turn improved the melt strength of PBS. It was noticed that the arc become broad and almost flattened after the incorporation of DCP into the PBS-RSF systems which confirms the presence of branching, cross-linking of the bio-composites without phase separation, which in turn enhance the melt strength of the bio-composites in presence of DCP [117].

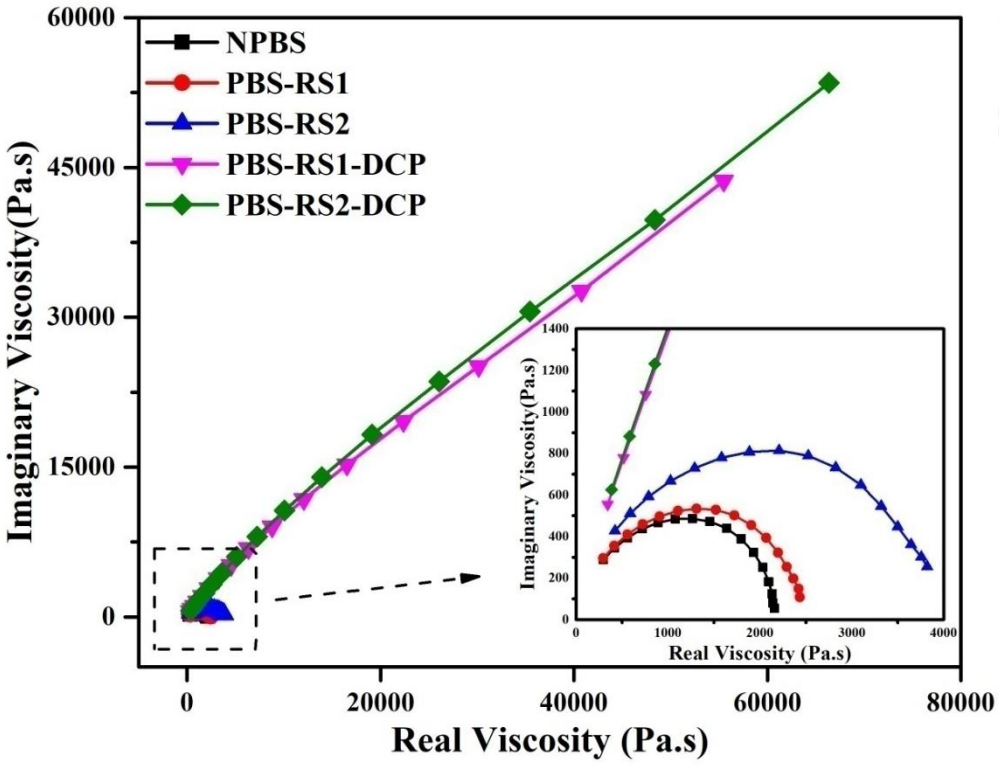

Fig. 3.12 Cole-Cole plot of NPBS and its bio-composites.

3.3 CONCLUSIONS

The present research describes the utilization of agricultural waste and its conversion to value-added products. PBS-RSF based biodegradable polymer composites were prepared by the melt extrusion process wherein the agricultural waste, RSF was used as a bio-filler and DCP was used as a cross-linking agent. Morphological, thermal, mechanical and rheological properties of the bio-composites were characterized thoroughly. FTIR analysis confirms the interaction of PBS and RSF in presence of DCP exist. XRD study showed that the addition of RSF in the PBS matrix did not change the crystal structure of the bio-composites whereas a layered like morphology of RSF was observed by FESEM analysis. It was observed that the UTS of the bio-composites decreased with increasing weight percentages of RSF (from 5wt.% to 10 wt.%) without the DCP content due to weak interfacial adhesion between the filler and the matrix. The UTS value of PBS-RS1 and PBS-RS2 composites decreased by ~21.6% and ~46.5%, respectively, as compared to the NPBS (19.4 MPa). Whereas, the values of elongation at break (%) are almost similar as compared to the NPBS (18.9) with the increasing weight percentages (5,10 wt.%) of RSF without DCP. Incorporation of DCP (2 wt.%) into the PBS-RSF systems leads to the significant improvement of the UTS value for both the PBS-RS1-DCP and PBS-RS2-DCP composites by a factor of 19.4 and 47 as compare to the PBS-RS1 and PBS-RS2 respectively. While the value of elongation at break (%), is increased rapidly specifically for the case of 5wt.% loading of RSF of PBS-RS1-DCP (96.48%). This is possibly due to the presence of more active free radical sites of peroxide at 2wt% loading of DCP which acts as a depolymerizing catalyst and leads to the fragmentation of some of PBS chains. The thermal stability of the bio-composites of PBS-RS1and PBS-RS2 improved with the addition of different loadings of RSF (5 wt.% and 10 wt.%) by a factor of 2 and 6 $^{\circ}$C as compare to the NPBS (367.6^{o}C) and all the thermal stability parameters are shifted towards the higher temperature, whereas the value of these parameters decreased slightly after the inclusion of

DCP content into the PBS-RSF systems as compared to NPBS. The glass transition temperature (T_g) and the melting temperature (T_m) values of NPBS and its composites are identical which signifies the similar secondary chain relaxation behaviour and similar melting nature of the crystallographic plane respectively. Rheological analysis of the fabricated bio-composites which were carried out by parallel plate geometry in the oscillatory shear mode, showed G'< G" over the frequency range until crossover. It confirmed the viscous nature of all the samples. With an increase in the weight percentages of RSF (for both 5 wt.% and 10 wt.% RS), both G' and G" increased with ω and this increment was even higher when DCP added to the PBS-RSF systems. The η' value was almost constant in the lower frequency region when ω was <1 and it decreased progressively for all the samples which implied the shear thinning behaviour of all the samples. Compared to NPBS, the torque of PBS-RSF (for both 5 wt.% and 10 wt.% of RSF) composites increased with frequency and this increment in the torque increased even further when DCP was added to the PBS-RSF systems. Addition of RSF and DCP into the NPBS resulted in a shift of the crossover point to a lower frequency value, which indicated high polydispersity index and increased the molecular weight of the bio-composites. Furthermore, Han plot and Cole-Cole plot demonstrated uniform miscibility and good compatibility with similar stress relaxation time of RSF on the PBS matrix, respectively. Hence, it could be concluded that RSF was well dispersed on the PBS matrix and acted as a reinforcing agent and increased the melt strength of the bio-composites. In addition, RSF reduced the cost of PBS based product, and thus the product could be used in the packaging field.

Chapter 4

Synthesis of nano silica from waste RS and fabrication of PLA-nano silica-based nanocomposites and evaluation of their properties

Abstract

This present work aims to investigate the effect of adding various amounts of nano-silica (NS), derived from rice straw particles on the poly (lactic acid)-NS-based nanocomposites using Luban gum (G), a compatibiliser. Crystallisation, mechanical, and rheological properties of the nanocomposites as a function of NS isolated from waste rice straw (RS) were analysed extensively. Morphological properties of the nanocomposites depict that adding LG improves the miscibility between the sphere-shaped NS and the PLA matrix. The value of different thermal properties from the DSC analysis showed that the glass transition temperature (T_g) and melting temperature (T_m) of the bio-composites with varying percentages of the weight of NS with and without G is almost identical. In contrast, due to the nucleation effect, the crystallisation temperature (T_c) of the PLA-NS-based systems increased with and without LG, which improved the crystallisation process. Mechanical properties, i.e., tensile strength (UTS) and Young's modulus (Y) values of the nanocomposites, were increased because of the improvement of the dispersion of NS into the PLA matrix. The results of the rheological tests indicated a rapid increase of the storage modulus, G', and the complex viscosity of the nanocomposites with the addition of G, which improves the melt strength of the nanocomposites. Shear thinning behaviour was observed. All the above results indicated that PLA-NS-based nanocomposites could be the potential material for application in the packaging field.

4.1 INTRODUCTION

In the last few years, the fabrication of green, sustainable, biodegradable polymers, nanomaterials, and composites from renewable resources has been one of the hottest topics of discussion among researchers [81-83]. Biodegradable polymers are gaining importance as they have several significant applications in the biomedical, structural, and packaging fields and are prospective replacements for synthetic polymeric products [84]. One of the most used bio-polymer, Poly (lactic acid) [118], has gained considerable interest in the commercial market because of its biocompatibility, easy processability, and comparable mechanical properties and thermal properties to conventional non-biodegradable synthetic plastics materials such as polyethylene (PE), polypropylene (PP), polyethylene terephthalate (PET) [119-121]. However, brittle in nature, poor melt strength, poor gas barrier properties, poor thermal stability, and heat distortion temperature (~ 55°C) restrict its applications [122, 123]. Therefore, blending with other polymers, co-polymerization, and mixing with inorganic fillers are the widely used strategies for improving the properties of PLA [124-130]. It was reported that mixing with inorganic additives such as carbon nanotube, ZnO, MgO, and TiO_2 helps to boost the performance of PLA [124-126].

Nano-silica (NS) or SiO_2 was a very promising filler for improving the performance of many polymeric materials [131, 132]. The main reason for using NS as a filler is because of some excellent properties: chemically, physically, and thermally stable, compatible with various materials, large surface area, largely available, and relatively inexpensive [133-135]. Many studies have found that the silica nanoparticles were extracted from natural sources like rice husk [136-138] and fly ash. Although, the utilization of rice straw (RS) for producing NS has yet to be widely researched. Rice is the largest cereal crop in the world. Amongst these, RS accounts for 45% of the total volume of rice production. Usually, rice millers dispose of and burn rice straw waste in an open environment, creating a severe environmental threat to society.

As a result, rice straw waste can be utilised to extract NSs, a value-added product. NS can be used as a nucleating agent in thermoplastic polymer-based nanocomposites, enhancing the thermal, mechanical, and rheological properties of NPLA [139]. However, miscibility and the phase separation between the polymer matrix and NS is still challenging for the scientific community as NS tends to aggregate due to small size effects, high surface energy, and relatively poor interaction between NS and polymer matrix.

The use of compatibilizers is one method in which the compatibility between the matrix and the filler is improved during melt processing. A compatibilizer could enhance interfacial adhesion by reducing the interfacial tension between the two immiscible phases, improving the mechanical properties of the composites.

This study aims to synthesize the nano-silica (NS) particles from an agricultural waste, RS, and prepare Poly (lactic acid)-NS-based nanocomposites, adding Luban gum (G) as a compatibiliser by melt extrusion process. This work also investigates the influence of NS content on the thermal, mechanical, and rheological properties of the nanocomposites. The structure-properties relationship of the nanocomposites will be explored in terms of the mechanical properties, crystallisation behaviour, and rheological properties.

4.2 RESULTS AND DISCUSSIONS

4.2.1 Morphological properties

The surface morphology of the nano silica (NS), isolated from RS is investigated using the FESEM image as shown in Fig 4.1. A sphere-shaped morphology is observed in the NSs with an average diameter of 50 nm.

The morphological structures of the NPLA and PLA-NS-based composites with or without Luban gum (G) are observed by FESEM analysis. The fractured surface of NPLA that appears to be rough is shown in Fig. 4.2. (a). The addition of NS into the PLA matrix with and without 'G' is displayed in Figs. 4.2. (b, c). It can be seen from Fig. 4.2. (b) that the sphere-shaped NS (6 wt.%) is well dispersed into the PLA matrix, which indicates good miscibility between the nanofiller, NS, and the PLA matrix without 'G', showing a good adhesion. Fig. 4.2. (c) depicts that the incorporation of Luban gum into the PLA-NS-based systems smoothened the surface of the composites as the gum here acted as a compatibilising agent for which NS was well distributed into the PLA matrix.

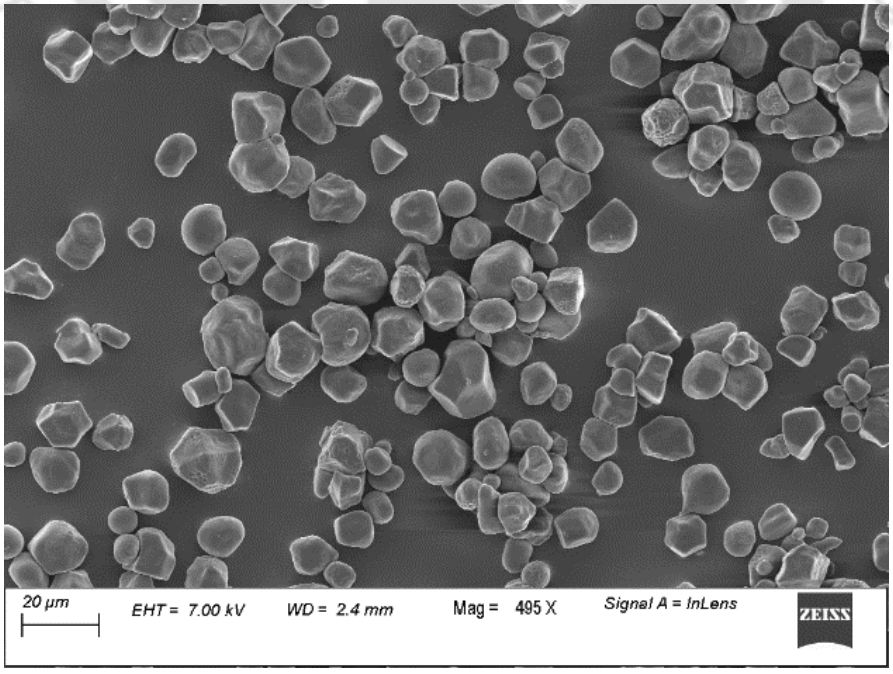

Fig. 4.1. FESEM images of nano silica (NS)

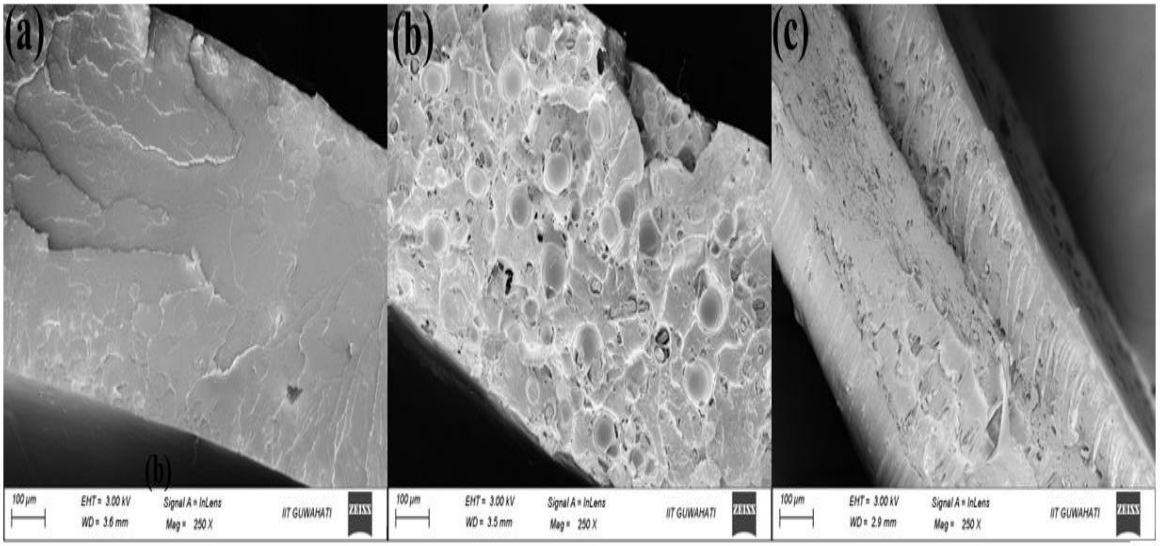

Fig. 4.2. FESEM images of NPLA and its nanocomposites (a) NPLA, (b) PLA-NS (6%), (c) PLA-NS (6%)-G (1%).

4.2.2. FTIR analysis

FTIR analysis investigates the structural modification of NPLA and PLA-NS-based nanocomposites with or without Luban gum (G). The FTIR spectrum of NS is shown in Fig. 4.3. (a). Fig. 4.3.(b, c, d) shows the FTIR spectra of the NPLA and its nanocomposites. The vibration bands at 1071, 791, 458 cm^{-1}were assigned to the asymmetric and symmetric stretching and bending vibration of O−Si−O [136, 140-141], as shown in Fig. 4.3. (a). Generally, NPLA showed four typical chemical groups, i.e., $-CH_3$, −CH, −C−O−C−, −C=O. The FTIR peaks at 1749, 1266, 1182, 1129, 1082, 1045, 868 cm^{-1} corresponding to −C=O stretching of aliphatic ester, asymmetric and symmetric stretching vibration of −C−O−C−, side group vibrations of C−OH, C−C stretching vibration and −CH stretching are the typical characteristic peaks of PLA [142]. The peaks at 2998, 1453, and 1370 cm^{-1} corresponded to −CH vibration, asymmetric vibration of $-CH_3$, and deformation of $-CH_3$ groups, respectively. The peaks at 2946, 2925, 2854 cm^{-1} represents the asymmetric stretching vibration of the −CH group and asymmetric and symmetric stretching vibrations of $-CH_2$ respectively. It could be

concluded that adding ‘G’ into the PLA-NS-based nanocomposites doesn't alter or shift the peak position.

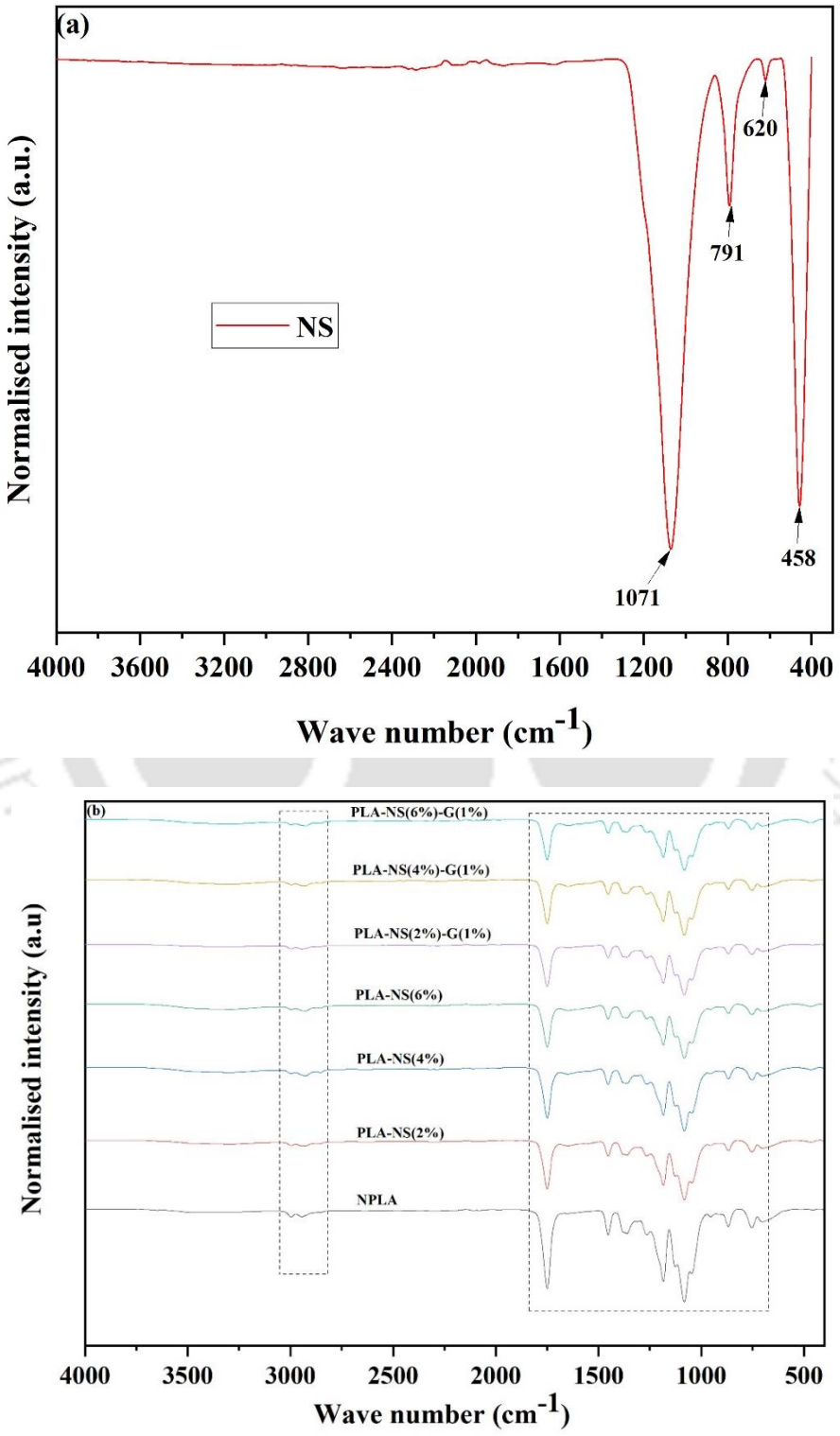

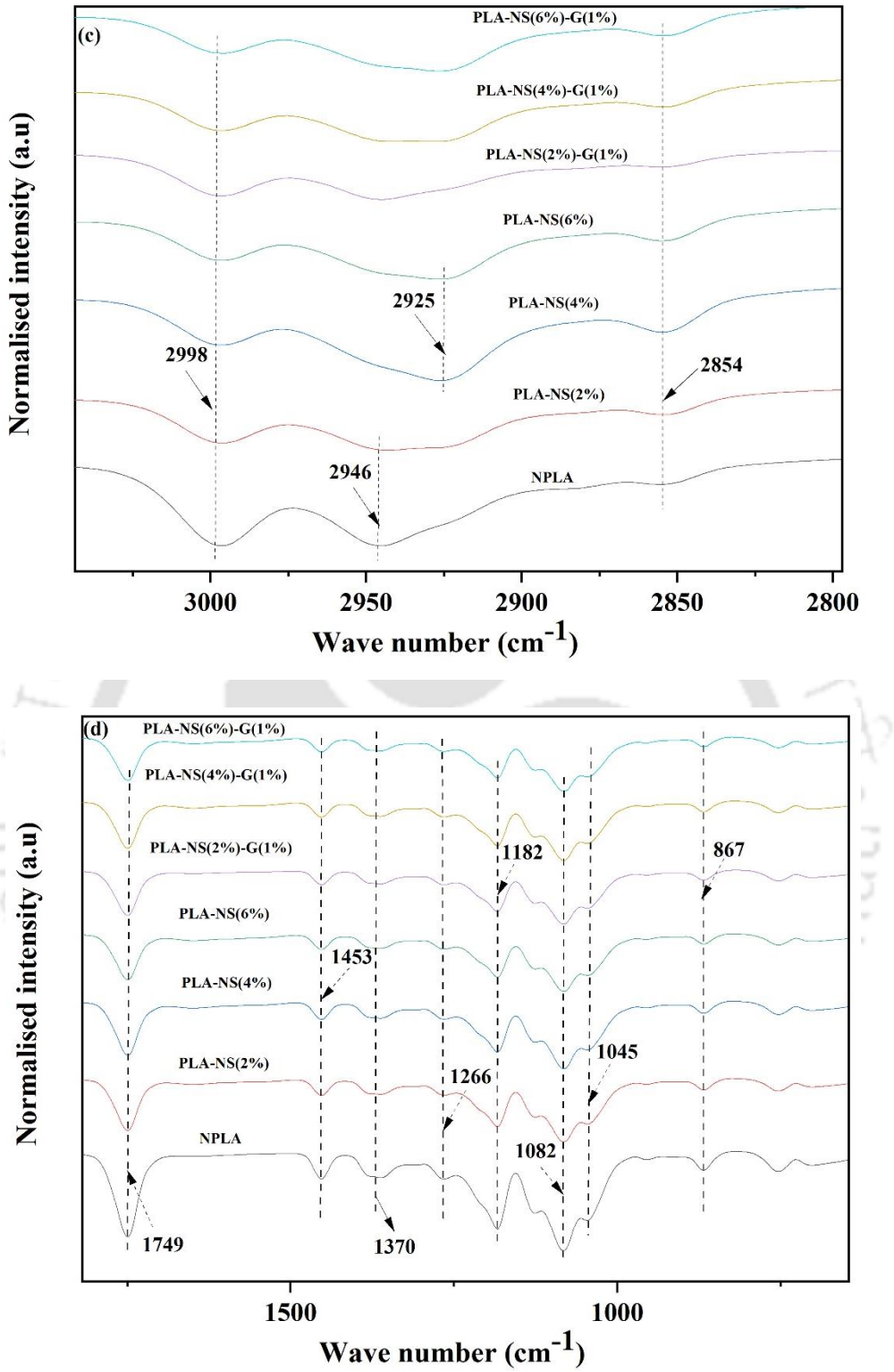

Fig. 4.3. (a) FTIR spectrum of nano silica (NS), **(b)** Comparison of FTIR spectrogram of neat PLA and its nanocomposites with the selected regions (marked in black boxes) analysed at **(c)** 3000-2800 cm^{-1} **(d)** 1800-600 cm^{-1} wavenumber range and the representative peaks marked with black arrows.

4.2.3. XRD analysis

The crystalline structure of NPLA and its composites is studied with XRD analysis. A wide diffraction from 2θ = 10º to almost 20º, as shown in Fig. 4.4, was observed for all the samples. This is because of the scattering of the PLA matrix. The diffraction peak at 2θ = 22º confirms the presence of NS in the PLA matrix, and the intensity of this diffraction peak is enhanced when the gum is added to the PLA-NS-based composites, which increases the crystallinity of the nanocomposites. A low-intensity peak at 2θ = 26.6º was observed for the PLA-NS-based composites in the presence of Luban gum (G) (PLA-NS (2%)-G (1%)).

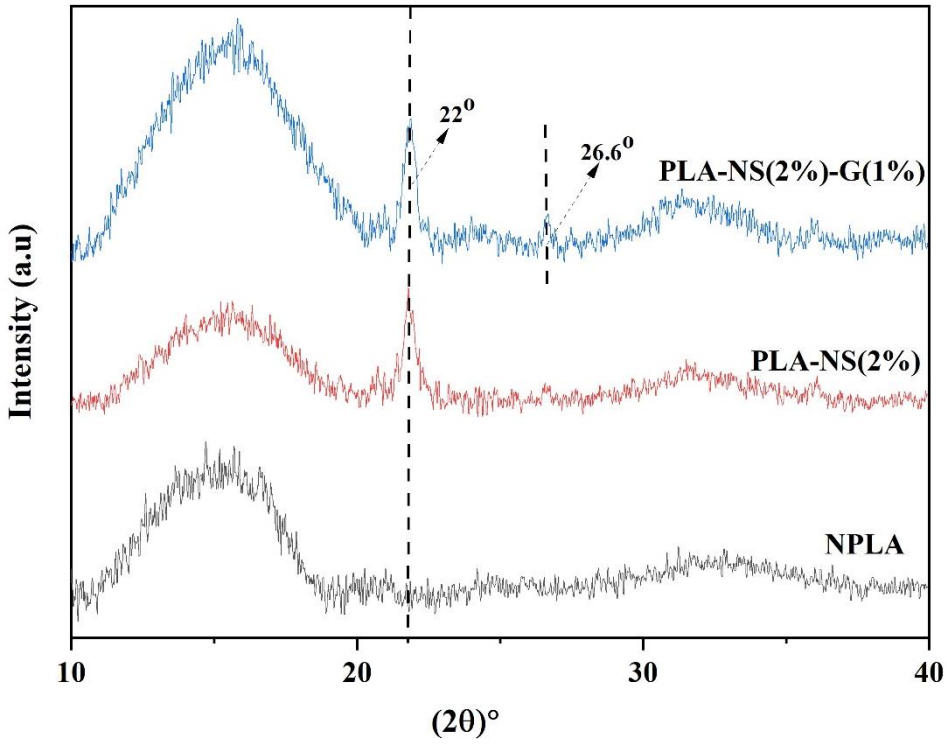

Fig. 4.4. XRD diffraction patterns of NPLA and its nanocomposites

4.2.4 DSC analysis

DSC measurements were carried out to investigate the chain folding behaviour of NPLA and its bio-composites in the presence of NS and Luban gum (G). The obtained second heating curves are depicted in Fig. 4.5, and the different thermal properties parameters are listed in Table 4.1. The glass transition temperature (T_g) values of NPLA (59.1 ºC) and its composites with and without 'G' are similar, which signifies the similar secondary chain relaxation behaviour. Similarly, the melting temperature (T_m) values of NPLA (152.4 ºC) and its composites with and without 'G' are identical, which indicates the similar melting nature of the crystallographic plane. The crystallisation temperature (T_c) of NPLA was 123.6 ºC. It was observed that with the addition of different weight percentages of NS and 'G' into the PLA matrix, the crystallisation temperature increases compared to NPLA (except for the PLA-SiO_2(2 wt.%)). It indicates that both the NS and the 'G' acted as good nucleating agents in the PLA matrix, which improved the crystallisation process.

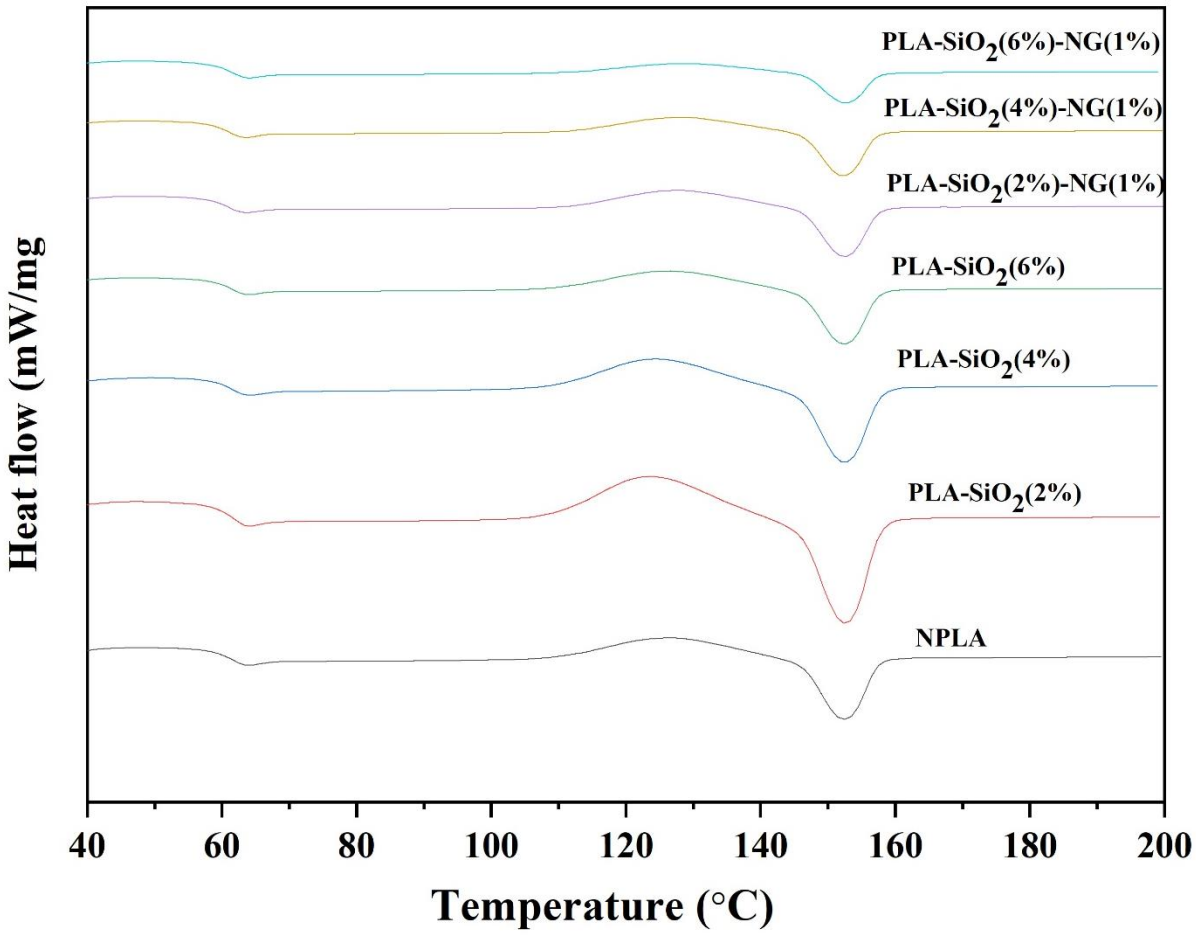

Fig. 4.5. DSC thermograms for neat PLA and its nanocomposites

Table 4.1 Thermal properties of NPLA and its nanocomposites from DSC analysis

Sample	T_g (°C)	T_c (°C)	T_m (°C)
NPLA	59.1	123.6	152.4
PLA-NS (2%)	59.4	123.8	152.6
PLA-NS (4%)	59.5	124.6	152.6
PLA-NS (6%)	59.3	126.5	152.6
PLA-NS (2%)-G (1%)	58.8	127.1	152.4
PLA-NS (4%)-G (1%)	58.8	127.6	152.4
PLA-NS (6%)-G (1%)	59.1	128.4	152.8

4.2.5. Mechanical property analysis

The tensile properties of the composites were studied extensively to assess the mechanical performance of the PLA-NS-based composites. The tensile strength results of the composites are shown in Fig. 4.6. (a, b), and the effect of NS loading with and without the presence of Luban gum (G) on the strength and modulus are presented in Table 4.2. The ultimate tensile strength (UTS) and Young's modulus (Y) of the pristine PLA (NPLA) were 36.1 MPa and 1013.7 MPa, respectively. It can be observed that with the addition of NS (for the loading of 2, 4, and 6 wt.%) in PLA without gum, both the strength and the modulus are increased—the incorporation of 2 wt.% NS in PLA, 8.6% increment of UTS, and 12.6% increment of Y were observed compared to NPLA. Similarly, for 4 wt.% of NS, an increment of 19.9% of UTS and 44.8% of Y was observed, and for 6 wt.% of NS, the increment of UTS and Y were 14.9% and 24.2%, respectively, compared to NPLA. This is probably because of the good interfacial adhesion between the filler and the matrix [143, 144]. NS could be effectively used as a filler in the PLA matrix to strengthen the interface. However, a slight decrement was observed in the UTS (4.15%) and Y (14.2%) values for the 6 wt.% NS in PLA compared to 4 wt.% NS in PLA. This is because of the aggregation between the nanoparticles for the higher loading of NS (6 wt.%). This aggregation could generate large cracks around the nanoparticles, which promotes the fracture failure of the composites. When the ‘G’ (1 wt.%) is added as a compatibiliser to the PLA-NS-based system, the tensile properties of the composites are increased rapidly. The maximum value of the UTS and Y of the composites (B7) are 51.6 MPa and 1923 MPa, respectively. This profound enhancement of the mechanical properties of the composites is because of the improvement of dispersion between the NS and the PLA matrix and the better orientation of the individual silica nanoparticles.

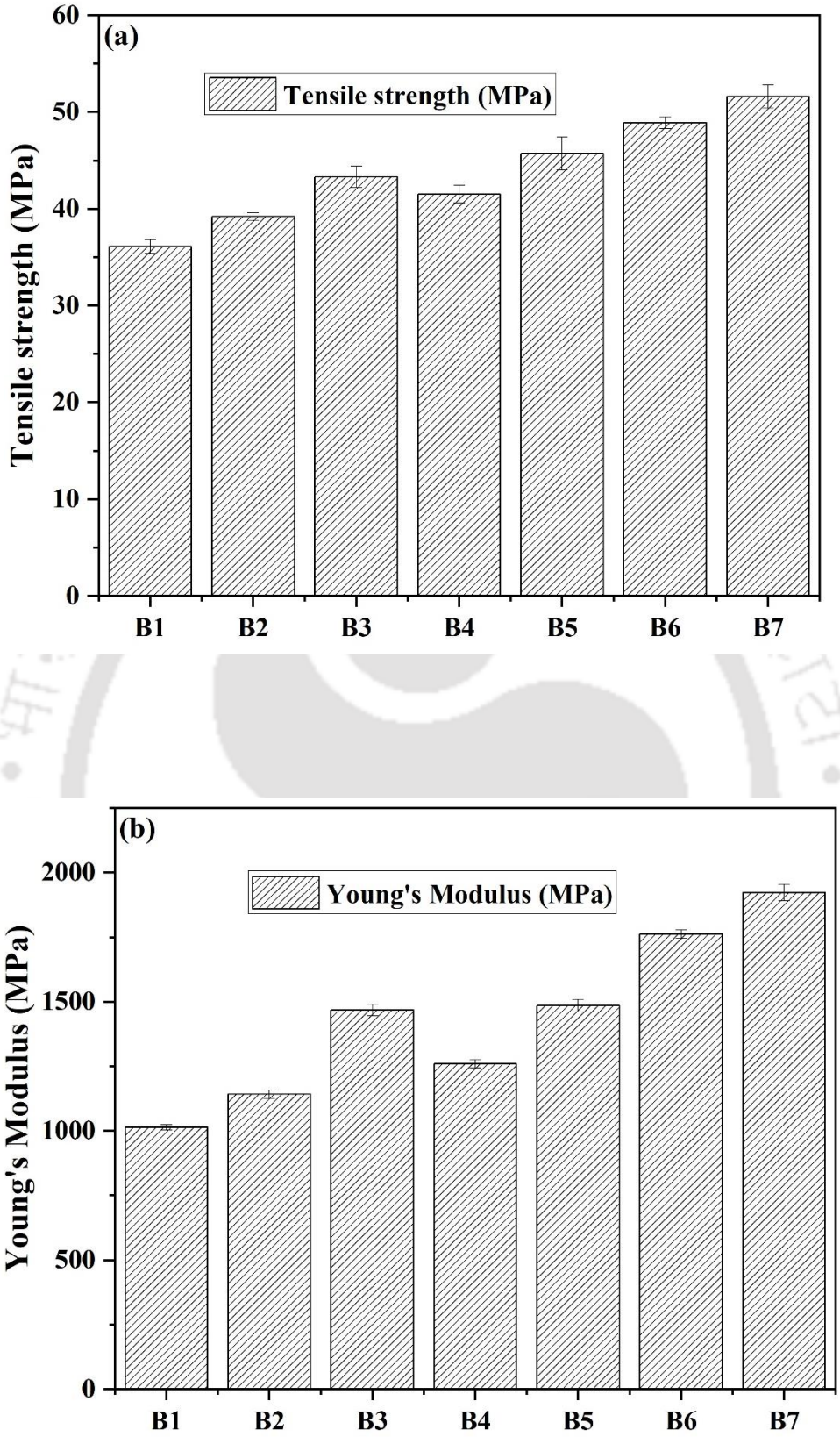

Fig. 4.6. Mechanical properties: **(a)** ultimate tensile strength (UTS), **(b)** Young's modulus (Y) of the extruded NPLA and its nanocomposites.

Table 4.2 Mechanical properties of NPLA and its nanocomposites from tensile analysis

Sample	Tensile strength (MPa)	Young's Modulus (MPa)
NPLA (B1)	36.1±0.7	1013.7± 10.6
PLA-NS (2%) (B2)	39.2±0.4	1142± 16.0
PLA-NS (4%) (B3)	43.3±1.1	1468± 22.0
PLA-NS (6%) (B4)	41.5±0.9	1259± 15.6
PLA-NS (2%)-G (1%) (B5)	45.7±1.7	1485± 24.0
PLA-NS (4%)-G (1%) (B6)	48.9±0.6	1762± 17.0
PLA-NS (6%)-G (1%) (B7)	51.6±1.2	1923± 32.0

4.2.6 Rheological property analysis

Parallel disc oscillatory shear test was performed to find the relationship between the melt rheological properties of the materials and their frequency at a specific temperature without affecting the internal structure of the materials. The storage modulus (G') and complex viscosity (η^*) of NPLA and its composites are shown in Fig. 4.7. (a, b) Dynamic rheological measurement performed at 180 °C in the frequency range of 0.1−500 rad/s within the viscoelastic region (5% strain is taken on the basis of the small amplitude strain sweep analysis). According to the linear viscoelastic theory, G' increase monotonically with an increase in angular frequency, ω, in the polymer composites. It could be clearly observed from Fig. 4.7 (a) that the PLA based bio-composites obey the linear viscoelastic theory showing an increase in G' with increasing ω. As the experiment was conducted at 180 °C, all the samples

were in the molten state. It implied that viscous nature was dominant in NPLA and its composites. On increasing the content of NS from 2→6 wt.%, the storage modulus, G' of the composites was almost found similar compares to NPLA. It was also observed that the incorporation of Luban gum (G) (1 wt.%) into the PLA-NS system resulted in a rapid increase in G' compared to NPLA. It suggested the characteristics of intense grafting.

The data of complex viscosity (η^*) as a function of angular frequency is displayed in Fig.4.7. (b) It was found that η^* decreased with an increase in ω for all the samples and a similar trend was observed for NPLA and PLA-NS based systems without gum. The samples showed Newtonian fluid-like behaviour when η^* was nearly independent of ω (ω $\leq$1 rad/s), and followed non-Newtonian fluid-like behaviour when η^* was dependent on ω (ω>1rad/s), which is termed as the Power-law region. In comparison to NPLA, the complex viscosity of the composites increased with an increase in the content of NS (2→6 wt.%), as addition of fillers hindered the movement of PLA chains.

In this study, NS acted as a reinforcing agent. Furthermore, when 'G' (1 wt.%) was added to the PLA-NS based systems, the complex viscosity enhanced even more. The reason for this pronounced improvement in complex viscosity is the effect of cross-linking and long chain branching due to the formation of entangled networks by the restriction of mobility of the macromolecules. Shear thinning behaviour was observed in all the samples of NPLA and its composites.

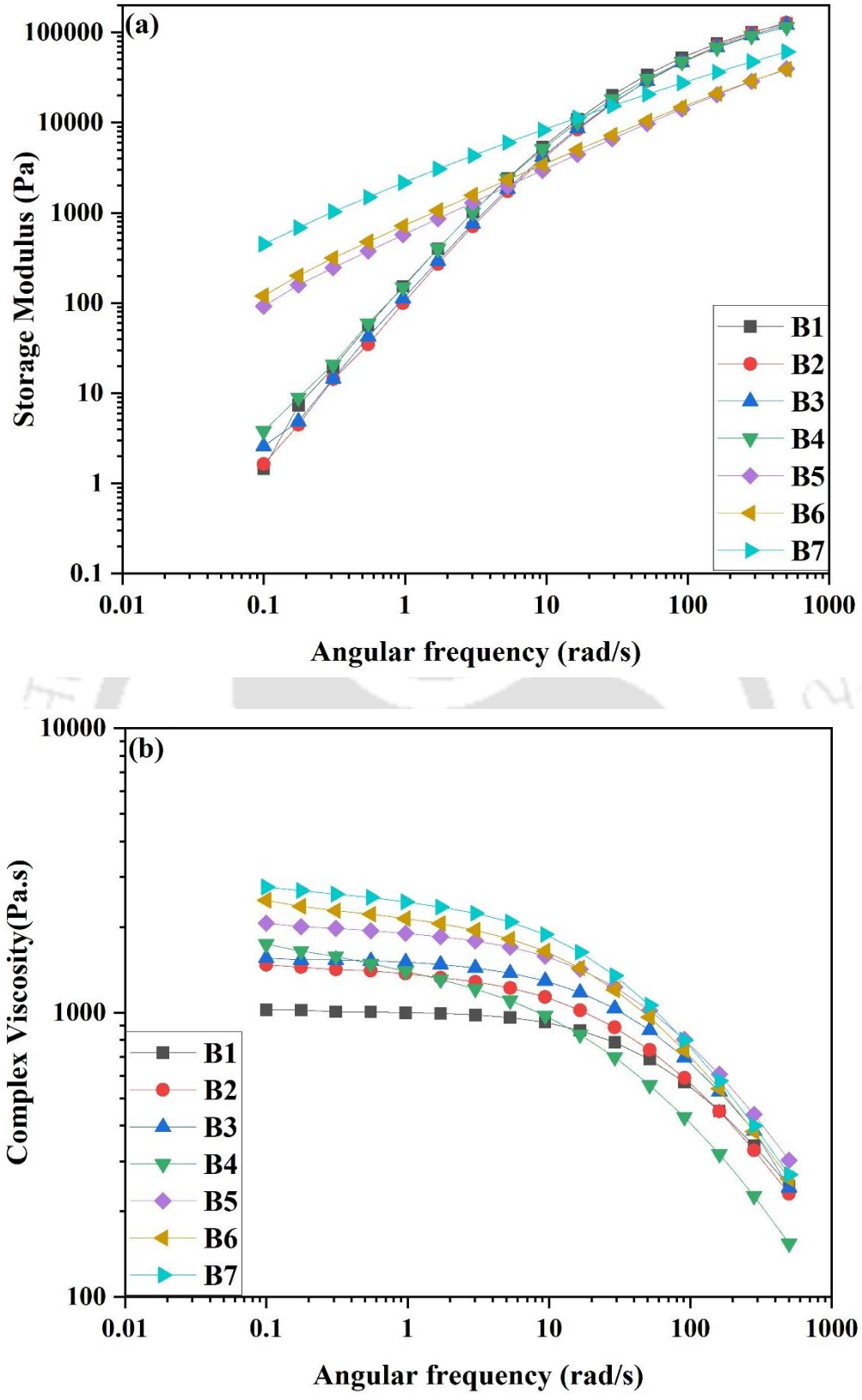

Fig. 4.7. Rheological properties: **(a)** storage modulus, and **(b)** complex viscosity of neat PLA and its nanocomposites.

4.3 CONCLUSIONS

In this work, nano-silica (NS) was isolated from an agricultural waste, RS, and was used as a filler to prepare the PLA-based nanocomposites using Luban gum (G) as a compatibiliser. Morphological, thermal, mechanical, and rheological properties of the nanocomposites were characterized extensively. XRD studies showed that adding NS and 'G' into the PLA matrix enhanced the crystallinity of the nanocomposites compared to NPLA. Morphological properties of the nanocomposites depict that adding 'G' improves the miscibility between the sphere-shaped NS and the PLA matrix. With the addition of different weight percentages of NS into the PLA matrix, both the values of UTS and Y increased. For instance, 6 wt.% of NS, the increment of UTS and Y were 14.9% and 22.8%, respectively, compared to NPLA. This is probably because of the good interfacial adhesion between the filler and the matrix. NS could be effectively used as a filler in the PLA matrix to strengthen the interface. The glass transition temperature, T_g, and the melting temperature, T_m, of the nanocomposites were almost identical, which signifies the similar secondary chain relaxation behaviour and the similar melting nature, respectively. But, the crystallisation temperature, T_c of the nanocomposites increased progressively with the addition of different percentages of the weight of NS and 'G' due to the nucleation effect. The results of the rheological tests indicated a rapid increase of the storage modulus, G', and the complex viscosity of the nanocomposites with the addition of 'G', which improves the melt strength of the nanocomposites. Shear thinning behaviour was observed. Finally, the PLA-NS-based nanocomposites with the presence of 'G' have the true potential for application in the packaging field.

Chapter 5

Extraction of Cellulose nanocrystals (CNC) from Rice Straw (RS)) and fabrication and characterisation of Poly (lactic acid) (PLA) – CNC based bio-nanocomposites by Melt Extrusion Process

Abstract

The present study reports a single-step melt extrusion process for the fabrication of poly (lactic acid) (PLA) and cellulose nanocrystal (CNC) based bio-nanocomposites using maleic anhydride (MA) as a compatibiliser. A rice-grain-like morphology of CNC (diameter: 40±5 nm; length: 300±15 nm) was observed, extracted from the waste rice straw (RS) by the acid hydrolysis (64 wt.% of H_2SO_4) treatment followed by alkali and bleaching process. Thermogravimetric analysis (TGA) showed that incorporating nanofiller, CNC improved the thermal stability of the bio-composites. The value of different thermal properties from the DSC analysis showed that the glass transition temperature (T_g) and melting temperature (T_m) of the bio-composites with varying percentages of the weight of CNC are almost identical. In contrast, due to the nucleation effect, the cold crystallisation temperature (T_{cc}) of the PLA-CNC-based systems decreased progressively with and without MA. The addition of MA (3 wt.%) into the PLA-CNC-based composites increased both the value of tensile strength (UTS) and Young's modulus (Y) because of the improvement of the dispersion of CNC into the PLA matrix. Rheological investigation of the bio-composites showed storage modulus (G') <loss modulus (G") over the angular frequency (ω) range until crossover, corroborating the viscous behaviour of the samples. The complex viscosity, η', was constant when ω<1 rad/s for all the samples, showing Newtonian characteristics. Shear thinning behaviour was observed when ω>1 rad/s.

GRAPHICAL ABSTRACT:

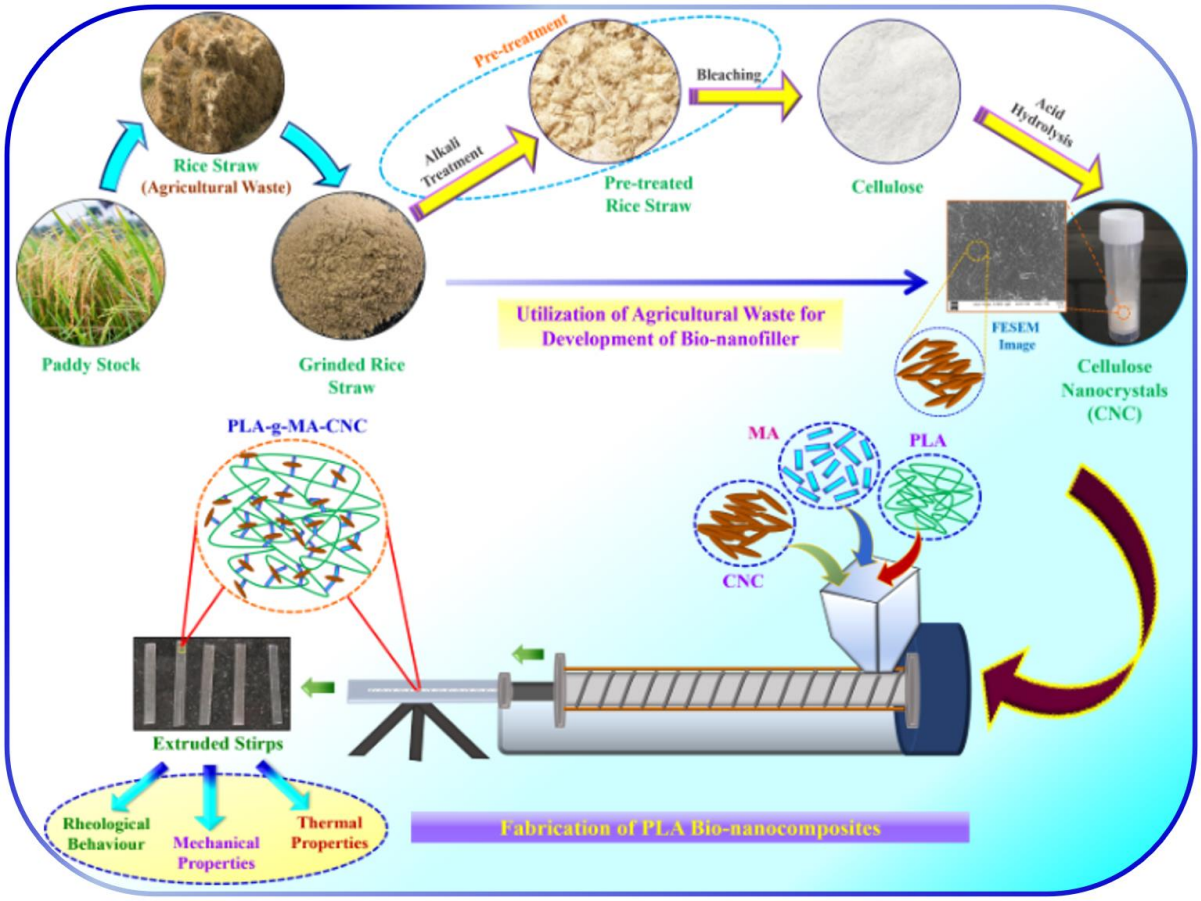

5.1 INTRODUCTION

With the rising prices of petrochemicals and the depletion of fossil fuel resources, the quest to develop green, sustainable, biodegradable polymers, nanomaterials, and composites from renewable resources has increased extensively as petroleum-derived products are a severe cause of concern for global warming [81-83]. Nowadays, biodegradable polymers are gaining importance to researchers as they have several significant applications in the biomedical, structural, and packaging fields and are a prospective replacement for synthetic polymeric products [84]. Poly (lactic acid) (PLA), a biobased linear thermoplastic polyester prepared from lactic acid, has gained considerable interest in the commercial market [118] because of its biocompatibility, easy processability, and comparable mechanical properties, thermal properties to the conventional non-biodegradable synthetic plastics [119-121]. However, brittle in nature, poor melt strength, poor gas barrier properties, poor thermal stability, and heat distortion temperature (~ 55°C) restrict its applications for manufacturing commodity products [122-123]. Chemical modifications, including copolymerization and blending with other biodegradable polymers, such as poly (butylene succinate) (PBS), poly (caprolactone) (PCL) [145], poly(hydroxybutyrate) (PHB) [146], are the widely used strategies for the improvement of the properties of PLA such as toughness, heat distortion temperature (HDT), compatibility and crystallization rate. But require a large addition ratio, which restricts its industrial uses. Therefore, adding various nanofillers into the PLA matrix, another blending method has been processed rapidly for the last decades [147].

Among these nanofillers, scientists are fascinated with cellulose nanocrystals (CNCs) as they are biodegradable, non-abrasive, non-toxic, and biocompatible [148-150]. Hydrogel, surface coating materials, and reinforcing agents for developing green nanocomposites are some of the typical applications of CNCs. Fabrication of CNCs from various lignocellulosic biomass resources [151], i.e., agricultural wastes, municipal wastes, food wastes, and forest residues, is

currently the need of interest in research, extracted by the acid hydrolysis method of the crystalline part of cellulose. Many studies have been found on the production of CNCs from various agricultural wastes, i.e., coconut husk fibres, banana rachis, soybean pods, soy hulls, and corn stalks. Although, the utilization of rice straw (RS) for producing CNCs as a natural resource has yet to be widely researched. Rice is the largest cereal crop in the world. Amongst these, RS accounts for 45% of the total volume of rice production. The composition of RS consists of 38.3% cellulose, 31% hemicellulose, 11.8% lignin, and 18.3% silica, and it has the high cellulose content available in the crop residues of the world. Usually, rice millers dispose of and burn rice straw waste in an open environment, creating a severe environmental threat to society. As a result, this high cellulosic source-based rice straw waste can be utilised to extract CNCs, a value-added product. The rod-shaped structure, abundant hydroxyl groups, large surface area, and high flexural rigidity make CNCs an ideal reinforcing agent in the thermoplastics polymer matrix such as PLA to develop high-performance and lightweight nanocomposites.

Several studies have reported that the hydrophobic PLA matrix and hydrophilic CNC have shown poor compatibility, causing nonhomogeneous dispersion of CNCs in the PLA matrix, leading to a decrease in the mechanical strength of PLA [152-154]. As a result, different hydrophobic treatments like acetylation [155], lactic acid graft [156], and acetate [157] were performed to better compatibility between the matrix and the filler. However, the improvement of the mechanical properties was limited due to the weak chemical interaction between the matrix and fillers.

Reactive compatibilization in the presence of a compatibilizer is one method in which the compatibility between the matrix and the filler is improved during melt processing [158-160]. A compatibilizer could enhance interfacial adhesion by reducing the interfacial tension between the two immiscible phases, improving the mechanical properties of the composites.

Presently, maleic anhydride (MA) is among the well-known compatibilizing agents used on bio-composites because of its low toxicity and good chemical reactivity [161]. Several studies have been reported on the grafting of MA as a compatibilizer onto polyolefins during melt processing [162, 163].

The perspective of this research is to extract the CNC from the agricultural waste, RS, by acid hydrolysis process, which has been used as a reinforcing agent to prepare PLA/CNC-based bio-composites by melt extrusion. This study uses maleic anhydride (MA) as a compatibilizer on the bio-composites to improve the interfacial adhesion between the matrix and fillers. We report a one-step reactive compatibilization process for the fabrication of bio-composites. The impact of different loadings of CNC on the melt-extruded PLA-based bio-composites, with or without MA content, was studied extensively. The influence of varying CNC concentrations on the morphological, thermal, mechanical, and rheological properties of the nanocomposites was analysed.

5.2 RESULTS AND DISCUSSIONS

5.2.1. Characterisation of CNC

The surface morphology of the acid hydrolysed CNC extracted from RS is investigated using the FESEM image as shown in Fig 5.1. (a). Rice grain-like morphology is observed in the CNCs with an average diameter of 40±5 nm and an average length of 300±15 nm. However, due to the strong intermolecular hydrogen bonding of CNCs, agglomeration was observed.

The FTIR spectra of CNCs, as shown in Fig 5.1. (b), showed prominent peaks at 1430 and 1372 cm^{-1} corresponding to symmetric $-CH_2$ bending, $-CH_2$ wagging, respectively. The absorbance bands at 2902 and 1640 cm^{-1} indicate the presence of C−H and O−H groups, respectively. The band at 1163 cm^{-1} corresponds to −C−O−C− asymmetric stretching of β-glucosidic linkages, C−OH stretching in a plane at C-6, which is evident for CNC. The peak at 1059 and 897 cm^{-1} represents the stretching vibration of the −C−O−C− pyranose ring and −CH vibration of β-glucosides of CNC [164]. Stretching vibration of free O−H groups and adsorbed water were observed by a broad peak from 3400-3200 cm^{-1}.

Fig 5.1. (c) exhibits the crystalline structure of CNC. The XRD pattern of the fabricated CNC shows peaks at 14.6°, 16.5°, 22.5° and 34.4°, which corresponds to the (1 1 0), (1 1 0), (2 0 0), (0 0 4) planes respectively, representing the cellulose I crystal structure. The peaks at 12.5° and 20.0º represent the cellulose II structure [165]. Two different intensified cellulosic polymorphs (cellulose I and cellulose II) were observed in CNCs, and this could be due to the pre-treatment processing steps.

The thermal degradation profile of CNC, as shown in Fig. 5.1.(d) generally follows two states of degradation, the first and second steps of degradation following the ranges of 100−200 and 250−500 °C representing the removal of moisture and sulphates and the degradation of cellulose, respectively. A TGA investigation for CNC materials was carried out to determine

their change in weight with respect to change in temperature: only 4 and 11 wt. % losses in the product occur in the temperature ranges 100-200 and 290-380°C, respectively. Further, cellulose generally shows a loss of inbound water at a higher temperature of around 100-200°C.

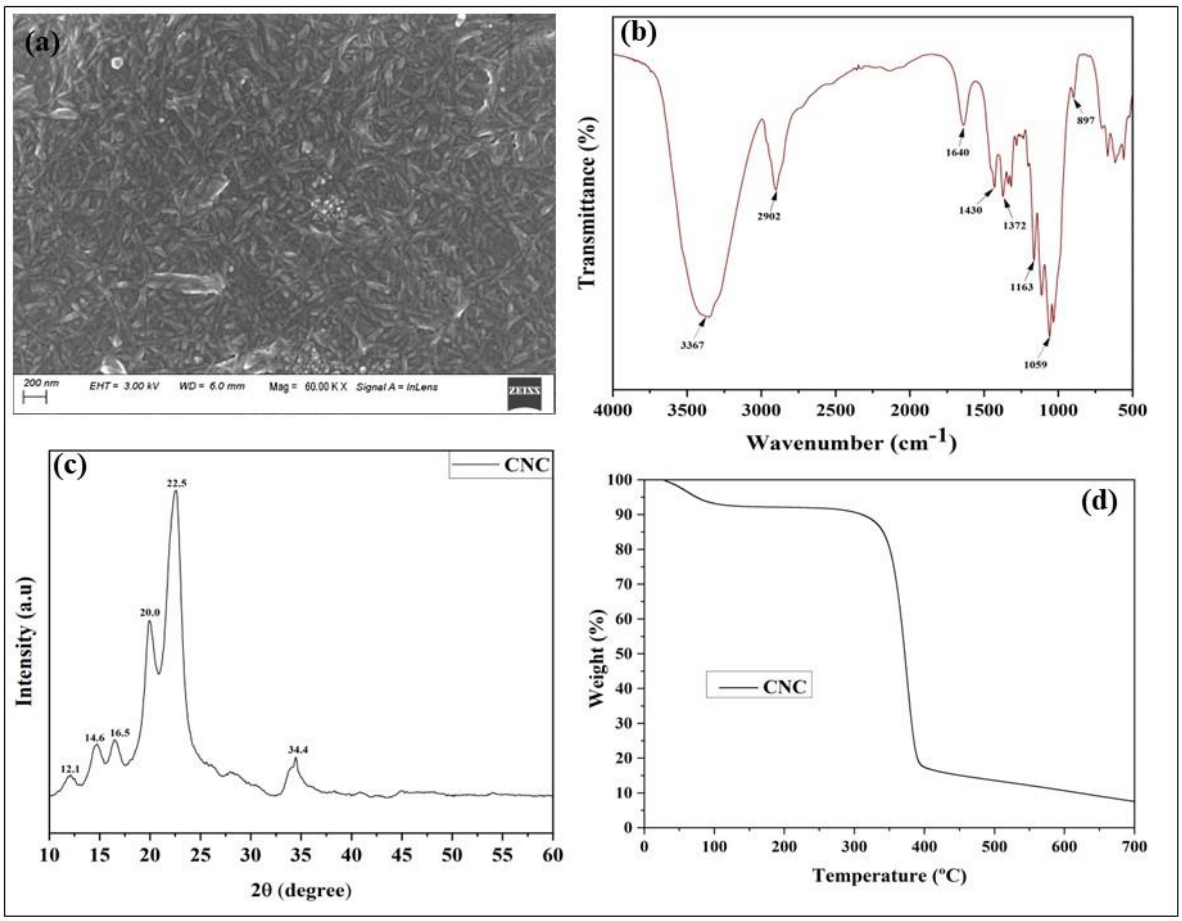

Fig. 5.1. (a) FESEM micrograph of the fabricated CNC, extracted from RS through sulphuric acid hydrolysis, **(b)** FTIR spectrum of CNC, **(c)** XRD pattern of CNC, **(d)** TGA profile of CNC.

5.2.2 FTIR analysis

FTIR analysis is used to characterise the chemical structure of the PLA and its bio nanocomposites. Fig. 5.2. shows the FTIR spectra of the bio-composites. Generally, PLA showed four typical chemical groups, i.e., $-CH_3$, $-CH$, $-C-O-C-$, $-C=O$ [142]. The FTIR peaks at 1749, 1265, 1181, 1129, 1080, 1042, 956, 868 cm^{-1} corresponding to $-C=O$ stretching of aliphatic ester, asymmetric and symmetric stretching vibration of $-C-O-C-$, side group vibrations of $C-OH$, $C-C$ stretching vibration and $-CH$ stretching are the typical characteristic peaks of PLA. The peaks at 2995, 1450, and 1382 cm^{-1} corresponded to $-CH$ vibration, asymmetric vibration of $-CH_3$, and deformation of $-CH_3$ groups, respectively. The peaks at 2945 and 1360 cm^{-1} represent the asymmetric stretching and bending vibration of the $-CH$ group, respectively. Asymmetric and symmetric stretching vibrations of $-CH_2$ from CNC are observed at 2923 cm^{-1} and 2852 cm^{-1}. It could be concluded that adding MA into the PLA-CNC-based composites doesn't alter or shift the peak position.

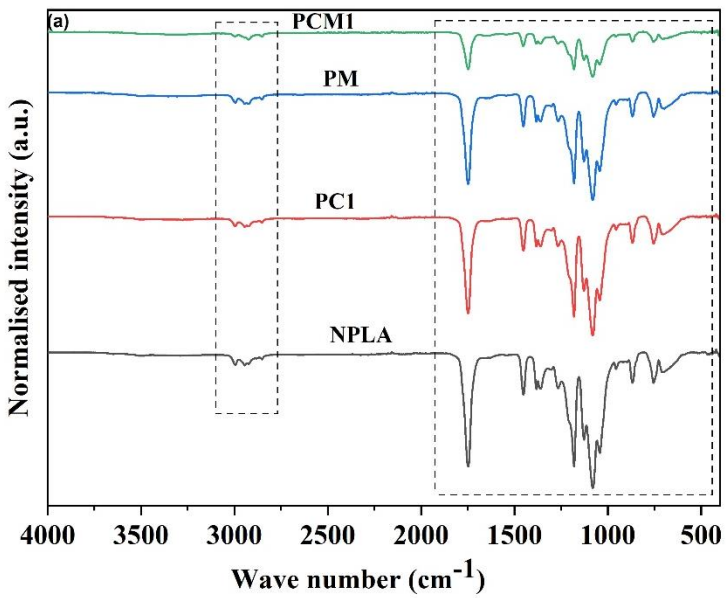

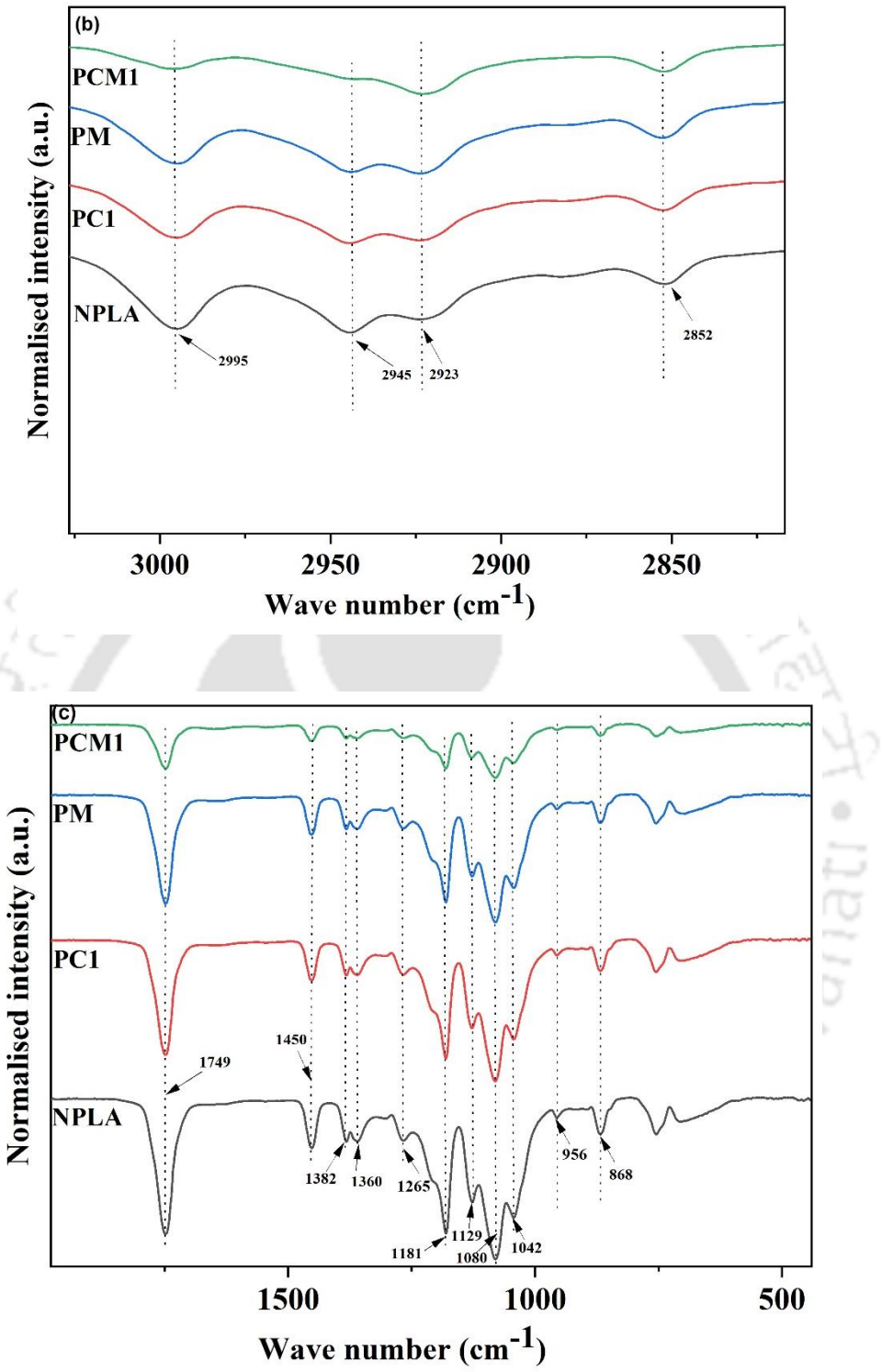

Fig. 5.2. (a) Comparison of FTIR spectrogram of neat PLA and its bio-composites with the selected regions (marked in black boxes) analysed at **(b)** 3000-2700 cm^{-1} **(c)** 2000-500 cm^{-1} wavenumber range and the representative peaks marked with black arrows.

5.2.3 XRD analysis

XRD studies were carried out to investigate the crystal structure of the nanocomposites. Fig. 5.3. shows the XRD patterns of the PLA-CNC-based nanocomposites in the presence of a compatibiliser, MA. PLA showed a representative peak at 16.4º and 18.8º corresponding to the α form of the PLA crystal with (010) and (110/200) planes [166]. Although there is no marked difference in the diffraction angle at 16.4º for all the nanocomposites, the incorporation of the nanofiller, CNC, into the PLA matrix led to an increase in the intensity of the diffraction peak at 16.4º. It suggests an enhancement of the crystallinity of PLA [166, 167]. This is because of the formation of C−C bonds between the PLA matrix and the CNCs. This enhancement in the crystallinity of the PLA-CNC-based composites is even more when MA is added to the system. This is due to the ordered arrangement of the amorphous PLA chains on the CNC surface, which increases the crystallinity of the nanocomposites. The diffraction peak at 22.3º confirms the presence of CNC in the PLAgMA corresponding to the cellulose I crystal structure.

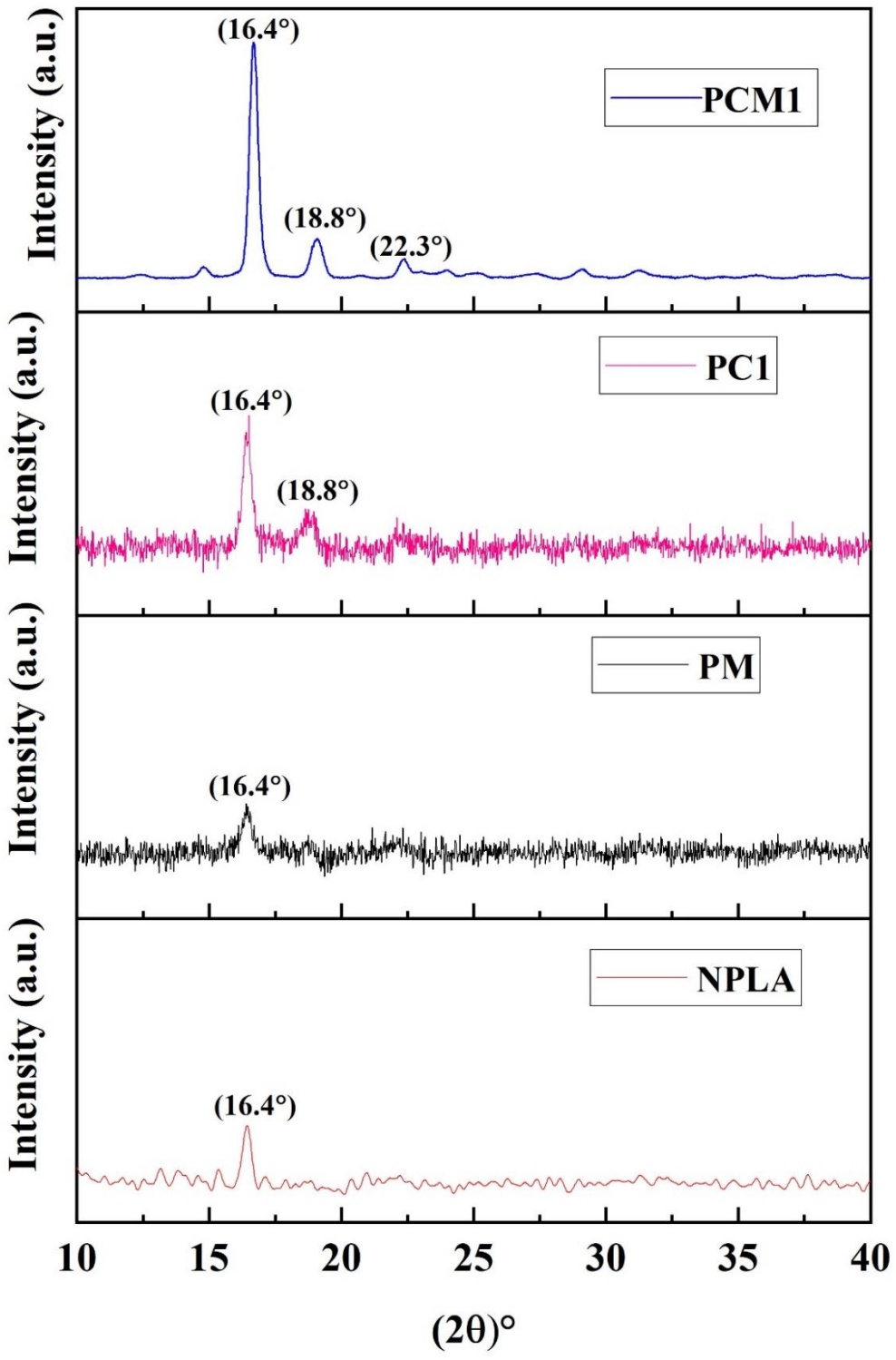

Fig. 5.3. XRD diffraction patterns of neat PLA and its bio-composites.

5.2.4 TGA analysis

Thermogravimetric Analysis (TGA) is used to determine the thermal stability of a polymer and its composites. TGA analysis was done to investigate the different thermal stability parameters, such as T_{10} (the temperature at which 10% weight loss occurs) and T_{max} (maximum decomposition temperature) of the extruded samples. The values of these parameters are given in Table 5.1. Fig. 5.4. (a) & (b) depicts the thermal behaviour with TGA and DTG thermograms of the PLA-CNC-based bio-composites with and without MA. All the samples follow a two-stage degradation process, as depicted in Fig. 5.4. (b), revealed by the first derivative thermograms. The value of T_{10} of NPLA was 339.3ºC. Adding different weight percentages of CNCs (2,4,6 wt.%) without a compatibiliser (MA) into PLA improves the thermal stability of the bio-composites, and all the thermal stability parameters are shifted to a higher temperature. The T_{10} value of PC1 (PLA-CNC(1wt.%)), PC2 (PLA-CNC(2wt.%)) and PC3 (PLA-CNC(3wt.%)) was increased by 7.8 ºC, 8.2 ºC, and 16.9 ºC compared to NPLA. The T_{max} values of the composites also follow a similar trend compared to NPLA. It implies that the enhancement in thermal stability was due to the incorporation of the nanofiller, CNCs into the PLA matrix. This is possibly due to the good interfacial adhesion between the matrix and the filler and also because of the rice grain-like morphology of CNCs, which retards the emission of the degraded gas. On the contrary, the incorporation of MA into the PLA-CNC-based systems had little effect on the thermal stability of the bio-composites compared to the effect of CNC on the PLA matrix. The $T_{10,}$ T_{max} values of the bio-composites have not much changed after the addition of MA.

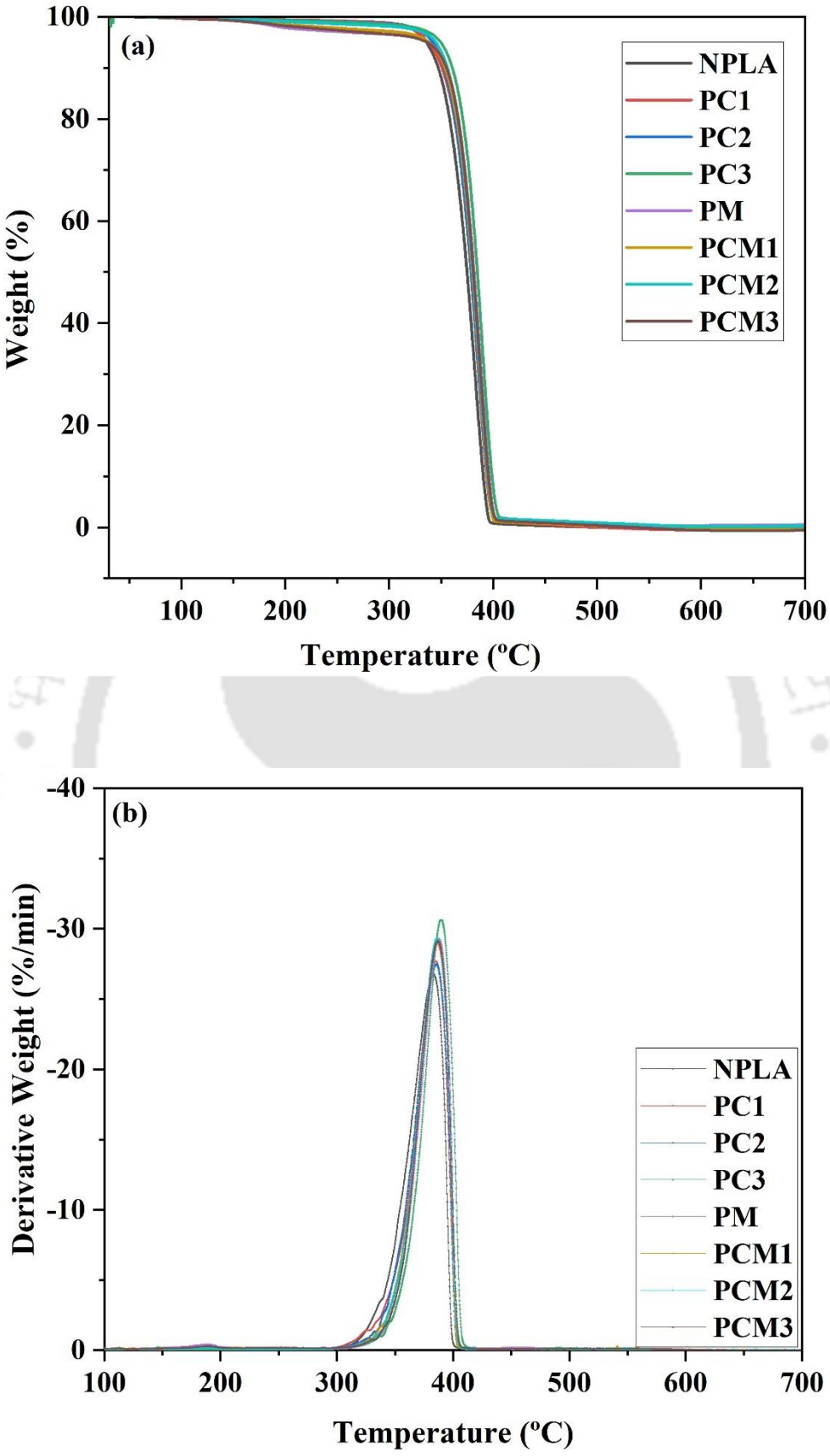

Fig. 5.4. Comparison of **(a)** TGA and **(b)** DTG curves of neat PLA and its bio-composites

Table 5.1 Thermal stability parameters of NPLA and its composites from TGA analysis

Sample	T_{10} (°C)	T_{max}(°C)
NPLA	339.3	383.5
PC1	347.1	385.1
PC2	347.5	385.9
PC3	356.2	389.5
PM	352.6	387.9
PCM1	349.1	386.7
PCM2	352.3	386.1
PCM3	349.3	386.6

5.2.5 DSC analysis

DSC measurements were carried out to investigate the chain folding behaviour of NPLA and its bio-composites in the presence of CNC and MA. The obtained second heating curves are depicted in Fig. 5.5., and the different thermal properties parameters are listed in Table 5.2. The glass transition temperature (T_g) values of NPLA (61.5 °C) and PLA-CNC-based composites are similar, which signifies the similar secondary chain relaxation behaviour. With the addition of MA into the PLA-CNC-based systems, the T_g values are slightly decreased compared to PLA-CNC blends without MA. This could be attributed to the plasticizing effect of MA. The cold crystallisation temperature (T_{cc}) values of the PLA-CNC-based systems with and without MA decreased progressively compared to NPLA (123.9 °C). This is probably due to the increased polymer chain mobility or the nucleation effect. The melting temperature (T_m) values of NPLA (166.9 °C) and PLA-CNC-based composites without MA are identical, which indicates the similar melting nature of the crystallographic plane. In addition, a double melting peak was observed in the PLA-CNC-based bio-composites with and without compatibilization. The low (T_{m1}) and high (T_{m2}) melting temperature peaks corresponded to the α′and α crystals,

indicating the polymorphism of PLA [168]. The crystallisation temperature of NPLA was 123.6 ºC.

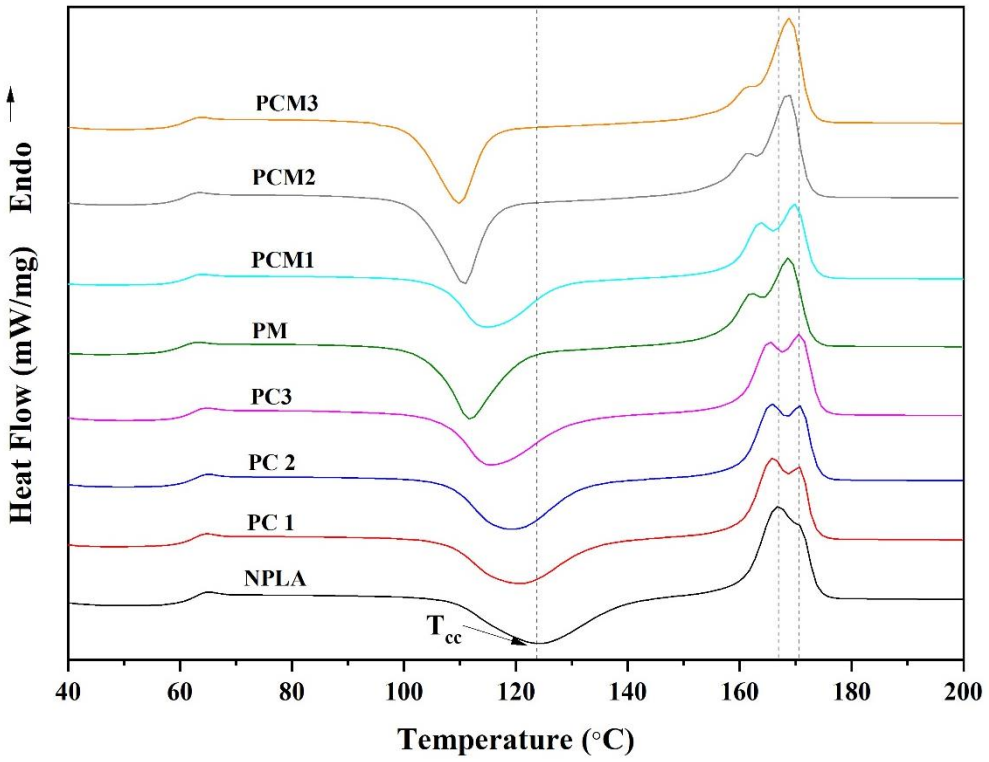

Fig. 5.5. DSC thermograms for neat PLA and its bio-composites

Table 5.2 Thermal properties of PLA and its bio-composites from DSC analysis

Sample	T_g (ºC)	T_{cc} (ºC)	T_m (ºC)
NPLA	61.5	123.9	166.9
PC1	60.9	120.6	166.0
PC2	61.5	119.5	165.8
PC3	60.2	115.7	165.4
PM	58.3	111.7	162.1
PCM1	59.2	114.7	163.8
PCM2	59.5	110.7	168.6
PCM3	59.5	109.9	168.8

5.2.6 *Mechanical property analysis*

The different mechanical properties, i.e., ultimate tensile strength (UTS) and Young's modulus (Y), give an idea about the plasticity and the toughness characteristics of a polymer and its composites. Figure 5.6. (a, b) displays the mechanical properties of pristine PLA and its bio-composites. Their average Ultimate tensile strength (UTS) and Young's modulus (Y) values are summarised in Table 5.3. NPLA presented a stiff and semi-ductile behaviour [153] with a UTS of 49.3 MPa, and YM of 1024.9 MPa. For PLA composites, the incorporation of CNCs (PC) did not improve but resulted in continuously decreased UTS and Y with the increased CNC loadings (1→3 wt.%). For instance, UTS decreased from 49.3 MPa of neat PLA to 37.9 MPa of PLA with 3 wt.% CNC addition (23.1% decrement); similarly, Y decreased from 1024.9 MPa to 815.6 MPa with the addition of 3 wt.% CNC (20.4% decrement). This is probably because of the poor dispersion of CNCs in the PLA matrix and the poor interfacial adhesion between them, generating stress concentration at the interface [169]. When the compatibiliser, MA, is incorporated into the PLA matrix, the value of UTS and Y is increased compared to NPLA. It increases rapidly when it is incorporated into the PLA-CNC systems. For instance, the UTS value increased from 49.3 MPa of NPLA to 56.9 MPa with 3 wt.% CNC (15.4% increment) when MA (3 %) is added to the systems. Similarly, the increment of the Y was 12.8% compared to NPLA. This profound enhancement of the mechanical properties of the composites is because of the improvement of dispersion between the CNC and the PLA matrix and the better orientation of the individual CNCs.

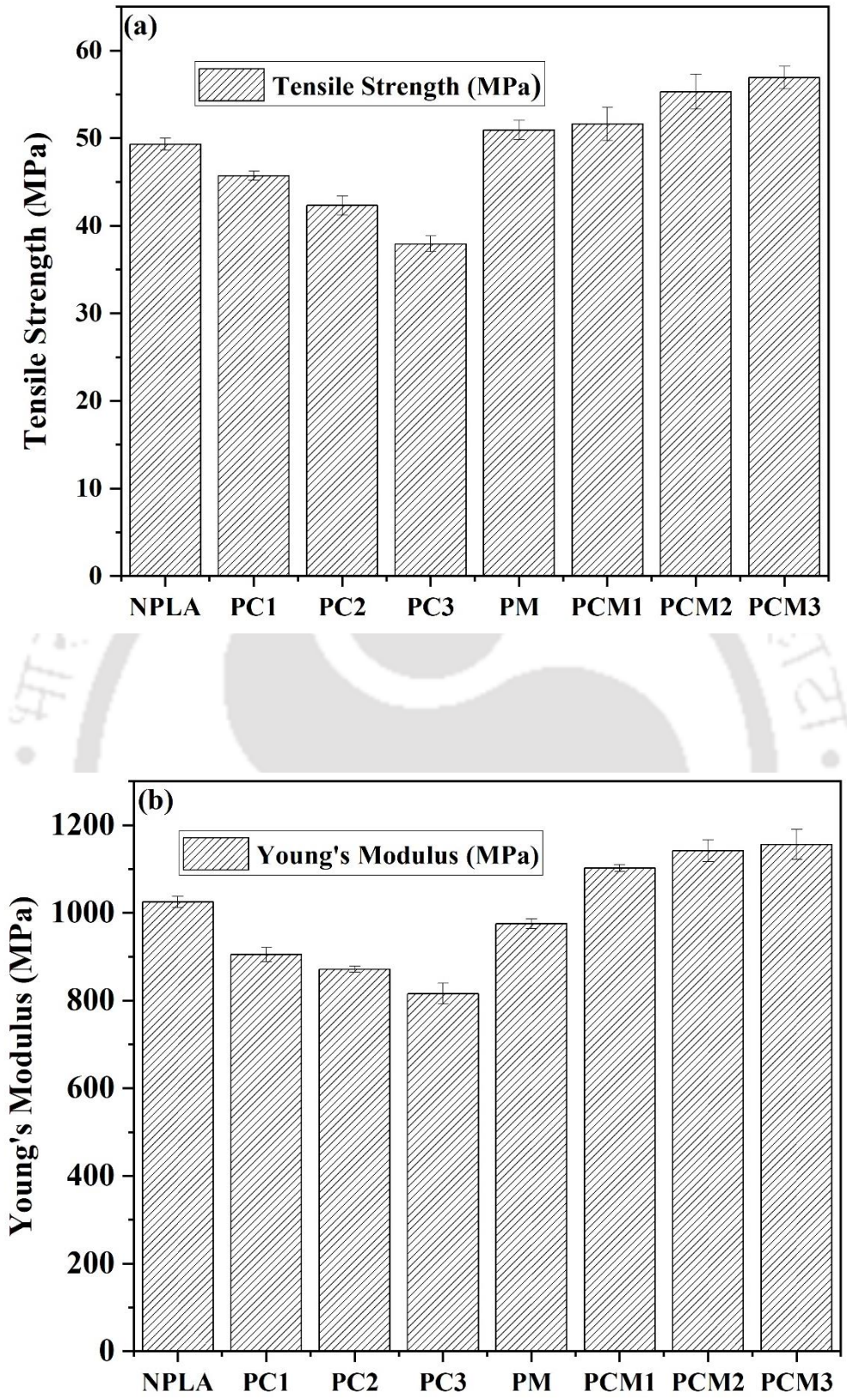

Fig. 5.6. Mechanical properties: **(a)** ultimate tensile strength (UTS), **(b)** Young's modulus (Y) of the extruded NPLA and its bio-composites.

Table 5.3 Mechanical properties of PLA and its bio-composites from tensile analysis

Sample	Tensile strength (MPa)	Young's Modulus (MPa)
NPLA	49.3± 0.7	1024.9± 12.8
PC1	45.7±0.5	904.7± 16.0
PC2	42.3±1.1	871.4± 7.0
PC3	37.9±0.9	815.6± 23.6
PM	50.9±1.1	974.5± 11.0
PCM1	51.6±1.9	1102± 8.0
PCM2	55.3±2.0	1142± 25.0
PCM3	56.9±1.3	1156± 34.0

5.2.7 Rheological property analysis

Parallel disc oscillatory shear test was performed to find the relationship between the melt rheological properties of the materials and their frequency at a specific temperature without affecting the internal structure of the materials. Dynamic rheological measurement performed at 180 °C in the frequency range of 0.1−500 rad/s within the viscoelastic region (5% strain is taken on the basis of the small amplitude strain sweep analysis). The storage modulus (G') and loss modulus (G") of NPLA and its composite samples are shown in Fig. 5.7. (a, b)

According to the linear viscoelastic theory, G' and G" increase monotonically with an increase in angular frequency, ω, in the polymer composites. It could be clearly observed from Fig. 5.7. (a, b) that the PLA based bio-composites obey the linear viscoelastic theory showing an increase in both G' and G" with increasing ω. As the experiment was conducted at 180 °C, all the samples were in the molten state. It implied that viscous nature was dominant in NPLA and

its composites when G' was less than G" for the samples over the frequency range until the crossover point. On increasing the content of CNC from 1-3 wt.%, both G' and G" increased slightly due to better dispersion of CNC on the PLA matrix. It was also observed that the incorporation of MA (3 wt.%) into the PLA-CNC system resulted in a rapid increase in G' and G".

The data of complex viscosity (η*) as a function of angular frequency is displayed in Fig. 5.8. It was found that η* decreased with an increase in ω for all the samples and a similar trend was observed for NPLA and PLA-CNC systems with and without MA. The samples showed Newtonian fluidlike behaviour when η* was nearly independent of ω ($\omega \leq 1$ rad/s), and followed non-Newtonian fluid-like behaviour when η* was dependent on ω ($\omega > 1$ rad/s), which is termed as the Power-law region. In comparison to NPLA, the complex viscosity of the composites increased with an increase in the content of CNC (1-3 wt.%), as the addition of the fillers hindered the movement of the PLA chains.

In this study, CNC acted as a reinforcing agent. Furthermore, when MA (3 wt.%) was added to the PLA-CNC based systems, the complex viscosity enhanced even more. The reason for this pronounced improvement in complex viscosity is the effect of cross-linking and long chain branching due to the formation of entangled networks by the restriction of mobility of the macromolecules. Shear thinning behaviour was observed in all the samples of NPLA and its bio-composites.

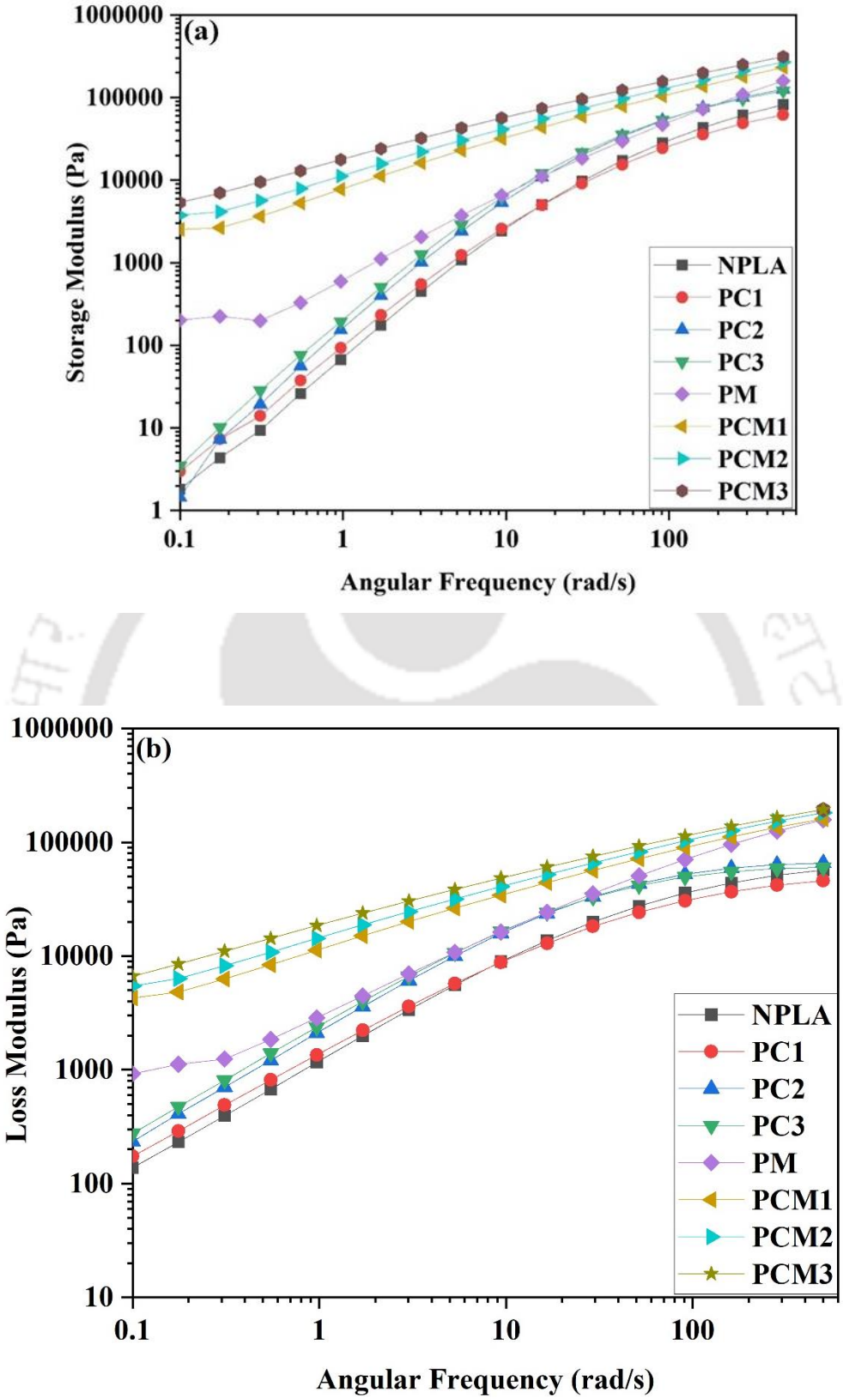

Fig. 5.7. Rheological property: **(a)** Storage modulus, **(b)** Loss modulus of neat PLA and its bio-composites.

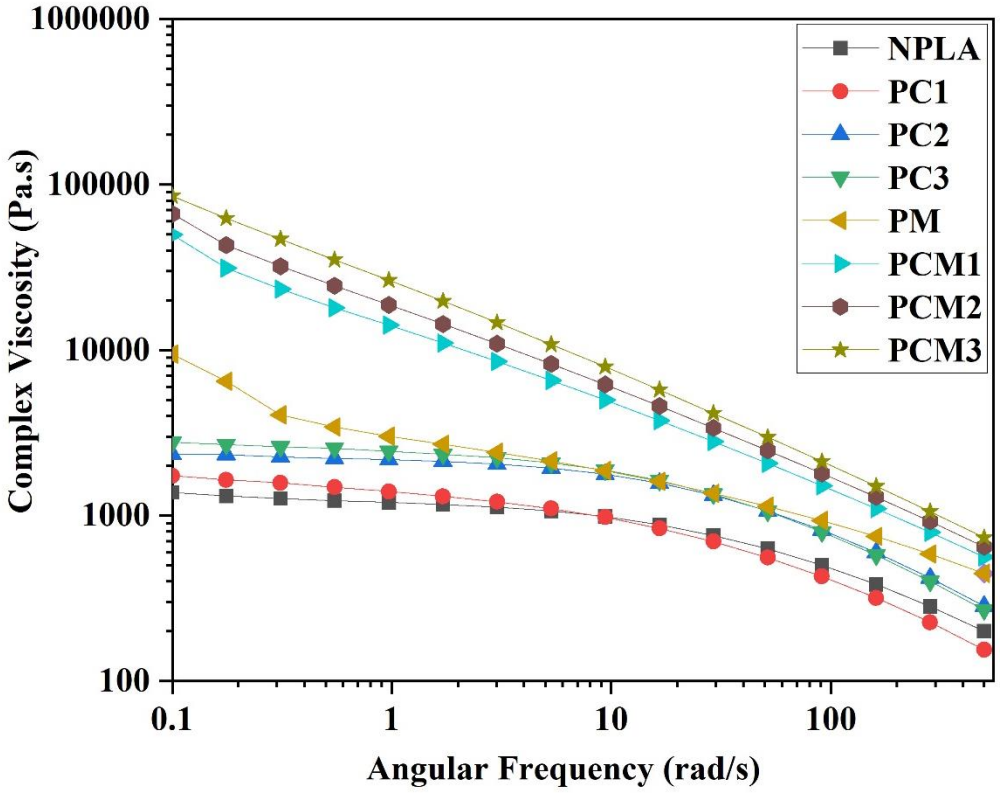

Fig. 5.8. Complex viscosity as a function of angular frequency (ω) of the extruded neat PLA and its bio-composites.

5.3 CONCLUSIONS

The present research describes the valorisation of agricultural waste (RS) and its conversion to a value-added product, CNC. In this study, PLA-CNC-based bio-nanocomposites were prepared by a melt extrusion process. The CNC and MA were used as nanofillers and compatibilising agents. Thermal, mechanical, and rheological properties of the bio-nanocomposites were characterized thoroughly. XRD studies showed an enhancement in the crystallinity of the bio-nanocomposites with the addition of CNC and MA. Incorporating MA (3 wt.%) into the PLA-CNC-based systems improved the mechanical properties of the nanocomposites due to the better dispersion of individual CNCs into the PLA matrix. For instance, the UTS value increased from 49.3 MPa of NPLA to 56.9 MPa with 3 wt.% CNC (15.4% increment) when MA (3 %) is added to the systems. Similarly, the increment of the Y was 12.8% compared to NPLA. The addition of nanofiller into the PLA matrix increased the thermal stability parameters of the nanocomposites due to the good interfacial adhesion between the matrix and the filler. All the thermal stability parameters are shifted to a higher temperature**.** The glass transition temperature (*Tg*) and melting temperature (*Tm*) of the bio-composites with varying percentages of the weight of CNC are almost identical. In contrast, due to the nucleation, the cold crystallisation temperature (*Tcc*) of the PLA-CNC-based systems decreased progressively with and without MA. Rheological investigation of the bio-composites showed storage modulus (G') <loss modulus (G") over the angular frequency (ω) range until crossover, corroborating the viscous behavior of the samples. The complex viscosity, η', was constant when ω<1 rad/s for all the samples, showing Newtonian characteristics. Shear thinning behavior was observed when ω>1 rad/s**.** Hence, it could be concluded that CNC was well dispersed on the PLA matrix, acted as a reinforcing agent, and increased the melt strength of the bio-composites. Finally, these extruded bio nanocomposites could be potential candidates in the packaging industry.

Chapter 6

Conclusions & Future Prospects

6.1 CONCLUSIONS

This chapter summarizes the key findings of the current research work and further provides future perspectives on the complex rheological behaviour of bio-composites and nanocomposites.

The main objective of the research work was to utilize agricultural waste in the form of rice straw (RS) to develop different polymeric composites which can be applied in the packaging field industry. The major innovations and diverse applications of the RSs presented in this thesis include: (i) the fabrication of silica nano particles from the extraction of renewable resources, followed by its utilization as reinforcing agents. (ii) development of CNCs from RS with a strategy to convert 'waste to wealth', followed by its utilization as a reinforcing agent. (iii) to develop completely 'green' and biodegradable polymeric nanocomposites for packaging applications. The research work presented in this thesis focuses on the influence of different nanofiller content on the thermal, mechanical, and rheological properties of the bio-composites and nanocomposites. The structure-properties relationship of the composites was explored in terms of the mechanical properties, thermal properties, crystallisation behaviour, and rheological properties. The major findings and conclusions drawn from the research work are summarized next.

- PBS-RSF based biodegradable polymer composites were prepared by the melt extrusion process wherein the agricultural waste, RSF was used as a bio-filler and DCP was used as a cross-linking agent. Morphological, thermal, mechanical and rheological properties of the bio-composites were characterized thoroughly. The thermal stability

of the bio-composites of PBS-RS1and PBS-RS2 improved with the addition of different loadings of RSF (5 wt.% and 10 wt.%) by a factor of 2 and 6 ºC as compare to the NPBS (367.6ºC) and all the thermal stability parameters are shifted towards the higher temperature, whereas the value of these parameters decreased slightly after the inclusion of DCP content into the PBS-RSF systems as compared to NPBS. The glass transition temperature (T_g) and the melting temperature (T_m) values of NPBS and its composites are identical which signifies the similar secondary chain relaxation behaviour and similar melting nature of the crystallographic plane respectively. Addition of RSF and DCP into the NPBS resulted in a shift of the crossover point to a lower frequency value, which indicated high polydispersity index and increased the molecular weight of the bio-composites. Furthermore, Han plot and Cole-Cole plot demonstrated uniform miscibility and good compatibility with similar stress relaxation time of RSF on the PBS matrix, respectively. Hence, it could be concluded that RSF was well dispersed on the PBS matrix and acted as a reinforcing agent and increased the melt strength of the bio-composites. In addition, RSF reduced the cost of PBS based product, and thus the products could be used in the packaging field.

- Nano-silica (NS) was isolated from an agricultural waste, RS, and was used as a filler to prepare the PLA-based nanocomposites using Luban gum (G) as a compatibilizer. With the addition of different weight percentages of NS into the PLA matrix, both the values of UTS and Y increased. For instance, 6 wt.% of NS, the increment of UTS and Y were 14.9% and 22.8%, respectively, compared to NPLA. This is probably because of the good interfacial adhesion between the filler and the matrix. NS could be effectively used as a filler in the PLA matrix to strengthen the interface. The crystallisation temperature, T_c of the nanocomposites increased progressively with the addition of different percentages of the weight of NS and LG due to the nucleation

effect. The PLA-NS-based nanocomposites with the presence of 'G' have the true potential for application in the packaging field.

- PLA-CNC-based bio-nanocomposites were prepared by a melt extrusion process. The CNC and MA were used as nanofillers and compatibilising agents. Incorporating MA (3 wt.%) into the PLA-CNC-based systems improved the mechanical properties of the nanocomposites due to the better dispersion of individual CNCs into the PLA matrix. The addition of nanofiller into the PLA matrix increased the thermal stability parameters of the nanocomposites due to the good interfacial adhesion between the matrix and the filler. All the thermal stability parameters are shifted to a higher temperature**.** The glass transition temperature (T_g) and melting temperature (T_m) of the bio-composites with varying percentages of the weight of CNC are almost identical. In contrast, due to the nucleation the effect was that the cold crystallisation temperature (T_{cc}) of the PLA-CNC-based systems decreased progressively with and without MA. Finally, these extruded bio nanocomposites could be potential candidates in the packaging industry.

6.2 FUTURE SCOPE OF RESEARCH

The work presented in the thesis can be further advanced in several directions as listed below.

- Development of a CNC based piezoelectric material for the application in the biomedical field.
- Fabrication of PLA-POSS based bio-composites through melt extrusion process.
- Fabrication of PLA/magnetic CNC based elastomers where different rheological models can be simulated to find the structure-property relationship.
- Chemical modification of CNC and preparation of magneto rheological fluid (MRF) and evaluation of their rheological properties.

Research Output

List of Publications:

Journals:

Sayan Kumar Bhattacharjee, Gourhari Chakraborty, Sourav Pratim Kashyap, Raghvendra Gupta, Vimal Katiyar. "Study of the Thermal, Mechanical and Melt Rheological Properties of Rice Straw Filled Poly (Butylene Succinate) Bio-composites Through Reactive Extrusion Process", *Journal of polymers and the environment*. https://doi.org/10.1007/s10924-020-01973-8.

"Investigation on thermal, mechanical, and rheological properties of Poly (lactic acid)/ cellulose nanocrystal (derived from rice straw) based bio-nanocomposites by melt extrusion process". (Manuscript under preparation).

"Isolation of nano silica from waste rice straw and studies on the structure-property relationship of Poly (lactic acid)- nano silica-based nanocomposites by melt extrusion process". (Manuscript under preparation).

Akhilesh Kumar Pal, **Sayan Bhattacharjee**, Surendra Singh Gaur, Ajinkya Pal, Vimal Katiyar. "Chemo-mechanical, morphological, and rheological studies of chitosan- graft -lactic acid oligomer reinforced poly (lactic acid) bio-nanocomposite films", *JAPS*, 135(3) 45546.

Kona Mondal, **Sayan Kumar Bhattacharjee**, Chethana Mudenur, Tabli Ghosh, Vaibhav V. Goud, Vimal Katiyar. "Development of antioxidant-rich edible active films and coatings incorporated with de-oiled ethanolic green algae extract: a candidate for prolonging the shelf life of fresh produce", *RSC Advances.* https://doi.org/10.1039/D2RA00949H.

Srijeeb Karmakar, Arjun Sankhla, Tabli Ghosh, **Sayan Bhattacharjee**, Vimal Katiyar. "Insulin biomolecular condensate formed in ionic microenvironment modulates the structural

properties of pristine and magnetic cellulosic nanomaterials", *Journal of Molecular Liquids*. https://doi.org/10.1016/j.molliq.2022.119580

Gourhari Chakraborty, **Sayan kumar Bhattacharjee**, G. Pugazhenthi, Vimal Katiyar. "Melt rheology analysis through experimental and constitutional mechanical models of exfoliated graphene based polylactic acid (PLA) nanocomposites", *Journal of Polymer Research***.** https://doi.org/10.1007/s10965-022-03353-3

Kona Mondal, **Sayan kumar Bhattacharjee**, Vaibhav V. Goud, Vimal Katiyar. "Effect of waste *Dunaliella tertiolecta* biomass ethanolic extract and turmeric essential oil on properties of guar gum-based active films", *Food Hydrocolloids.* https://doi.org/10.1016/j.foodhyd.2023.109199.

Book Chapter:

Gourhari Chakraborty, **Sayan Kumar Bhattacharjee**, Vimal Katiyar. Rheological Studies of Biodegradable composites, *Biodegradable Composites for Packaging Applications CRC Press* (2022).

Conference

Sayan Kumar Bhattacharjee, Raghvendra Gupta, Vimal Katiyar. Melt rheological properties of Rice Straw filled Polly (butylene succinate) Bio-composites through melt extrusion process. International Symposium on Sustainable Polymers & National Symposium on Chemistry Education for Sustainable Engineering (August 23-25, 2019), IIT Guwahati, Guwahati, India**.**

References

[1] Imre B, Pukánszky B (2013) Compatibilization in bio-based and biodegradable polymer blends, Eur. Polym. J. 49:1215−1233.

[2] Scott G (2000) Fundamentals, Representative Applications and Future Perspectives of Green Chemistry: A Short Review, 'Green' polymers, Polym.Degrad. Stab. 68: 1−7.

[3] Eling B, Gogolewski S, Pennings AJ (1982) Biodegradable materials of poly (l-lactic acid): 1. Melt-spun and solution-spun fibres, Polymer. 23:1587−1593.

[4] Shalumon KT, Anulekha KH, Chennazhi KP, Tamura H, Nair SV, Jayakumar R (2011) Fabrication of chitosan/poly (caprolactone) nano-fibrous scaffold for bone and skin tissue engineering, Int. J. Biol. Macromol. 48 (4): 571-576.

[5] Lee SH, Wang S (2006) Biodegradable polymers/ bamboo fiberbiocomposite with bio-based coupling agent. Compos. PartA Appl. Sci. Manuf. 37: 80–91.

[6] Lu X, Huang J, He G, Yang L, Zhang N, Zhao Y, Qu J (2013) Preparation and characterization of cross-linked poly (butylene succinate) by multifunctional TDI-TMP. Industrial & Engineering Chemistry. 52(38):13677–13684

[7] Wang H, Xu M, Wu Z, Zhang W, Ji J, Chu PK (2012) Biodegradable poly (butyelene succinate) modified by gas plasmas and their in vitro functions as bone implants, ACS Appl. Mater. Inter. 4 (8): 4380-4386.

[8] Satheesh Kumar MN, Mohanty AK, Erickson L, Misra M (2009) Lignin and its applications with polymers. J. Biobased Mater. Bioenergy. 3: 1-24, doi:10.1166/jbmb.2009.1001.

[9] Sahoo S, Misra M, Mohanty AK (2011) Enhanced properties of lignin-based biodegradable polymer composites using injection moulding process, Compos. Part A Appl. Sci. Manuf. 42: 1710–1718.

[10] Ray SS, Okamoto K, Okamoto M (2003) Structure-property relationship in biodegradable poly (butylene succinate)/ layered silicate nanocomposites, Macromolecules. 36 (7):2355-2367.

[11] Chen R, Zou W, Zhang H, Zhang G, Yang Z, Jin G, Qu J (2015) Thermal behaviour, dynamic mechanical properties and rheological properties of poly (butylene succinate) composites filled with nanometer calcium carbonate, Polymer Testing. 42: 160-167.

[12] Park BD, Wi SG, Lee KH, Singh AP, Yoon TH, Kim YS (2003) X-ray photoelectron spectroscopy of rice husk surface modified with maleated polypropylene and silane Biomass Bioenerg 25(319).

[13] Bakker R, Elbersen W, Poppens R, Lesschen JP, (2013) Rice straw and Wheat straw. Potential feedstocks for the Biobased Economy. Wageningen UR, Food & Biobased Research.

[14] Rahman MH, Bhoi PR (2021) An overview of non-biodegradable bioplastics. J. Clean Prod 294: .https://doi.org/10.1016/j.jclepro.2021.126218

[15] Ahmed T, Shahid M, Azeem F, Rasul I, Shah AA, Noman M, Hameed A, Manzoor N, Manzoor I, Muhammad S (2018) Biodegradation of plastics: current scenario and future prospects for environmental safety. Environ Sci Pollut Res 25:7287-7298.

[16] Shah AA, Hasan F, Hameed A, Ahmed S (2008) Biological degradation of plastics: A comprehensive review: Biotechnol Adv 26:246-265

[17] Plastics-the Facts 2016: an Analysis of European Plastics Production, Demand and waste Data Plastics Europe (2016).

[18] Bioplastics market data, 2020 Bioplastics market data European Bioplastics. https://www.european-bioplastics.org/market/ (2020).

[19] Kumar et al. (2017) Bioplastic classification, production and their potential food applications, Journal of hill agriculture, 8, 118-129.

[20] Tachibana et al. (2009) Utilization of a biodegradable mulch sheet produced from Poly (lactic acid)/ecoflex/modified starch in mandarin orange groves, International Journal of molecular science 10: 3599-3615.

[21] Aguiree et al. (2016) Poly (lactic acid) – mass production, processing, industrial applications, and end of life, Advanced Drug Delivery System 107: 333-336.

[22] Hamad et al. (2015) Properties and mecial applications of poly (lactic acid): A review, eExpress Polymer Letters 9: 435-455.

[23] Brigham et al. (2012) Applications, Applications of poly (hydroxyalkanoates) in the medical industry, International Journal of Biotechnology for wellness Industries 1: 53-60.

[24] Auras et al. (2004) An overview of polylactide as packaging materials, Macromolecular Bioscience 4: 836-864.

[25] Muthuraj R, Misra M, Mohanty AK Binary Blends of Poly (Butylene Adipate-co-Terephthalate) and Poly (Butylene Succinate): A New Matrix for Bio-_composites Applications. AIP Conf. Proc. 1664, 150009-1–150009-5; doi: 10.1063.1.4918505.

[26] Habibi Y, Lucia LA, Rojas OJ (2010) Chem. Rev. 110: 3479–3500.

[27] Reid MS, Villalobos M, Cranston ED (2017) Langmuir 33: 1583–1598.

[28] Dufresne A (2013) Mater. Today 16: 220–227.

[29] Dhar P, Bhardwaj U, Kumar A, Katiyar V (2014) Food Addit. Packag. American Chemical Society 197–239.

[30] Jackson JK, Letchford K, Wasserman BZ, Ye L, Hamad WY, Burt HM (2011) Int. J. Nanomedicine 6: 321–330.

[31] Lin N, Dufresne A (2014) Eur. Polym. J. 59: 302–325.

[32] Sun X, Wu Q, Lee S, Qing Y, Wu Y (2016) Sci. Rep. 6 (31654).

[33] Peng BL, Dhar N, Liu HL, Tam KC (2011) Can. J. Chem. Eng. 89: 1191–1206.

[34] P. Liu, X. Guo, F. Nan, Y. Duan, J. Zhang, ACS Appl. Mater. Interfaces 9 (2017) 3085–3092.

[35] F. Hoeng, A. Denneulin, J. Bras, Nanoscale 8 (2016) 13131–13154.

[36] Luo W, Schardt J, Bommier C, Wang B, Razink J, Simonsen J, Ji X (2013) J. Mater. Chem. A 1: 10662–10666.

[37] Zhou Y, Fuentes-Hernandez C, Khan TM, Liu JC, Hsu J, Shim JW, Dindar A, Youngblood JP, Moon RJ, Kippelen B (2013) Sci. Rep. 3.

[38] Lu Y, Armentrout AA, Li J, Tekinalp HL, Ozcan S (2015) J Mater Chem A.

[39] Abitbol T, Rivkin A, Cao Y, Nevo Y, Abraham E, Ben-Shalom T, Lapidot S, Shoseyov O (2016) Curr. Opin. Biotechnol. 39: 76–88.

[40] Dhar P, Kumar A, Katiyar V (2016) ACS Appl. Mater. Interfaces 8: 18393−18409.

[41] Moon RJ, Martini A, Nairn J, Simonsen J, Youngblood J (2011) Chem. Soc. Rev. **40**: 3941 —3994

[42] Soni B, Hassan EB, Mahmoud B (2015) Carbohydr. Polym. 134: 581 —589

[43] Torres GF, Commeaux S, Troncoso OP (2012) J. Funct. Biomater. 3: 864 —878

[44] Tesfaye et al. (2017) Nanosilk grafted poly (lactic acid) films: Influence of crosslinking on rheology and thermal stability. ACS Omega 2: 7071-7984.

[45] Junutek et al. (2011) Thermal, morphological and mechanical properties of biobased and biodegradable blends of poly (lactic acid) and chemically modified thermoplastic starch. Polymer Engineering science 51: 826-834.

[46] Jaratrokamjorn et al. (2011) Toughness enhancement of poly (lactic acid) by melt blending with natural rubber. Journal of Applied Polymer Science 124: 5027-5036.

[47] Nerkar et al. (2015) Improvement in the melt and solid-state properties of poly (lactic acid), poly-3-hydroxyoctanoate and their blends through reactive modification. Polymer 64: 51-61.

[48] Ji et al. (2014) Morphology, rheology, crystallization behaviour and mechanical properties of poly (lactic acid)/poly (butylene succinate)/ducumyl peroxide reactive blends. Journal of Applied polymer science 131: 1-8.

[49] Sabzi M, Jiang L, Liu F, Ghasemi I, Atai M (2013) Graphene nanoplatelets as poly (lactic acid) modifier:linear rheological behavior and electrical conductivity. Journal of Materials Chemistry A 1:8253

[50] Jandas PJ, Mohanty S, Nayak SK (2013) Rheological and Mechanical Characterization of Renewable Resource Based High Molecular Weight PLA Nanocomposites. Journal of Polymers 403467:1-11

[51] Chakraborty G, Gupta A, Pugazhenthi G, Katiyar V (2018) Facile dispersion of exfoliated graphene/PLA nanocomposites via in situ polycondensation with a melt extrusion process and its rheological studies.2018. Journal of Applied Polymer Science 46476: 1-11

[52] Tesfaye M, Patwa R, Dhar P, Katiyar V (2017) Nanosilk-Grafted Poly (lactic acid) Films: Influence of Cross-Linking on Rheology and Thermal Stability. ACS Omega 2:7071-7084

[53] Karakuş S (2019) Preparation and rheological characterization of Chitosan-Gelatine@ZnOSi Nanoparticles. International Journal of Biological Macromolecules 137: 821–828

[54] Yuankun Wang, Wenyuan Xie, Defeng Wu. (2020) Rheological properties of magnetorheological suspensions stabilized with nanocelluloses. Carbohydrate Polymers 231: 115776.

[55] Tesfaye M, Patwa R, Gupta A, Kashyap MJ, Katiyar V (2017) Recycling of Poly (Lactic Acid)/Silk based Bionanocomposites Films and its Influence on Thermal Stability,

Crystallization Kinetics, Solution and Melt Rheology. International journal of biological macromolecules 101: 580-594.

[56] Shojaeiarania J, Bajwa DS, Stark NM, Bajwa SG (2019) Rheological properties of cellulose nanocrystals engineered polylactic acid nanocomposites. Composites Part B 161: 483–489

[57] Ko SW, Gupta RK, Bhattacharya SN, Choi HJ (2010) Rheology and Physical Characteristics of Synthetic Biodegradable Aliphatic Polymer Blends Dispersed with MWNTs. Macromolecular Materials and Engineering 295: 320–328.

[58] Lee S, Kim M, Song HY, Hyun K (2019) Characterization of the Effect of Clay on Morphological Evaluations of PLA/Biodegradable Polymer Blends by FT-Rheology. Macromolecules 52: 7904−7919

[59] Dhar P, Bhardwaj U, Kumar A, Katiyar V (2015) Investigations on Rheological and Mechanical Behavior of Poly(3-Hydroxybutyrate)/Cellulose Nanocrystal Based Nanobiocomposites. Polymer composites 1-10.

[60] Pal AK, Bhattacharjee SK, Gaur SS, Pal A, Katiyar V (2017) Chemomechanical, morphological, and rheological studies of chitosan-graft-lactic acid oligomer reinforced poly (lactic acid) bionanocomposite films. Journal of Applied Polymer Science 45546 :1-10.

[61] Joseph K, Carvalho LH (2000) Jute/cotton woven fabric reinforced polyester composites: effect of hybridization. Natural polymers and composites conference proceedings. 454–9.

[62] Plackett D, Andersen T, Pedersen W, Nielsen L (2003) Biodegradable composites based on L-polylactide and jute fibres. Composites science and Technology 63:1287-1296.

[63] Mangal R, Saxena N, Sreekala M, Thomas S, Singh K (2003) Thermal properties of pineapple leaf fiber reinforced composites. Materials Science and Engineering: A 339: 281-285.

[64] Wong S, Shanks R, Hodzic A (2004) Interfacial improvements in poly (3-hydroxybutyrate)-flax fibre composites with hydrogen bonding additives. Composites Science and Technology 64: 1321–30.

[65] Alvarez VA, Terenzi A, Kenny JM, Vazquez A (2004) Melt rheological behavior of starch-based matrix composites reinforced with short sisal fibers. Polymer Engineering and Science 44: 1907–14.

[66] Pothan L, Thomas S, Groeninckx G (2006) The role of fibre/matrix interactions on the dynamic mechanical properties of chemically modified banana fible/polyester composites. Composites Part A: Applied Science and Manufacturing. 37: 1260-1269.

[67] Zini E, Focarete ML, Noda I, Scandola M (2007) Bio-composite of bacterial poly(3-hydroxybutyrate-co-3-hydroxyhexanoate) reinforced with vegetable fibers. Composites Science and Technology 67: 2085–94.

[68] Huda MS, Drzal LT, Mohanty AK, Misra M (2007) The effect of silane treated- and untreated-talc on the mechanical and physicomechanical properties of poly (lactic acid)/newspaper fibers/talc hybrid composites. Composites Part A: Applied Science and Manufacturing 38: 367–379.

[69] Xu H, Wang L, Teng C, Yu M (2008) Biodegradable composites: ramie fibre reinforced PLLA–PCL composite prepared by in situ polymerization process. Polymer Bulletin 61: 663–670.

[70] Bledzki AK, Jaszkiewicz A, Scherzer D (2009) Mechanical properties of PLA composites with man-made cellulose and abaca fibres. Composites Part A: Applied Science and Manufacturing 40: 404–12.

[71] Marsyahyo E, Jamasri, Rochardjo HSB, Soekrisno (2009) Preliminary investigation on bulletproof panels made from ramie fiber reinforced composites for NIJ Level II, IIA, and IV. Journal of Indian Textile 39: 13–26.

[72] Melo JDD, Carvalho LFM, Medeiros AM, Souto CRO, Paskocimas CA (2012) A biodegradable composite material based on polyhydroxybutyrate (PHB) and carnauba fibers. Composites: Part B 43: 2827-2835.

[73] Mi HY, Jing X, Peng J, Salick MR, Peng XF, Turng LS (2014) Poly(ε-caprolactone) (PCL)/cellulose nano-crystal (CNC) nanocomposites and foams. Cellulose 21: 2727-2741.

[74] Arias A, Heuzey MC, Huneault MA, Ausias G, Bendahou A (2015) Enhanced dispersion of cellulose nanocrystals in melt-processed polylactide-based nanocomposites. Cellulose 22: 483-498.

[75] Dhar P, Tarafdar D, Kumar A, Katiyar V (2016) Thermally recyclable polylactic acid/cellulose nanocrystal films through reactive extrusion process. Polymer 87: 268-282.

[76] Noshi N, Hong W, Ghanbarzadeh B, Fasihi H, Montazami R (2018) Study of cellulose nanocrystal doped starch-polyvinyl alcohol bionanocomposite films. International Journal of Biological Macromolecules. 107: 2065-2074.

[77] Borkotoky SS, Dhar P, Katiyar V (2017) Biodegradable Poly (lactic acid)/Cellulose Nanocrystals (CNCs) Composite Microcellular Foam: Effect of Nanofillers on Foam Cellular

Morphology, Thermal and Wettability Behaviour. International Journal of Biological Macromolecules. 106: 433-446.

[78] Dhar P, Gaur SS, Soundararajan N, Gupta A, Bhasney SM, Mili M, Kumar A, Katiyar V (2017) Reactive Extrusion of Polylactic Acid/Cellulose Nanocrystal Films for Food Packaging Applications: Influence of Filler Type on Thermomechanical, Rheological, and Barrier Properties. Industrial & Engineering Chemistry Research. 56(16).

[79] Kaili Song, Helan Xu, Kongliang Xie, Yiqi Yang (2017) Keratin-Based Biocomposites Reinforced and Cross-Linked with Dual-Functional Cellulose Nanocrystals. ACS Sustainable Chemistry & Engineering. 5: 5669-5678.

[80] Shaoying Cui, Pingfu Wei, Li LI (2018) Preparation of poly (propylene carbonate)/graphite nanoplates-spherical nanocrystal cellulose composite with improved glass transition temperature and electrical conductivity. Composites Science and Technology. 168: 63-73.

[81] Imre B, Pukánszky B (2013) Compatibilization in bio-based and biodegradable polymer blends. Eur Polym J 49:1215−1233.

[82] Scott G (2000) 'Green' polymers. Polym Degrad Stab 68: 1−7.

[83] Eling B, Gogolewski S, Pennings AJ (1982) Biodegradable materials of poly(l-lactic acid): 1. Melt-spun and solution-spun fibres. Polymer 23:1587−1593.

[84] Shalumon KT, Anulekha KH, Chennazhi KP, Tamura H, Nair SV, Jayakumar R (2011) Fabrication of chitosan/poly (caprolactone) nano-fibrous scaffold for bone and skin tissue engineering. Int J Biol Macromol 48 (4):571-576.

[85] Lee SH, Wang S (2006) Biodegradable polymers/ bamboo fiber bio-composite with bio-based coupling agent. Compos PartA Appl Sci Manuf 37: 80–91.

[86] Lu X, Huang J, He G, Yang L, Zhang N, Zhao Y, Qu J (2013) Preparation and characterization of cross-linked poly (butylene succinate) by multifunctional TDI-TMP polyurethane pre-polymer. Ind Eng Chem Res 52 (38): 13677-13684.

[87] Wang H, Xu M, Wu Z, Zhang W, Ji J, Chu PK (2012) Biodegradable poly (butyelene succinate) modified by gas plasmas and their in vitro functions as bone implants. ACS Appl Mater Inter 4 (8): 4380-4386.

[88] Satheesh Kumar MN, Mohanty AK, Erickson L, Misra M (2009) Lignin and its applications with polymers. J Biobased Mater Bioenergy 3:(1-24), doi:10.1166/jbmb.2009.1001.

[89] Sahoo S, Misra M, Mohanty AK (2011) Enhanced properties of lignin-based biodegradable polymer composites using injection moulding process. Compos Part A Appl Sci Manuf 42:1710–1718.

[90] Sinha Ray S, Okamoto K, Okamoto M (2003) Structure-property relationship in biodegradable poly (butylene succinate)/ layered silicate nanocomposites. Macromolecules 36 (7): 2355-2367.

[91] Chen R, Zou W, Zhang H, Zhang G, Yang Z, Jin G, Qu J (2015) Thermal behaviour, dynamic mechanical properties and rheological properties of poly (butylene succinate) composites filled with nanometer calcium carbonate. Polymer Testing 42: 160-167.

[92] Park BD, Wi SG, Lee KH, Singh AP, Yoon TH, Kim YS (2003) Biomass Bioenerg 25: 319.

[93] Ohkita T, Lee SH (2005) Crystallization behaviour of poly (butylene succinate)/corn starch biodegradable composite. J Appl Polym Sci 97: 1107–1114.

[94] Bao L, Chen Y, Zhou W, Wu Y, Huang Y (2011) Bamboo fibers @ poly(ethylene glycol) reinforced poly(butylene succinate) bio-composites. J Appl Polym Sci 122:2456–2466.

[95] Liu L, Yu J, Cheng L, Yang X (2009) Biodegradability of poly(butylene succinate) (PBS) composite reinforced with jute fibre. Polym Degrad Stab 94: 90–94.

[96] Ishiaku US, Khondker OA, Baba S, Nakai A, Hamada H (2005) Processing and characterization of short fiber reinforced jute/poly butylene succinate biodegradable composites: The effect of weld-line. J Polym Environ 13: 151–157.

[97] Bin T, Qu J, Liu L, Feng Y, Hu S, Yin X (2011) Non- isothermal crystallization kinetics and dynamic mechanical thermal properties of poly (butylene succinate) composites reinforced with cotton stalk bast fibers. Thermochim Acta 525:141–149.

[98] Nam TH, Ogihara S, Tung NH, Kobayashi S (2011) Effect of alkali treatment on interfacial and mechanical properties of coir fiber reinforced poly(butylene succinate) biodegradable composites. Compos Part B Eng 42: 1648–1656.

[99] Thirmizir MZA, Ishak ZAM, Taib RM, Rahim S, Jani SM (2011) Kenaf-bast-fiber-filled biodegradable poly (butylene succinate) composites: Effects of fiber loading, fiber length, and maleated poly (butylene succinate) on the flexural and impact properties. J Appl Polym Sci 122: 3055-3063.

[100] Han SO, Lee SM, Park WH, Cho D (2006) Mechanical and thermal properties of waste silk fiber reinforced poly (butylene succinate) bio-composites. J Appl Polym Sci 100: 4972-4980.

[101] Lee MW, Han SO, Seo YB (2008) Red algae fibre/ poly(butylene succinate) bio-composites: The effect of fibre content on their mechanical and thermal properties. Compos Sci Technol 68: 1266-1272.

[102] Flores ED, Funabashi M, Kunioka M (2009) Mechanical properties and biomass carbon ratios of poly (butylene succinate) composites filled with starch and cellulose filler using furfural as plasticizer. J Appl Polym Sci 112: 3410-3417.

[103] Kuan CF, Ma CCM, Kuan HC, Wu HL, Liao YM (2006) Preparation and characterization of the novel water cross-linked cellulose reinforced poly (butylene succinate) composites. Compos Sci Technol 66: 2231-2241.

[104] Sahoo S, Misra M, Mohanty AK (2011) Enhanced properties of lignin-based biodegradable polymer composites using injection moulding process. Compos Part A Appl Sci Manuf 42: 1710-1718.

[105] Dhar Prodyut, Tarafder Debashis, Kumar Amit, Katiyar Vimal (2016) Thermally recyclable polylactic acid/cellulose nanocrystal films through reactive extrusion process. Polymer 87: 268-282.

[106] Phua Y.J, Chow W.S, Mohd Ishak Z.A (2011) The hydrolytic effect of moisture and hydrothermal aging on poly (butylene succinate)/organo-montmorillonite nanocomposites. Polymer Degradation and Stability. 96: 1194-1203

[107] Mohkami M, Talaeipour M (2011) Bioresources. 1990.

[108] Kim HS, Lee BH, Lee S et al. (2011) Enhanced interfacial adhesion, mechanical, and thermal properties of natural flour-filled biodegradable polymer bio-composites. J Therm Anal Calorim 104: 331-338.

[109] Kim HS, Yang HS, Kim HJ (2015) Biodegradability and Mechanical Properties of Agro-Flour Filled Polybutylene Succinate Bio-composites. J Appl Polym Sci 97: 1513-1521.

[110] Hongsriphan N, Muangrak W, Soonthornvacharin K, Tulaphol T (2015) Mechanical Improvement of Poly (butylenes succinate) with Polyamide Short Fibers. Macromol Symp 354: 28-34.

[111] Chuanhui Gao, Zetian Li, Yuetao Liu, Xinhua Zhang, Jing Wang, Yumin Wu (2019) Thermal, Crystallographic, and Mechanical Properties of Poly (butylene succinate)/Magnesium Hydroxide sulphate Hydrate Whisker Composites Modified by in Situ Polymerization. I&EC research.

[112] Chakraborty Gourhari, Gupta Arvind, Pugazhenthi G, Katiyar V (2017) Facile dispersion of exfoliated graphene/PLA nanocomposites via in situ polycondensation with a melt extrusion process and its rheological studies. JAPS https://doi.org/10.1002/app.46476.

[113] Cox WP, Merz EH (1958) Journal of polymer science. 28 (1958): 619.

[114] Chuang HK, Han CD (1984) Rheological behaviour of polymer blends J Appl Polm Sci 29 (6): 2205-2209.

[115] Han CD, Kim J, Kim JK (1989) Determination of the order-disorder transition temperature of block copolymers. Macromolecules 22 (1): 383-394.

[116] Cole KS, Cole RH (1941) Dispersion and absorption in dielectrics I. Alternating current characteristics. J Chem Phys 9 (4): 341-351.

[117] Monika, Mulchandani N, Katiyar V (2019) Generalised kinetics for thermal degradation and melt rheology for poly (lactic acid)/ poly (butylene succinate) functionalised chitosan based reactive nanobiocomposite. IJBM (141): 831-842.

[118] Li Y, Wang S, Wang Q (2017) Enhancement of tribological properties of polymer composites reinforced by functionalised graphene. Compos Part B Eng 120: 83-91.

[119] Zawawi EZE, Hafizah AHN, Romli AZ, Yuliana NY, Bonnia NN (2020) Effect of nanoclay on mechanical and morphological properties of poly(lactide) acid (PLA) and polypropylene (PP) blends. Mater Today: Proc 46: 1778-82.

[120] Hayoune et al. (2020) Thermal decomposition kinetics and lifetime prediction of a PP/PLA blend supplemented with iron stearate during artificial aging. Thermochim Acta 690:178700

[121] Imre B, Pukanszky B (2013) Compatibilization in bio-based and biodegradable polymer blends. Eur Polym J 49:1215-33.

[122] Khankrua R et al. (2014) Polym. Degrad. Stabil. 108 (232).

[123] Gomez R et al. (2015) Polym. Eng. Sci. 55 (214).

[124] Hamad K, Kaseem M, Yang H.W, Deri F, Ko Y.G (2015) Properties and medical applications of polylactic acid: A review. Express Polym. Lett. 9: 435–455.

[125] Kaseem M, Hamad K, Deri F, Ko YG (2017) A review on recent researches on polylactic acid/carbon nanotube composites. Polym. Bull. 74: 2921–2937.

[126] Kaseem M, Ko YG (2017) Melt flow behavior and processability of polylactic acid/polystyrene (PLA/PS) polymer blends. J. Polym. Environ. 25: 994–998.

[127] Kaseem M, Hamad K, Rehman ZU (2019) Review of recent advances in polylactic acid/TiO_2 composites. Materials 12: 3659

[128] Hamad K, Kaseem M, Deri F (2012) Preparation and characterization of binary and ternary blends with poly (lactic acid), polystyrene, and acrylonitrile-butadiene-styrene. J. Biomater. Nanobiotechnol. 3: 405–412.

[129] Kaseem M (2019) Poly (lactic acid) composites. Materials 12: 3586

[130] Hamad K, Ko YG, Kaseem M, Deri F (2014) Effect of acrylonitrile–butadiene–styrene on flow behavior and mechanical properties of polylactic acid/low density polyethylene blend. Asia-Pac. J. Chem. Eng. 9: 349–353.

[131] Kadhum SA (2017) The Effect of two types of nano-particles (ZnO and SiO_2) on different types of bacterial growth. Biomed. Pharmacol. J. 10: 1701–1708.

[132] Li H, Liebscher M, Curosu I, Choudhury S, Hempel S, Davoodabadi M, Dinh TT, Yang J, Mechtcherine V (2020) Electrophoretic deposition of nano-silica onto carbon fiber surfaces for an improved bond strength with cementitious matrices. Cem. Concr. Compos. 114(103777).

[133] Galliker P, Hommes G, Schlosser D, Corvini PFX, Shahgaldian P (2010) J. Colloid Interface Sci. 349**(**1).

[134] Nandiyanto ABD, Suhendi A, Ogi T, Umemoto R, Okuyama K (2014) Chem. Eng. J. 256 **(**421).

[135] Nandiyanto A, Ogi T, Iskandar F, Okuyama K (2011) Chem. Eng. J. 167**(**409).

[136] Rafiee E, Shahebrahimi S, Feyzi M, Shaterzadeh M (2012) Int. Nano Letters 2 **(**1).

[137] Sousa AM, Visconte L, Mansur C, Furtado C (2009) Chem. Chem. Technol. 3 **(**321).

[138] Kalapathy U, Proctor A, Shultz J (2000) Bioresource. Technol. 73 **(**257).

[139] Tsai PA, Chiu WM, Lin CE, Wu JH (2013) Fabrication and characterization of PLA/SiO_2/Al_2O_3 composites prepared by Sol-Gel process. Polym. Plast. Technol. Eng. 52:1488–1495.

[140] Lu P, Hsieh YL (2012) Powder Technol. 225**,** 149.

[141] Soltani N, Bahrami A, Canul MIP, Gonzalez LA (2015) Chem. Eng. J. 264**,** 899.

[142] Nikolic L, Ristic I, Adnadjevic B, Nikolic V, Jovanovic J, Stankovic, M (2010) Novel microwave-assisted synthesis of poly (D, L-lactide): the influence of monomer/initiator molar ratio on the product properties. Sensors (Basel) 10: 5063–5073.

[143] Anderson I (2017) Mechanical properties of specimens 3D printed with virgin and recycled polylactic acid 3D print. Addit. Manuf. 4:110-115.

[144] Asmatulu E et al. (2018) Invesgating compression strengths of 3D printed polymeric infill specimens of various geometries. 21.

[145] Navarro-Baena I, Sessini V, Dominici F, Torre L, Kenny JM, Peponi L (2016) Design of biodegradable blends based on PLA and PCL From morphological, thermal and mechanical studies to shape memory behavior. Polym. Degrad. Stab. 132: 97–118.

[146] Arrieta MP, Fortunati E, Dominici F, Lopez J, Kenny JM (2015) Bionanocomposite films based on plasticized PLA-PHB/cellulose nanocrystal blends. Carbohydr. Polym. 121: 265–275.

[147] Goffin AL, Raquez JM, Duquesne E, Siqueira G, Habibi Y, Dufresne A, Dubois P (2011) From interfacial ring-opening polymerization to melt processing of cellulose nanowhisker-filled polylactide-based nanocomposites. Biomacromolecules 12: 2456–2465.

[148] Bras J, Hassan ML, Bruzesse C, Hassan EA, El-Wakil NA, Dufresne A (2010) Mechanical, barrier, and biodegradability properties of bagasse cellulose whiskers reinforced natural rubber nanocomposites. Ind. Crops Prod. 32: 627–633.

[149] Li MC, Wu Q, Song K, De Hoop CF, Lee S, Qing Y, Wu Y (2016) Cellulose nanocrystals and polyanionic cellulose as additives in bentonite water-based drilling fluids: rheological modeling and filtration mechanisms. Ind. Eng. Chem. Res. 55: 133–143.

[150] Zhou L, He H, Li MC, Song K, Cheng HN, Wu Q (2016) Morphological influence of cellulose nanoparticles (CNs) from cottonseed hulls on rheological properties of polyvinyl alcohol/CN suspensions. Carbohydr. Polym. 153: 445–454.

[151] Nechyporchuk O, Belgacem MN, Bras J (2016) Production of cellulose nanofibrils: a review of recent advances. Ind. Crops Prod. 93: 2–25.

[152] Arias A, Heuzey MC, Huneault MA, Ausias G, Bendahou A (2014) Enhanced dispersion of cellulose nanocrystals in melt-processed polylactide-based.

[153] Kamal MR, Khoshkava V (2015) Effect of cellulose nanocrystals (CNC) on rheological and mechanical properties and crystallization behavior of PLA/CNC nanocomposites. Carbohydr. Polym. 123: 105–114.

[154] Zhang C, Salick MR, Cordie TM, Ellingham T, Dan Y, Turng LS (2015) Incorporation of poly (ethylene glycol) grafted cellulose nanocrystals in poly (lactic acid) electrospun nanocomposite fibers as potential scaffolds for bone tissue.

[155] Lin N, Huang J, Chang PR, Feng J, Yu J (2011) Surface acetylation of cellulose nanocrystal and its reinforcing function in poly(lactic acid). Carbohydr. Polym. 83: 1834–1842.

[156] Lizundia E, Fortunati E, Dominici F, Vilas JL, Leon LM, Armentano I, Torre L, Kenny JM (2016) PLLA-grafted cellulose nanocrystals: role of the CNC content and grafting on the PLA bionanocomposite film properties. Carbohydr. Polym. 142: 105–113.

[157] Spinella S, Lo Re G, Liu B, Dorgan J, Habibi Y, Leclère P, Raquez J M, Dubois P, Gross RA (2015) Polylactide/cellulose nanocrystal nanocomposites: efficient routes for nanofiber modification and effects of nanofiber chemistry on PLA reinforcement. Polymer 65: 9–17.

[158] Paul et al. (1999) "Polymer blends". John Wiley & Sons, Hoboken.

[159] Baker et al. (2001) "Reactive Polymer Blending". Carl Hanser Verlag, Munich.

[160] Robeson LM. (2007) "Polymer Blends, A Comprehensive Review". Carl Hanser Verlag, Munich.

[161] Raquez et al. (2008) Recent Advances in Reactive Extrusion Processing of Biodegradable Polymer-Based Compositions Macromol. Mater. Eng. 293 (447).

[162] Gaylord et al. (1982) J. Polym. Sci. Polym. Lett. Ed. 20 (481).

[163] Gaylord et al. (1983) J. Polym. Sci., Part C: Polym. Lett. 21 (23).

[164] Lei W, Fang C, Zhou X, Yin Q, Pan S, Yang R, Liu D, Ouyang Y (2018) Cellulose nanocrystals obtained from office waste paper and their potential application in PET packing materials. Carbohydrate Polymers, 181: 376–385.

[165] Aguayo MG, P´erez AF, Reyes G, Oviedo C, Gacitúa W, Gonzalez R, Uyarte, O (2018). Isolation and characterization of cellulose nanocrystals from rejected fbers originated in the Kraft Pulping process. Polymers, 10(10).

[166] Mukherjee T, Sani M, Kao N, Gupta RK, Quazi N, Bhattacharya S (2013) Chem. Eng. Sci. 101: 655-662.

[167] Lin N, Huang J, Chang PR, Feng J, Yu J (2011) Carbohydr. Polym. 83: 1834-1842.

[168] Battegazzore et al. (2011) Crystallization kinetics of poly (lactic acid)-talc composites eXpress polymer Letters 5: 849-858.

[169] Zhang C, Salick MR, Cordie TM, Ellingham T, Dan Y, Turng LS (2015) Incorporation of poly (ethylene glycol) grafted cellulose nanocrystals in poly (lactic acid) electrospun nanocomposite fibers as potential scaffolds for bone tissue. Mater Sci Eng C Mater Biol Appl. 49: 463-471